Electronic Supplementary Information

Ferromagnetic α-Fe_2O_3 NPs: A potential catalyst in Sonogashira Hagihara cross coupling and Hetero-Diels-Alder reactions

Meenal Kataria, Subhamay Pramanik, Navleen Kaur, Manoj Kumar, Vandana Bhalla,*

Department of Chemistry, UGC Sponsored Centre for Advanced Studies-1, Guru Nanak Dev University, Amritsar 143005, and Punjab, India

E-mail: vanmanan@yahoo.co.in

vanmanan@yahoo.co.in

Table S1: Comparison of catalytic activity of α-Fe_2O_3 NPs for Sonogashira cross coupling reaction over other catalytic system reported in the literature.

Serial No.	Publication	Catalyst used	Use of Noble metal	Use of CuI	Use of Amine	Solvent	Nano catalysis	Recycling	Reaction time	Temp. required (in °C)	Isolated Yield (Product, %)
1	**Present manuscript**	**α-Fe_2O_3, K_2CO_3**	**No**	**No**	**No**	**Ethylene glycol (green solvent)**	**Yes**	**Yes (13 times)**	**13 h**	**80**	**84**
2	*Green Chem.*, 2015, **17**, 1893-1898	Pd-CS, Pd-CS-Glu and Pd-CS-SH, K_2CO_3	Yes	No	No	EtOH/Water	Yes	Yes (6 times)	6 h	65	98
3	*Green Chem.*, 2015, **17**, 1071-1076	Pd/C, DABCO	Yes	No	Yes	γ-Valerolactone	No	No	4 h	60-100	99
4	*Green Chem.*, 2014, **16**, 2515-2522	PEG-2000, $PdCl_2(PPh_3)_2$	Yes	No	Yes	Water, Et_3N	No	No	24 h	25	95
5	*Chem. Commun.*, 2015, **51**, 10871-10874	L_4–Pd	Yes	No	Yes	DMF	No	Yes (5 times)	1.5 h	90	97
6	*Chem. Eur. J.*, 2014, **20**, 1-13	PEGylated g-Fe_2O_3-Pd NPs	Yes	No	Yes	THF	Yes	Yes	24 h	65	86
7	*Org. Lett.*, 2014, **16**, 3724-3727	(N-heterocyclic carbene)-Cu and (N-heterocyclic carbene)-Pd complexes	Yes	Yes	No	DMSO	No	No	24 h	120	94
8	*J. Mater. Chem. A*, 2014, **2**, 484-491	Pd–PPh_2-MCM-41@SiO_2@Fe_3O_4 (Very complicated)	Yes (Pd)	No	No	Water	No	Yes	4 h	70	95
9	*Org. Lett.*, 2013, **15**, 65-67	Pd-Cu dual Reactor	Yes	Yes	No	DMF	No	No	-	120	95
10	*Angew. Chem. Int. Ed.* 2013, **52**, 11554-11559	Pd(0) nanoparticle, KOAc	Yes (Pd)	No	Yes	NMP (toxic)	Yes	No	24 h	160	83
11	*Green Chem.*, 2013, **15**, 2349-2355	Pd catalyst, K_2CO_3	Yes (Pd)	No	No	EtOH/Chlorobenzene (flammable)	No	Yes	18 h	60	88
12	*Green Chem.*, 2013, **15**, 2132-2042	Fe_3O_4@-SiO_2@PPh_2@Pd(0), NaOH (Very complicated)	Yes (Pd)	No	No	Water	No	Yes	15 min-4 h	80	91
13	*Chem. Eur. J.*, 2013, **19**, 14024-14029	5% Pd-Au/C, K_3PO_4	Yes (Pd, Au)	No	No	*i*PrOH/H_2O	No	No	20 h	80	73

14	*Adv. Synth. Catal.*, 2011, **353**, 125-132	Fe_3O_4	No	No	No	Ethylene glycol	Yes	Yes	35h	125	92
15	*Chem. Commun.,* 2010, **46**, 6524-6526	Pd@meso-SiO_2 (Very complicated)	Yes (Pd)	No	No	EtOH	No	Yes	30 h	80	55
16	*Angew. Chem. Int. Ed.* 2007, **46**, 1536-1538	Au(I), K_3PO_4	Yes (Au)	No	No	*O*-Xylene	No	No	24 h	130	54
17	*Langmuir,* 2010, **14**, 12225-12229	Au-Ag-Pd trimetallic nanoparticles	Yes (Pd, Au, Ag)	No	No	DMF-H_2O	No	No	2 h	120	94
18	*Org. Lett.,* **2** , 2000, 2935-2938	$Pd(PPh_3)_2$, Ag_2O	Yes (Pd, Ag)	No	No	THF	No	No	8 h	60	60

Table S2: Comparison of catalytic activity of α-Fe_2O_3 NPs for hetero-Diels–Alder reaction over other catalytic system reported in literature.

Sr. No.	Publication	Catalyst Used	Use of noble metal	Cost of catalyst	Use of Nano catalyst	Amount of Catalyst used	Use of activated diene/die nophile	Solvent	Additives	Tem p. (˚C)	Time	Yield %	Recycl ability
1	**Present manuscript**	**α-Fe_2O_3 NPs**	**No**	**Very cheap**	**Yes**	**1 mol %**	**No**	***p*-xylene (90%)/Neat condition (68%)**	**No**	**60**	**10h**	**Upto 90%**	**Yes**
2	*Org. Lett.*, 2015, **17**, 3506-3509	$LiClO_4$	No	Costly	No	1 equiv.	Yes	DCE/MeCN	Yes	80	2h	94	No
3	*Org. Lett.*, 2015, **17**, 3536-3539	CuI in 4Å MS	No	Costly and Sensitive	No	10 mol%	Yes	THF/t-BuOH (1:1)	Yes (Et_4NI, Cs_2CO_3)	25	1-48	90	No
4	*J. Am. Chem. Soc.* 2014, **136**, 17714−17717	PCN-223 porphyrinic ZrMOF	Yes	Costly	No	1 mol%	No	Toluene	$AgBF_4$	80	12 h	99	Yes
5	*Chem. Commun.*, 2014, **50**, 14187-14190	Calcium BINOL-derived phosphates	No	Yes	No	2.5 mol%	Yes	DCM	HCl	Rt	12h	94%	No
6	*Org. Lett.*, 2014, **16,** 3564-3567	Cu(I)OTF_2L	No	-	No	10 mol%	Yes	Toluene	Base	0˚C	Upto 24h	› 90%	No
7	*Org. Lett.*, 2013, **15**, 9-12	Rh$(cod)_2BF_4$	Yes	costly	No	5 mol %	No	DCM	Acid	80˚C	Upto 24h	Upto 90 %	No
8	*J. Am. Chem. Soc.*, 2012, **134**, 5512-5515	Iron(III) porphyrin catalyst	No		No		No	Benzene- upto 90%/ Neat condition-trace yield	No	80˚C	12h	Upto 90%	
9	*J. Am. Chem. Soc.*, 2009, **131**, 12882-12883	Chiral phosphoric acid	No	Yes	No	2-100 mol%	Yes	Toluene	-	RT	24 h	Upto 95 %	
10	*Org. Lett.,2008,* **10**, 13-16	1-Np-TADDOL	No	-	No	20 mol%	Yes	Toluene/DCM	Acid chloride	-78˚C	15 min		No
11	*Org. Lett.*, 2004, **6**, 13-16	$Ti(OiPr)_4$	No	costly	No	5 mol %	Yes	Toluene	TFA	0˚C	72 h	Upto 92%	No
12	*Org. Lett.*, 2003, **5**, 7-10	Diethyl Zinc	No	-	No	10 mol%	Yes	Toluene	Acid	-20˚C	30 h	Upto 99 %	No

Table S3: Comparison table between the present catalytic system and previously reported system for Sonogashira coupling reactions (*Angew. Chem. Int. Ed.* 2008, **47**, 4862-4865).

Sr. No.	Points of Comparison on Reaction Conditions	Present Manuscript	*Angew. Chem. Int. Ed.* 2008, 47, 4862-4865
1.	Reactivity towards Substrates	Both for aryl iodides and bromides	Only for aryl Iodides
2.	Recyclability of catalyst	Yes (13 times)	No
3.	Mechanistic Study	Yes	No
4.	Base	K_2CO_3 (mild, Cheap)	Cs_2CO_3 (Strong, Costly)
5.	Time	13-24 h	72 h
6.	Solvent	Ethylene Glycol (green solvent)	Toluene
7.	Catalyst Loading	Low catalyst loading (0.5 mol %)	High catalyst loading (15 mol %)

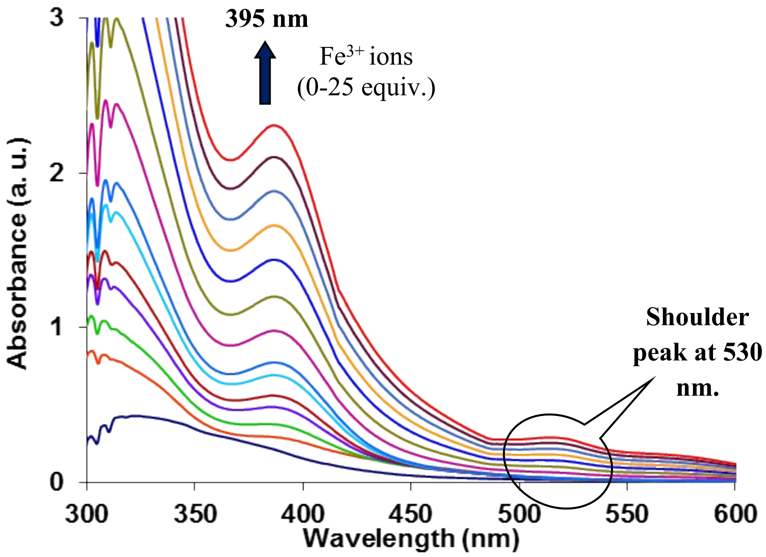

Figure S1: UV-vis. spectroscopic spectra of derivative 1 (5 μM) in H_2O/EtOH (7:3, v/v) upon the addition Fe^{3+} ions (0-25 equiv.).

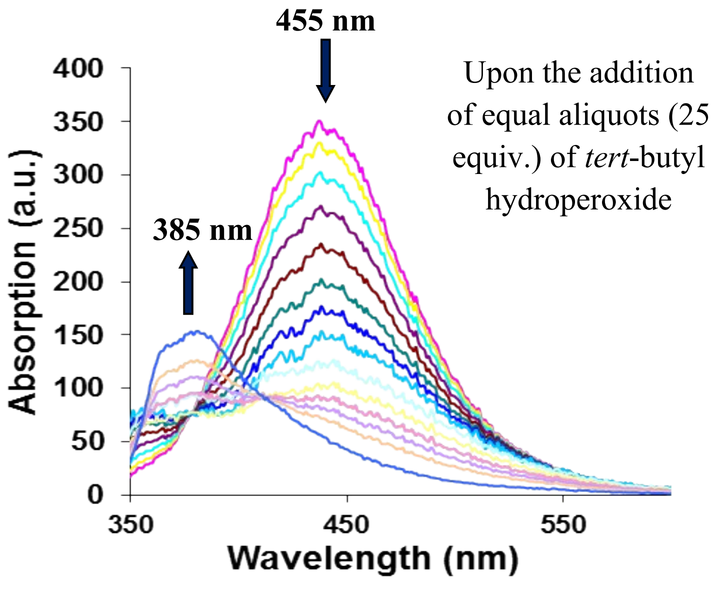

Figure S2: Fluorescence spectra of derivative **1** (5 μM) after the addition of equal aliquots of *tert*-butyl hydroperoxide (a oxidizing agent) in H_2O/EtOH (7:3, v/v) mixture.

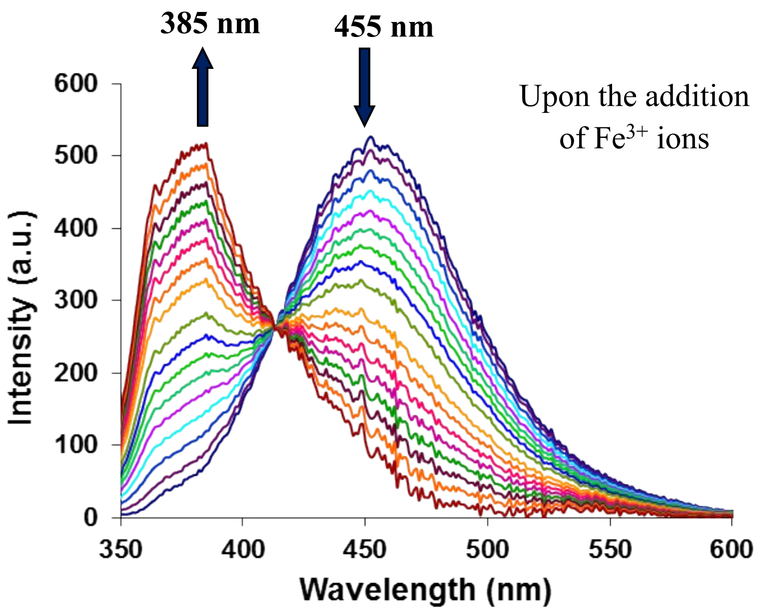

Figure S3: Fluorescence spectra of derivative **1** (5 μM) showing the variation on addition of Fe^{3+} ions (0-25 equiv.) in H_2O/EtOH (7:3, v/v) mixture.

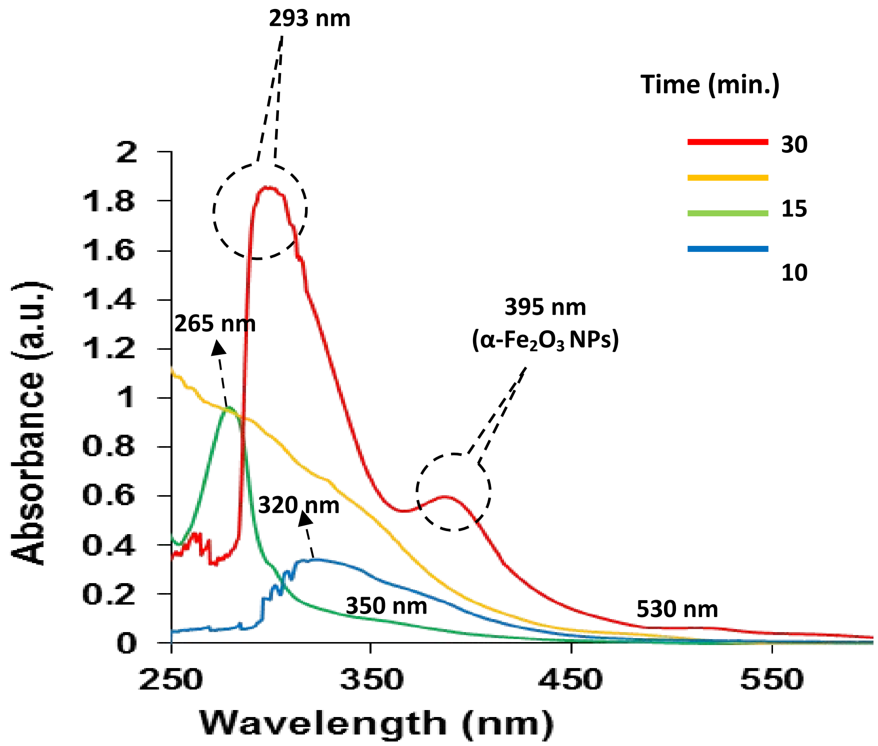

Figure S4: UV-vis Spectra showing the formation of Fe (0) Nps bands after keeping the solution of derivative **1** and Fe^{3+} ion (0-25 equiv.) in H_2O/EtOH (3:7, v/v) mixture under inert atmosphere for 10 min and followed by oxidation resulting in the *in situ* formation of Fe_2O_3 nanoparticles

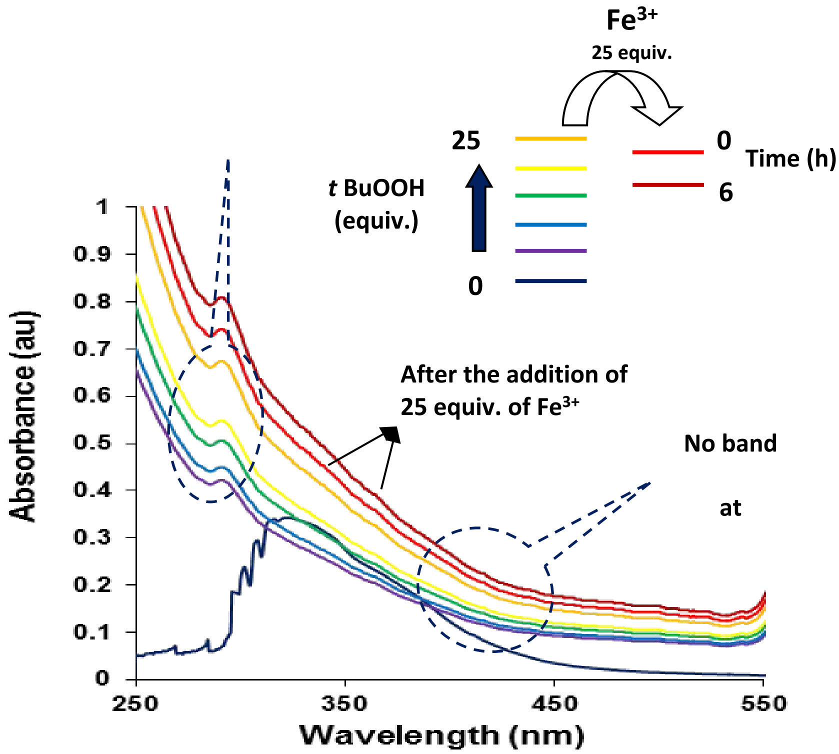

Figure S5: UV-vis Spectra of derivative **1** on addition of *tert*- butyl hydroperoxide (0-25 equiv.) in H_2O/EtOH (3:7, v/v) mixture followed by the addition of Fe^{3+} ion (0-25 equiv.).

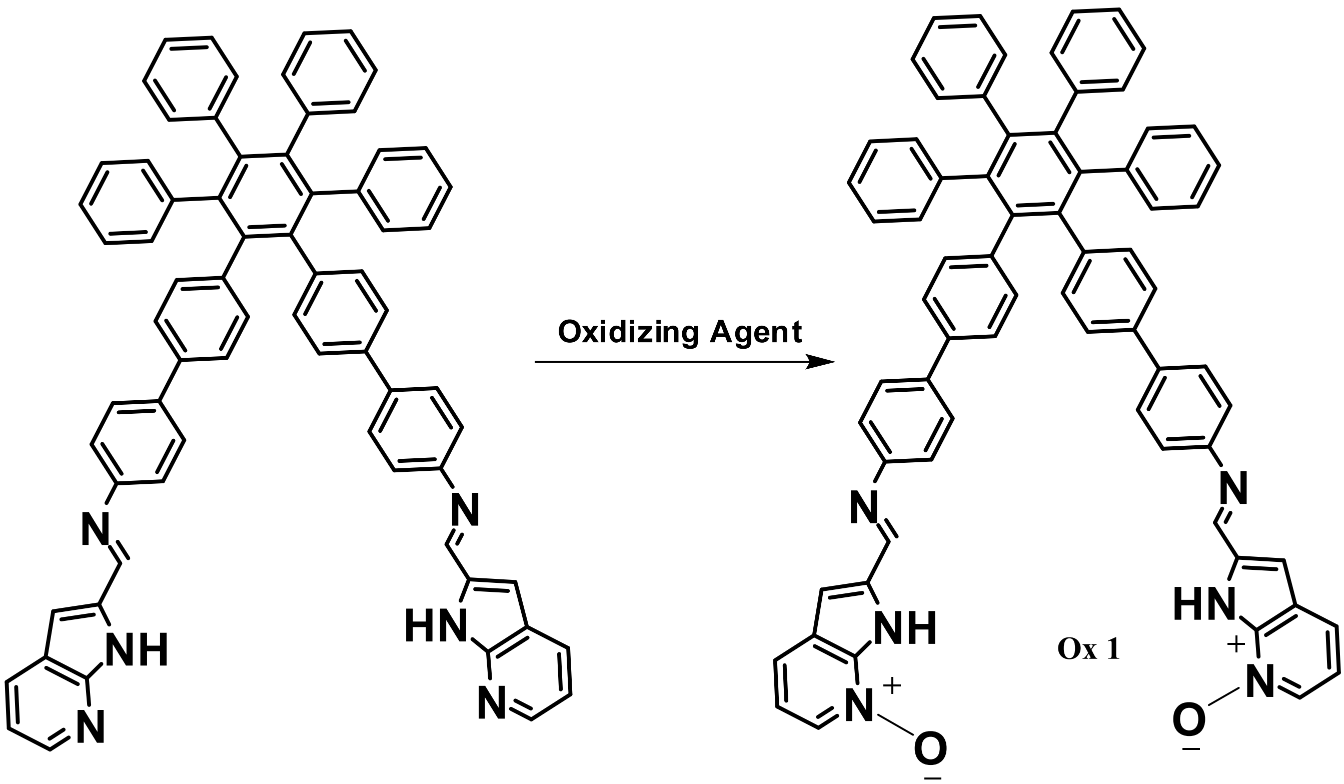

Scheme 1: Oxidation of derivative **1** by using *t* BuOOH to yield N-oxide derivative.

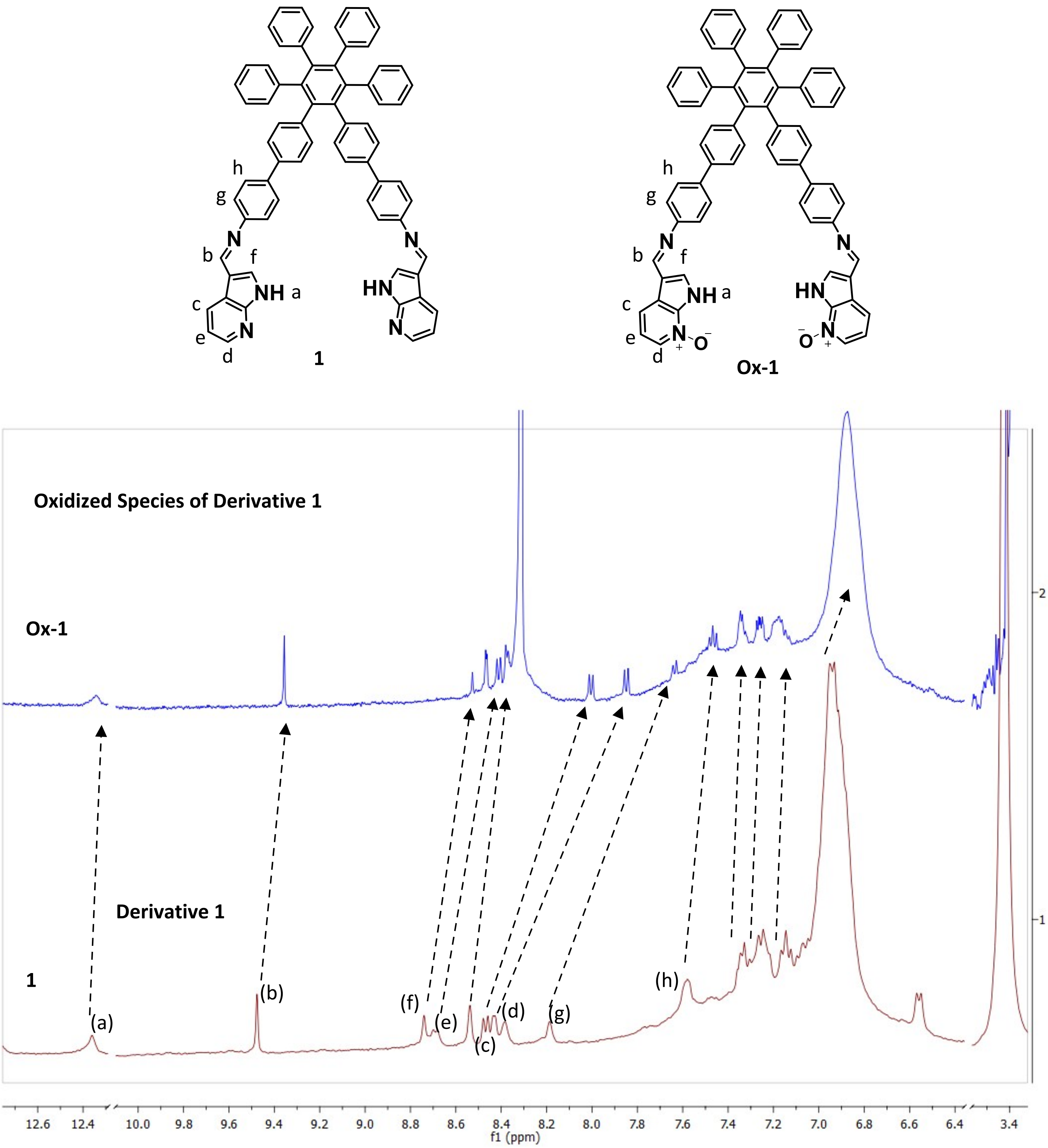

Figure S6: Overlay of [1]H NMR spectra of derivative **1** and oxidized species of derivative **1** showing the upfield shifting of all protons.

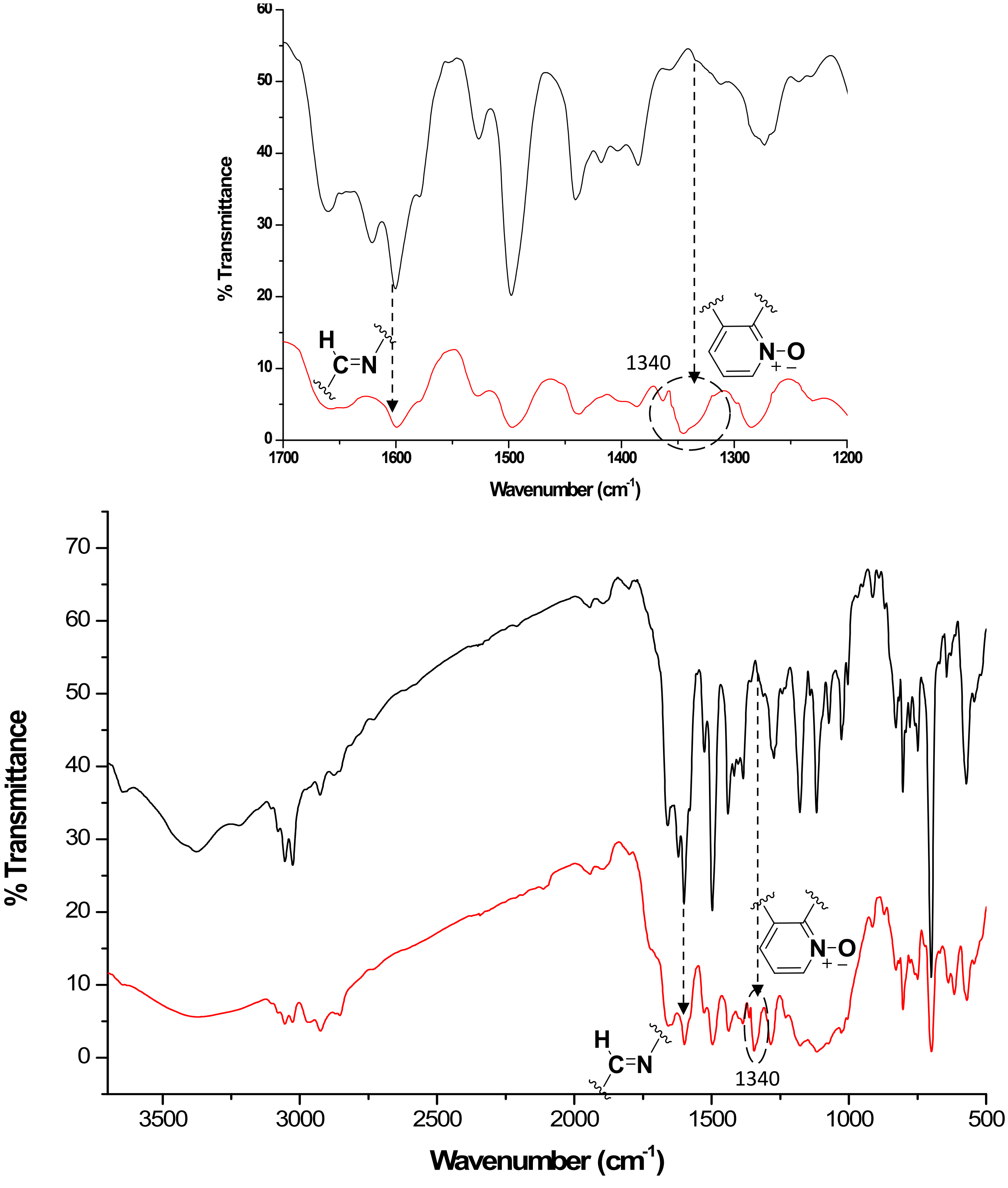

Figure S7: FT-IR spectrum of oxidized deivative **1** showed stretching band at around 1340 cm^{-1} corresponding to $N^{+}–O^{-}$ stretching frequency.

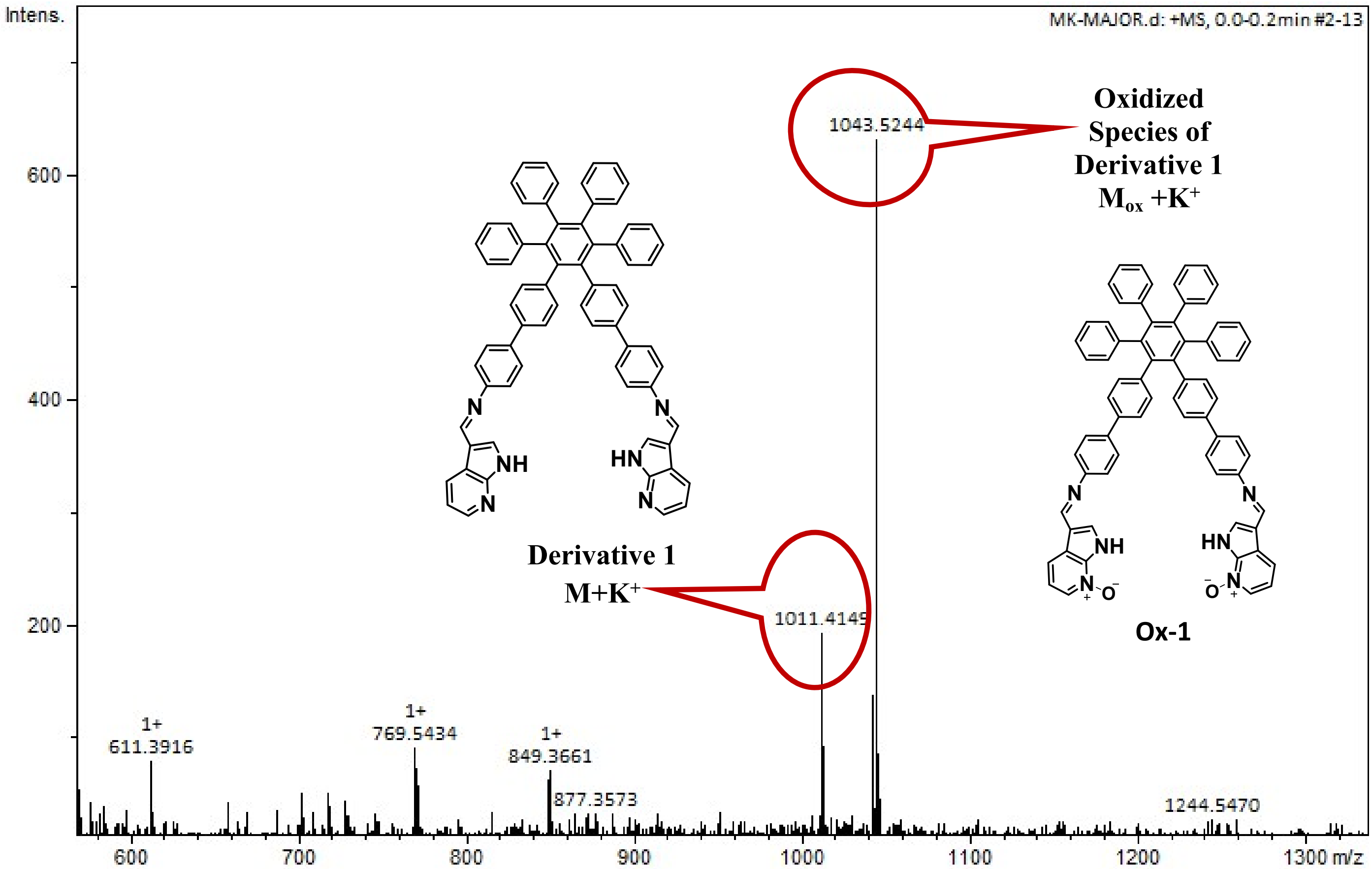

Figure S8: ESI-MS mass spectrum of residue obtained showed a parent ion peak, m/z = 1043 due to oxidized species of derivative **1.**

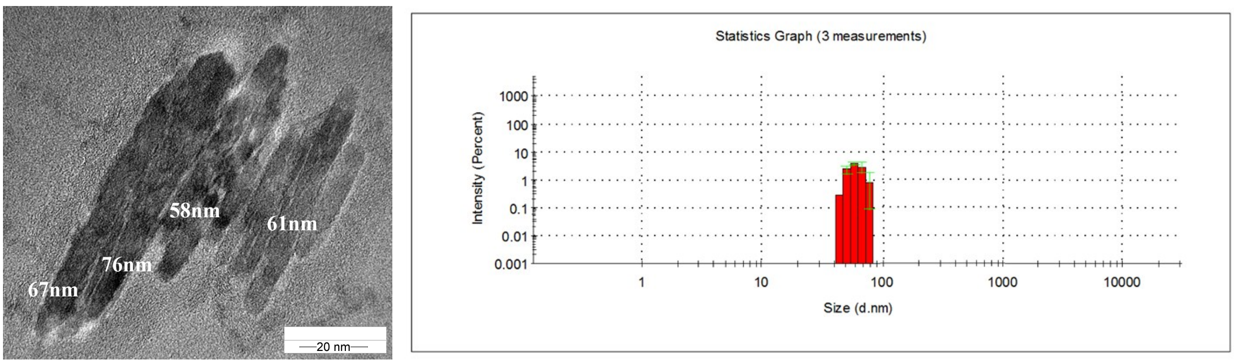

Figure S9: (A) TEM (Scale bar 20 nm) and (**B**) DLS analysis of compound **1** (5 µM) showing the size of Fe_2O_3 nanoparticles at temperature 70°C in the range of 60-80 nm.

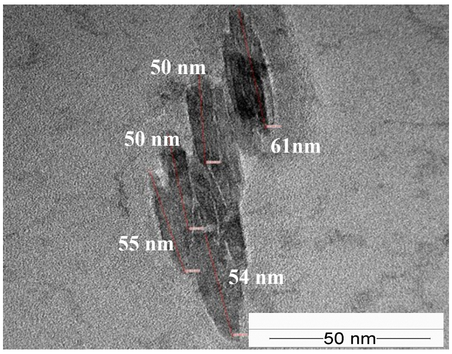

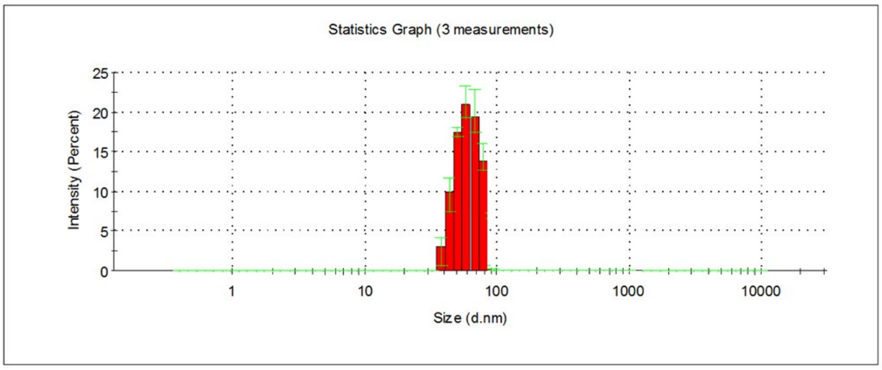

Figure S10: (A) TEM (Scale bar 50 nm) and (**B**) DLS analysis of compound **1** (5 μM) showing the size of Fe_2O_3 nanoparticles in the presence of sodium hydroxide (pH=12) in the range of 50-60 nm.

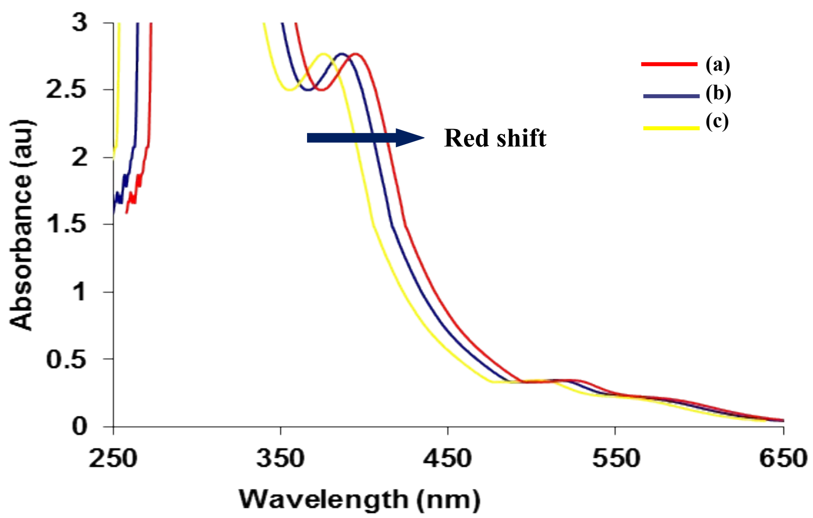

Figure S11: UV-vis. spectra by varying Fe^{3+} ions to ligand ratio a) 2:1, b) 1:1, c) 1:2.

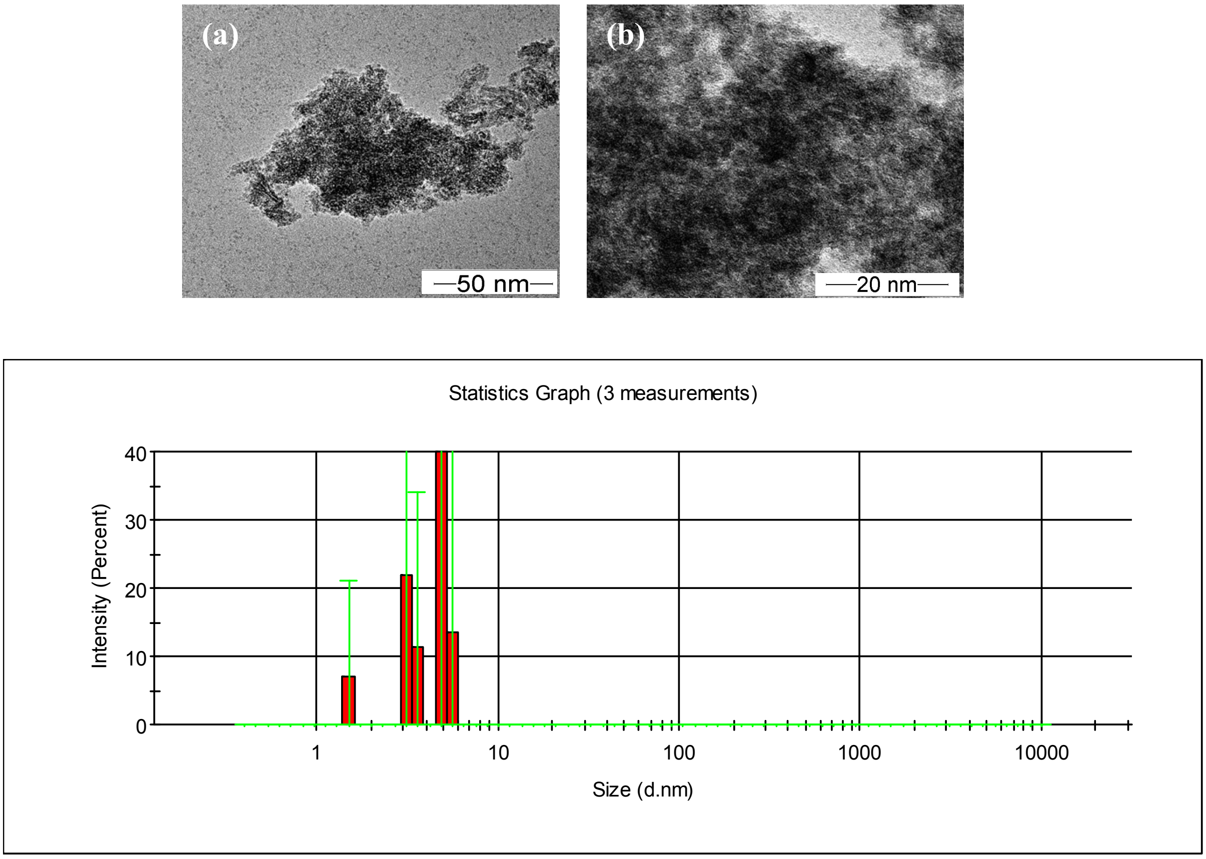

Figure S12: A) TEM images of spherical α-Fe_2O_3 NPs prepared by literature reported method (*J. Mater. Chem. A*, 2013, **1**, 830) B) DLS analysis showing the size of α-Fe_2O_3 NPs 4-6 nm.

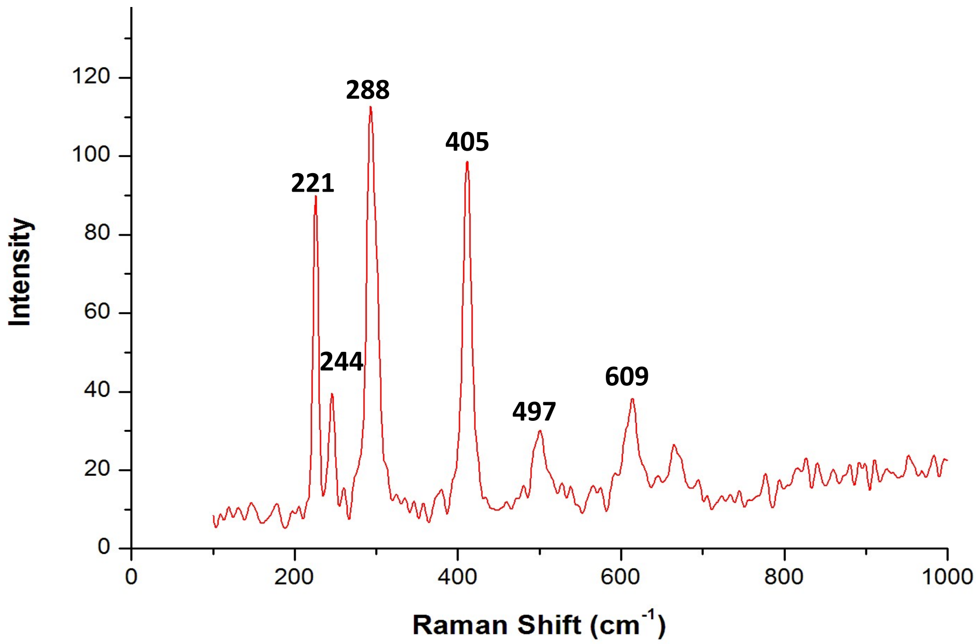

Figure S13: Raman spectrum of spherical α-Fe_2O_3 NPs prepared by literature reported method (*J. Mater. Chem. A*, 2013, **1**, 830); [Refrence 1: *CrystEngComm.*, 2014, **16**, 10618].

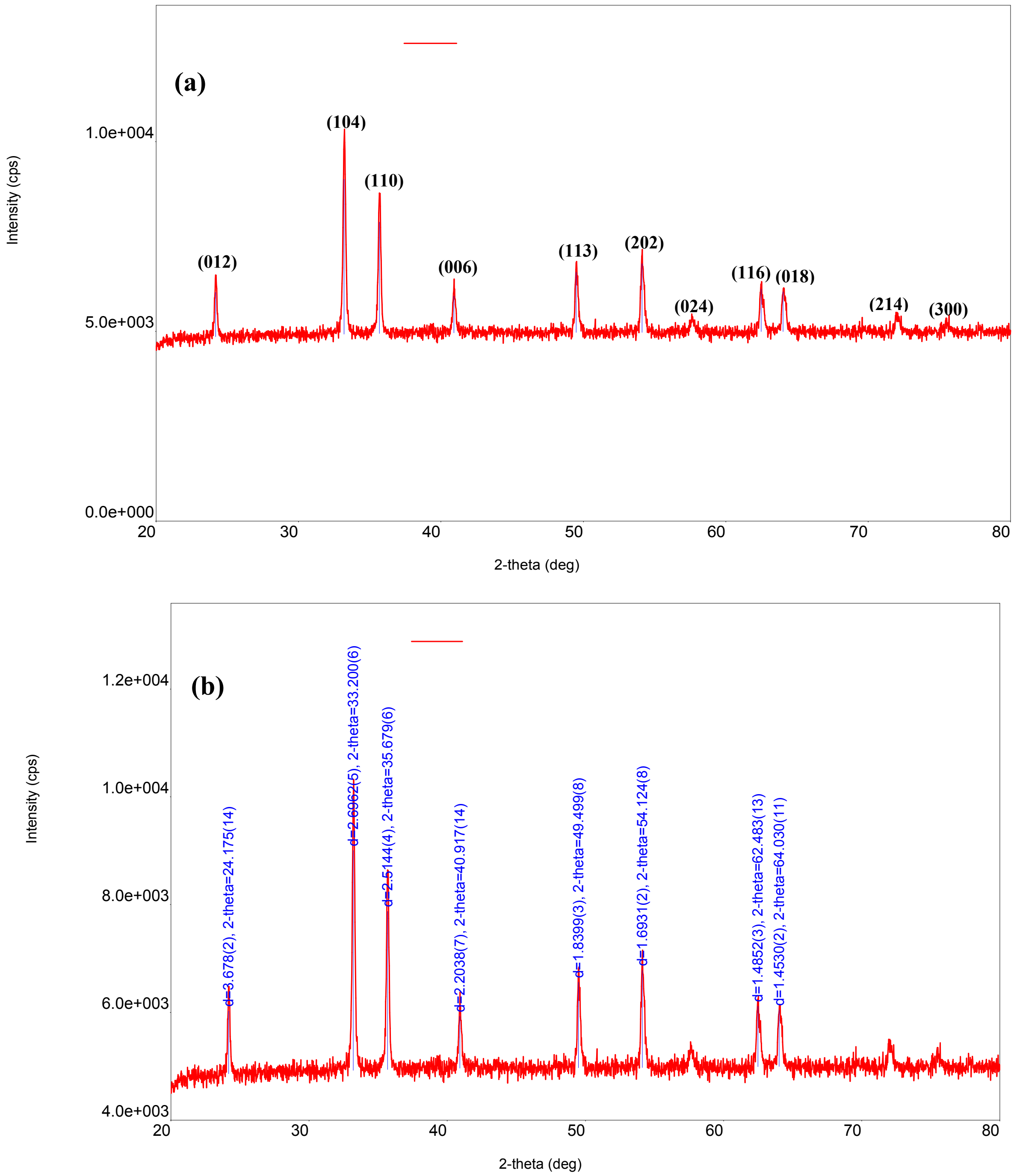

Figure S14: (a-b) XRD diffraction pattern of spherical α-Fe_2O_3 NPs prepared by commercial reported method.

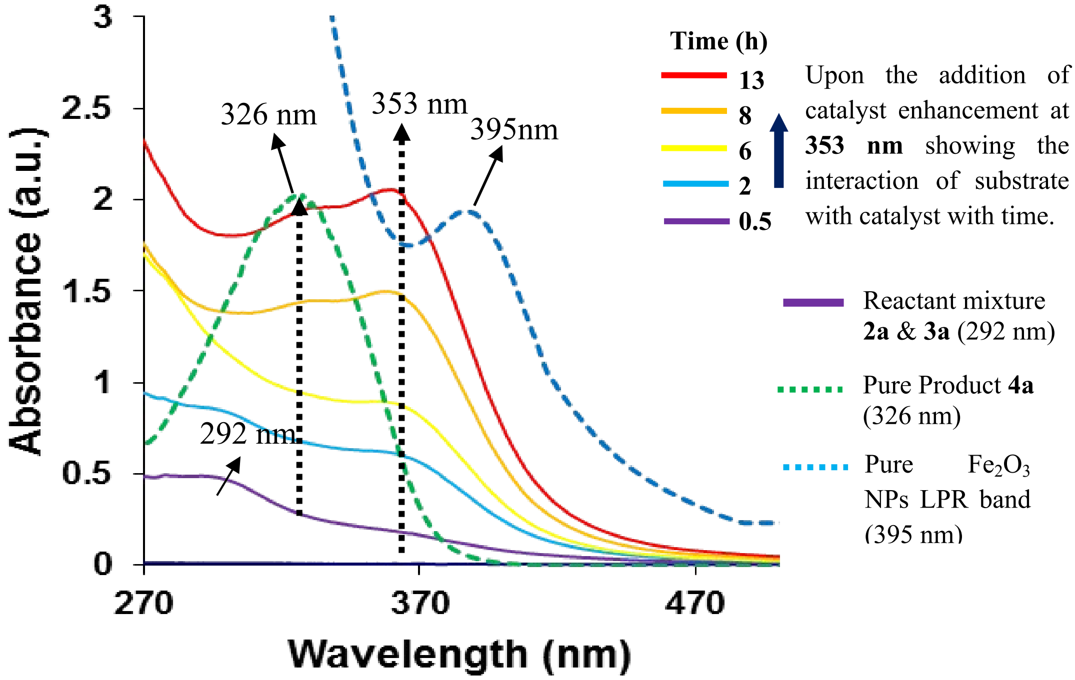

Figure S15: UV-vis. Spectra recorded during the reaction of **1a** and **2a** in the presence of in situ generated Fe_2O_3 NPs in ethylene glycol.

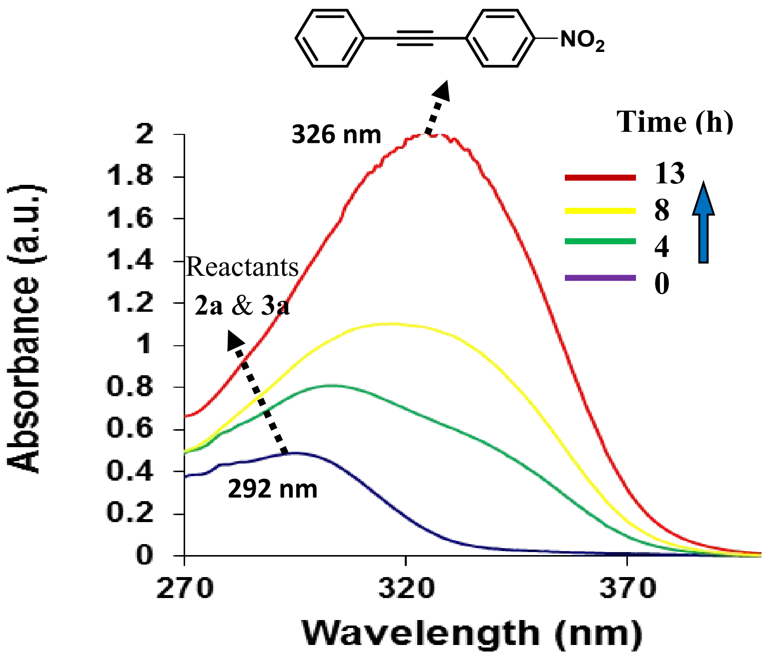

Figure S16: UV-vis spectra of reaction between **1a** and **2a** showing the completion of reaction to give product **4a** catalysed by Fe_2O_3 NPs when the catalyst loading was 0.005 mol.

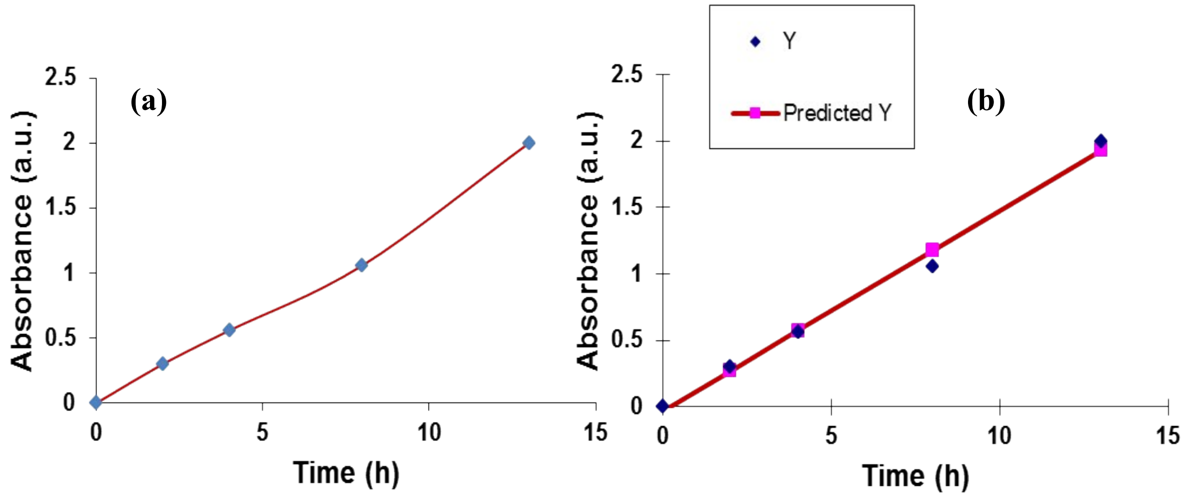

Figure S17: (a) Kinetic profile showing the formation of product with time when the catalyst loading is 0.005 mol; (b) calibration curve. Reactions were monitored by UV-vis. Spectroscopy.

Multiple R= 0.995
R^2 = 0.991
Slope = 0.150
Rate = (2.303×0.150)/3600 = 0.959×10^{-4} sec^{-1}

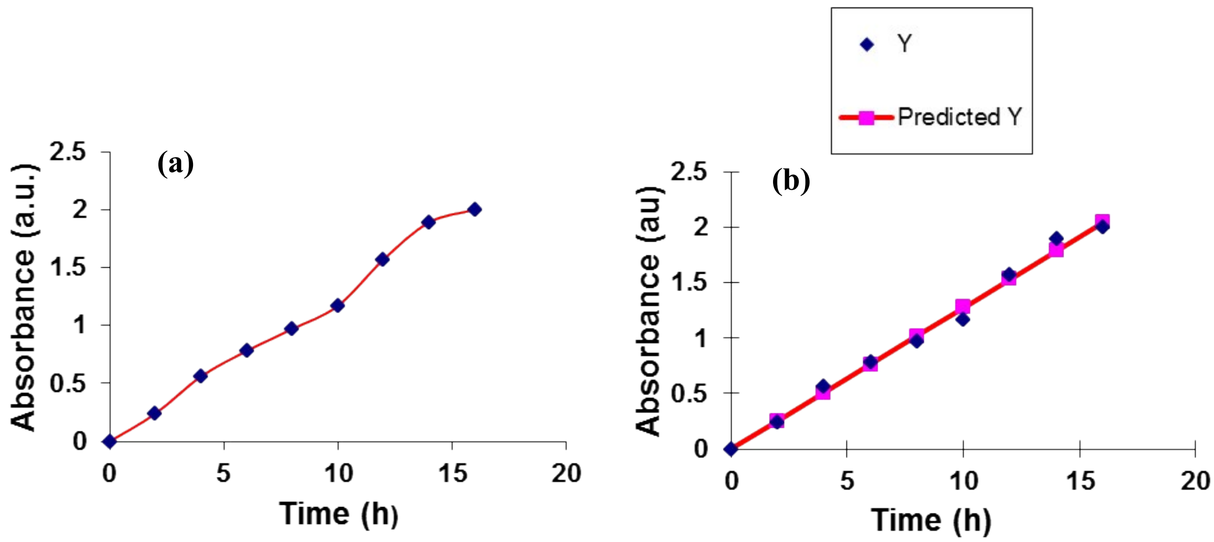

Figure S18: (a) Kinetic profile showing the formation of product with time when the catalyst loading is 0.004 mol, (b) calibration curve. Reactions were monitored by UV-vis. Spectroscopy.

Multiple R= 0.996
R^2 = 0.992
Slope = 0.128
Rate = (2.303×0.128)/3600 = 0.818×10^{-4} sec^{-1}

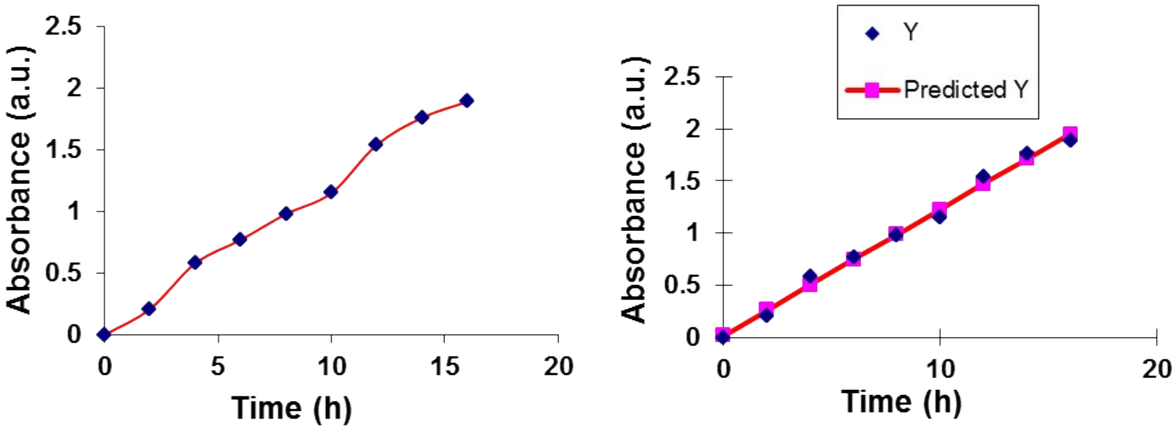

Figure S19: (a) Kinetic profile showing the formation of product with time when the catalyst loading is 0.0035 mol, (b) calibration curve. Reactions were monitored by UV-vis. Spectroscopy.

Multiple R= 0.996
$R^2 = 0.992$
Slope = 0.120
Rate = $(2.303\times0.120)/3600 = 0.767\times10^{-4}$ sec^{-1}

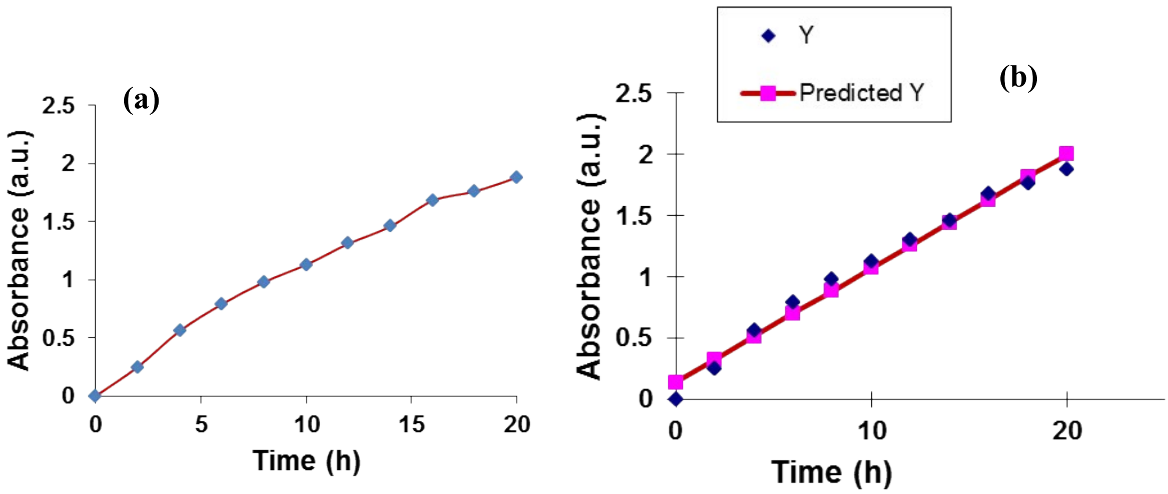

Figure S20: (a) Kinetic profile showing the formation of product with time when the catalyst loading is 0.0025 mol, (b) calibration curve. Reactions were monitored by UV-vis. spectroscopy.

Multiple R= 0.9901
$R^2 = 0.981$
Slope = 0.093
Rate = $(2.303\times0.093)/3600 = 0.59\times10^{-4}$ sec^{-1}

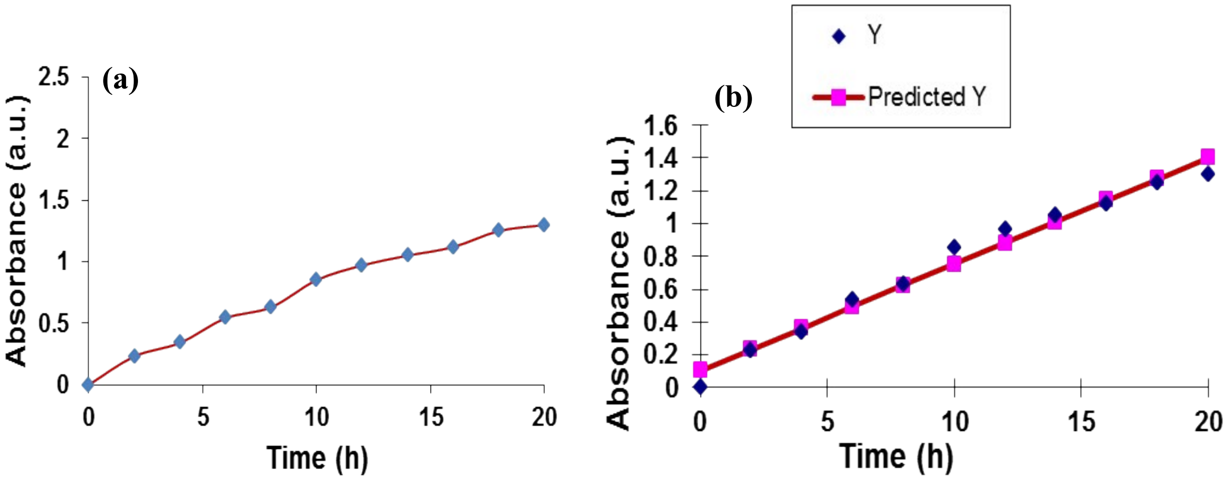

Figure S21: (a) Kinetic profile showing the formation of product with time when the catalyst loading is 0.0015 mol, (b) calibration curve. Reactions were monitored by UV-vis. Spectroscopy.

Multiple R= 0.988
R^2 = 0.977
Slope = 0.064
Rate = (2.303×0.064)/3600 = 0.409×10^{-4} sec^{-1}

(a) Sonogashira cross coupling reaction

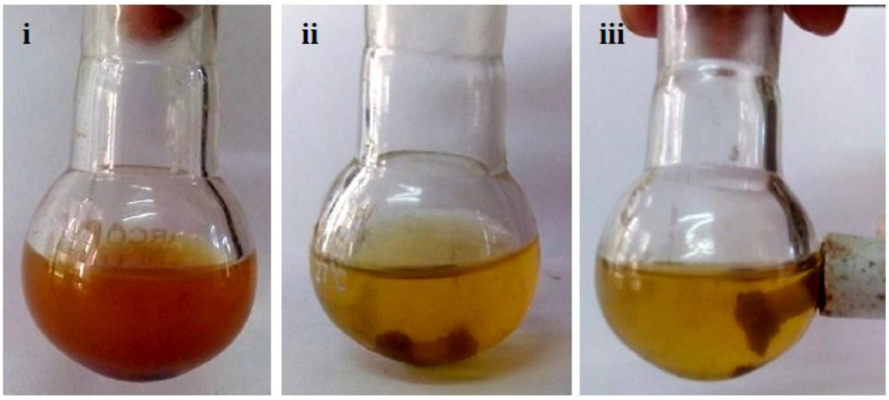

(a) Hetero-Diels-Alder reaction

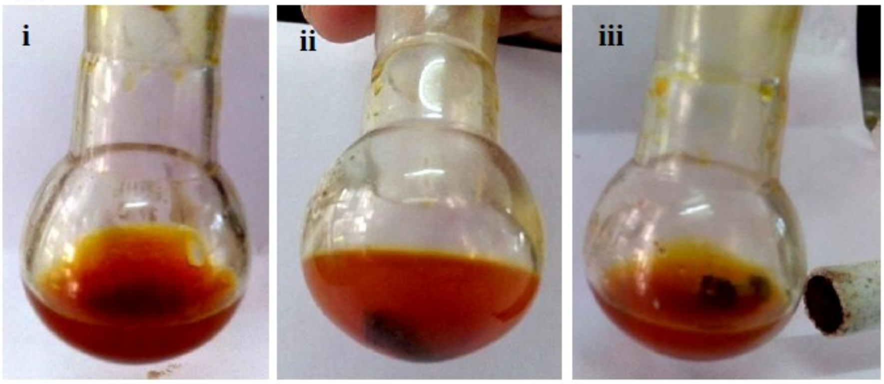

Figure S22: α-Fe_2O_3 nanoparticles (a) for Sonogashira cross coupling reaction i) dispersed in the reaction mixture, ii) adsorbed on a magnetic stirring bar, iii) an external magnet attracted stirring bar and α-Fe_2O_3 nanoparticles; (b) for Hetero-Diels-Alder reaction i) dispersed in the reaction mixture, ii) adsorbed on a magnetic stirring bar, iii) an external magnet attracted stirring bar and α-Fe_2O_3 nanoparticles.

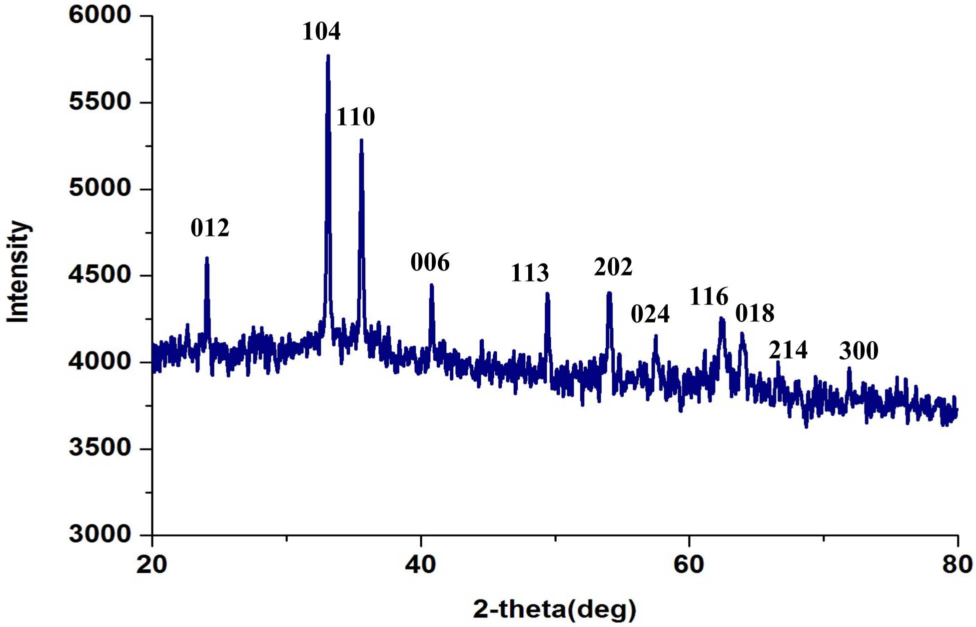

Figure S23: XRD of *in situ* generated rod like α-Fe_2O_3 NPs separated after 13 cycles recycling.

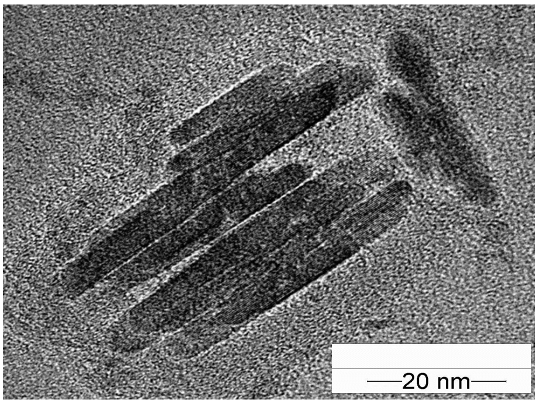

Figure S24: TEM image of *in situ* generated rod like α-Fe_2O_3 NPs separated after 13 cycles.

SpectrAA Report. **13:23 21-08-2015** **Page 1**

Analyst	
Date Started	12:44 21-08-2015 GMT: 07:14 21-08-2015
Worksheet	fe210815
Comment	
Methods	Fe
Computer name	HP-PC
Serial Number:	

Method: Fe (Flame)

Sample ID	Conc mg/L		%RSD	SD	Mean Abs	BG Abs	
CAL ZERO	0.000		62.8	0.0006	-0.0009	0.0010	
	Readings						
	-0.0015	-0.0005	-0.0007		21-08-2015	12:49:34	
		ISF					
		1.0000					
STANDARD 1	5.000		1.9	0.0055	0.2947	0.0010	
	Readings						
	0.2886	0.2963	0.2993		21-08-2015	12:50:14	
		ISF					
		1.0000					
STANDARD 2	10.000		0.4	0.0022	0.5006	0.0027	
	Readings						
	0.5022	0.4981	0.5016		21-08-2015	12:50:48	
		ISF					
		1.0000					
STANDARD 3	15.000		1.0	0.0066	0.6595	0.0044	
	Readings						
	0.6563	0.6552	0.6671		21-08-2015	12:51:16	
		1.0000					
Sample 001	0.166		2.7	0.0003	0.0098	0.0418	
	Readings						
	0.0098	0.0096	0.0101		21-08-2015	12:57:40	
		ISF					
		1.0000					

Figure S25: Atomic Absorption Studies (AAS) of the residual liquid left after the magnetic separation of catalyst and found that only 0.166 mg/lit = 0.166 ppm of iron leached into the solution.

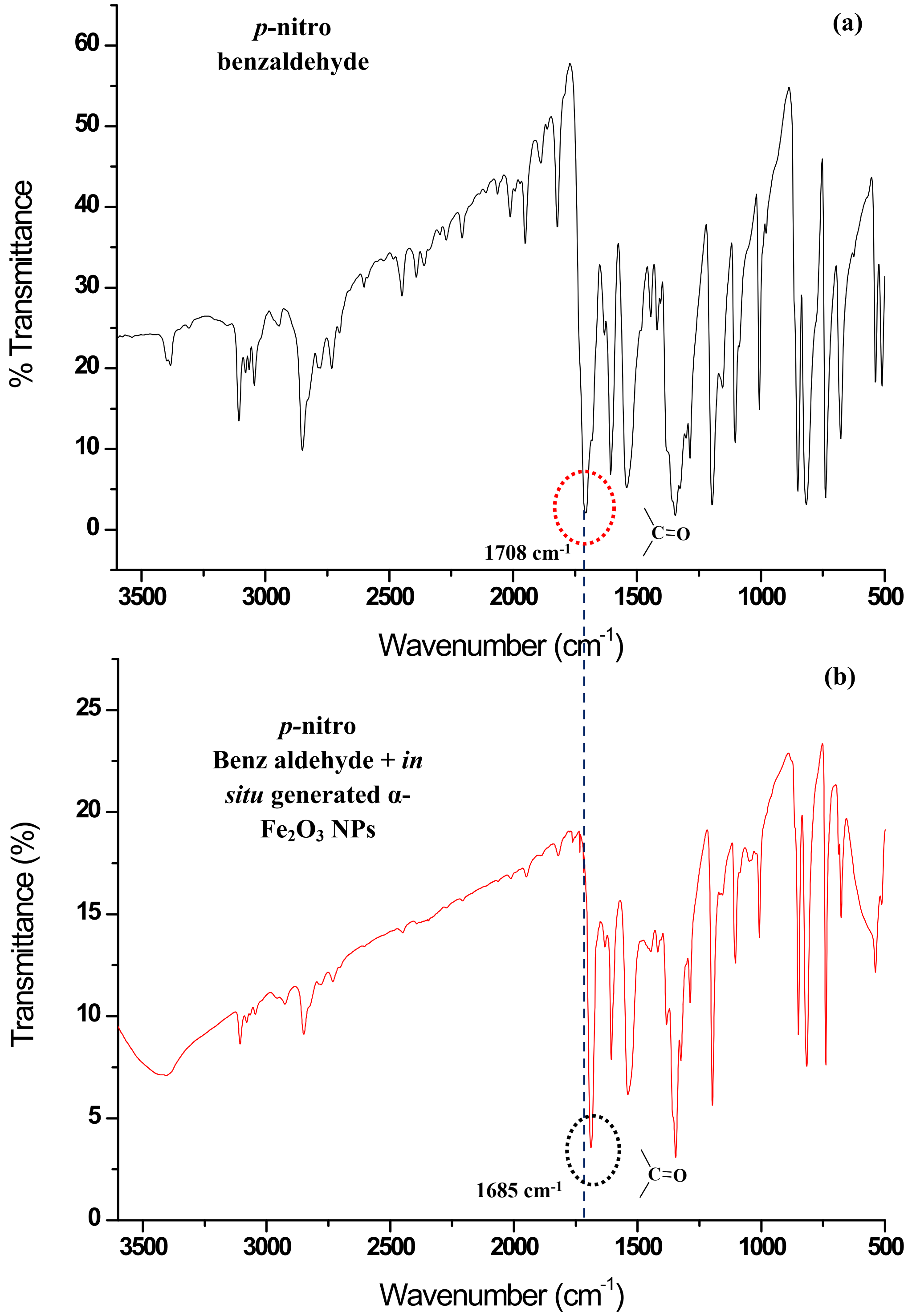

Figure S26: IR spectra of (a) *p*-nitrobenzaldehyde; (b) separated reaction mixture containing *p*-nitrobenzaldehyde and α-Fe_2O_3 NPs.

Fig. S27A: ^{1}H NMR Spectra ($CDCl_3$, 500 MHz, ppm) of compound 4a:

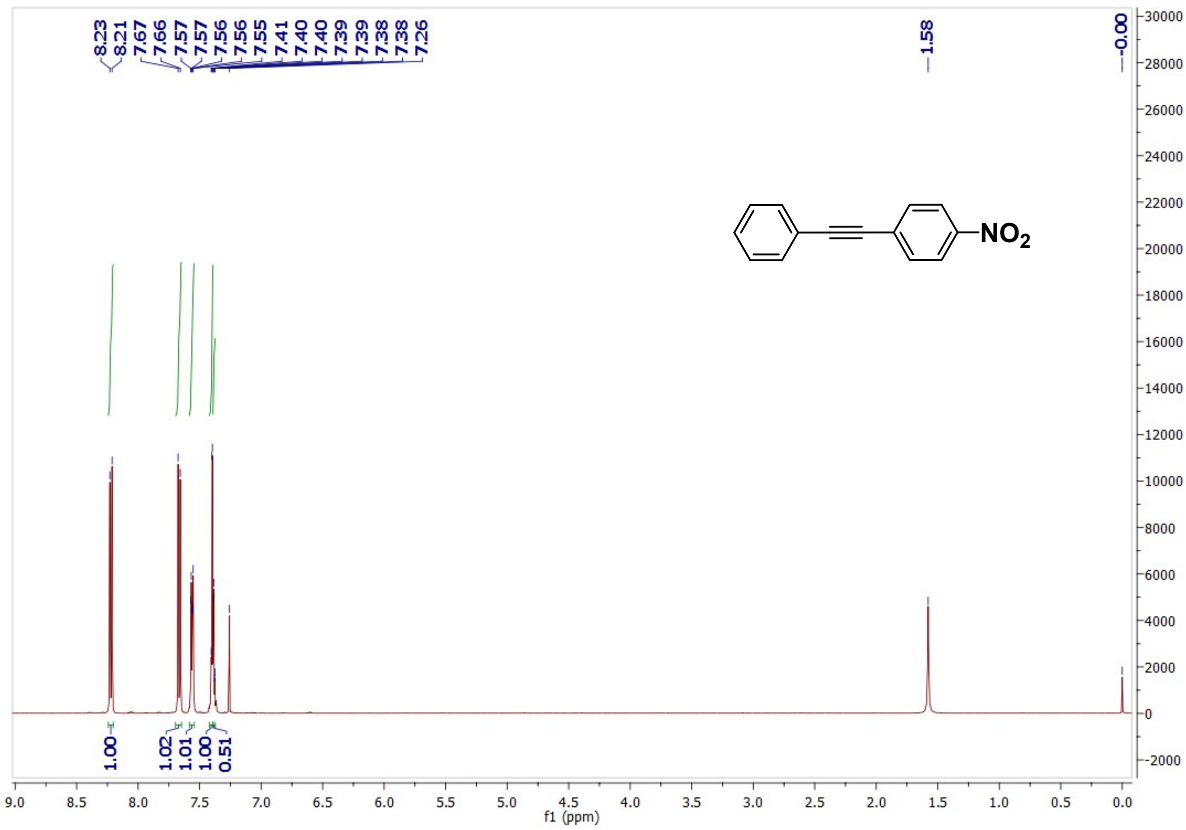

Fig. S27B: ^{13}C NMR Spectra ($CDCl_3$, 125 MHz, ppm) of compound 4a:

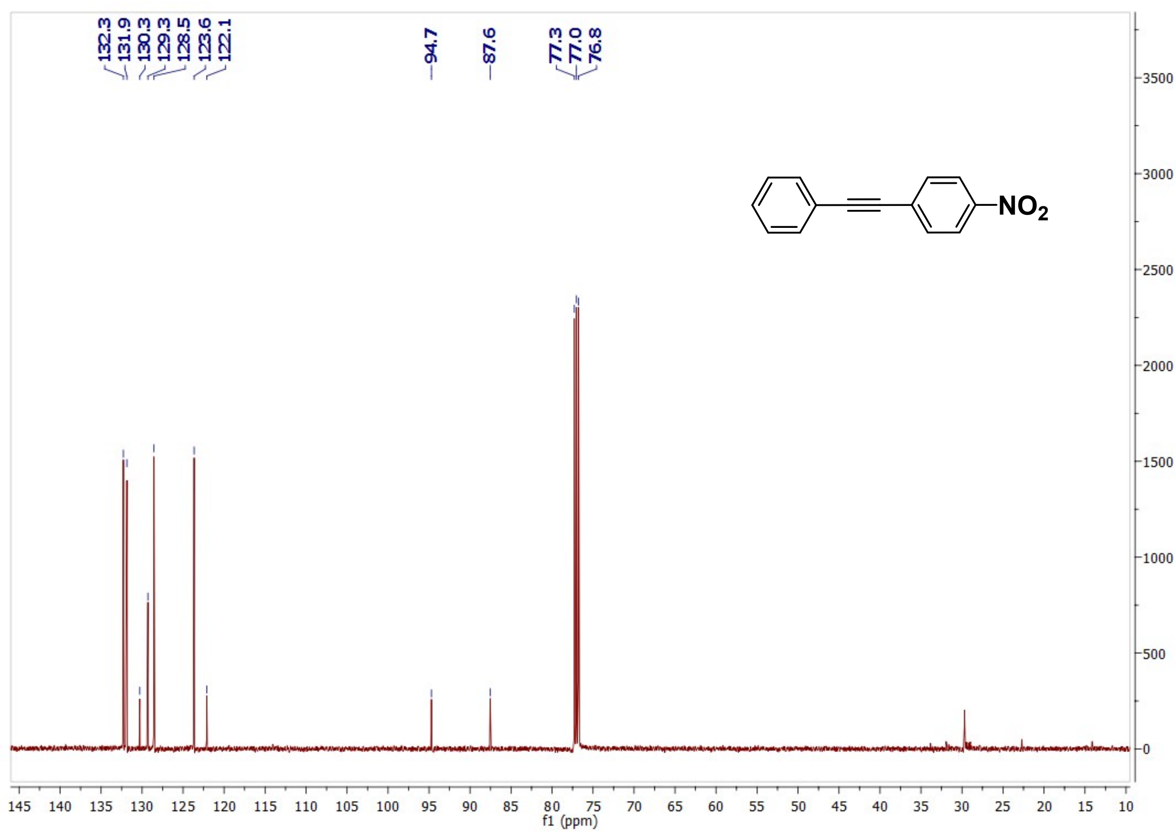

Fig. S28A: ^{1}H NMR Spectra ($CDCl_3$, 500 MHz, ppm) of compound 4b & 4c:

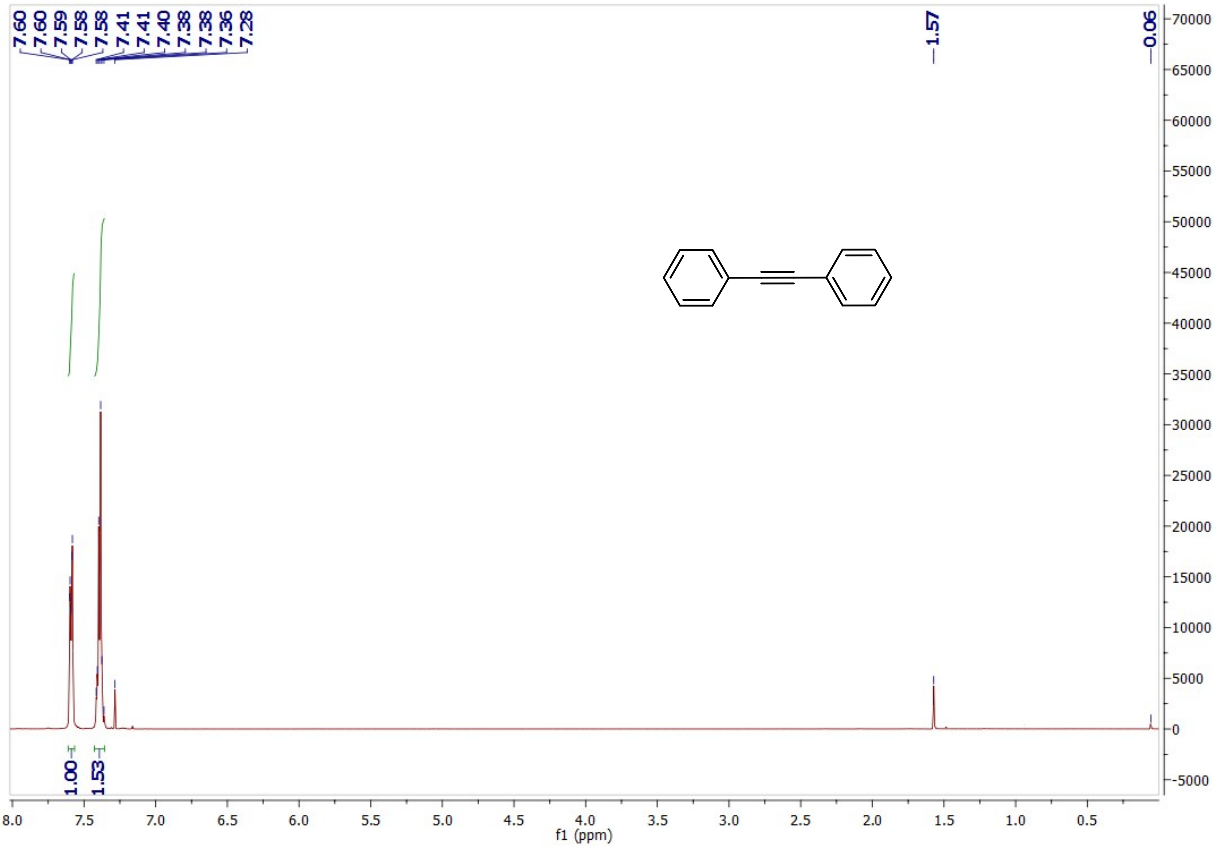

Fig. S28B: ^{13}C NMR Spectra ($CDCl_3$, 125 MHz, ppm) of compound 4b & 4c:

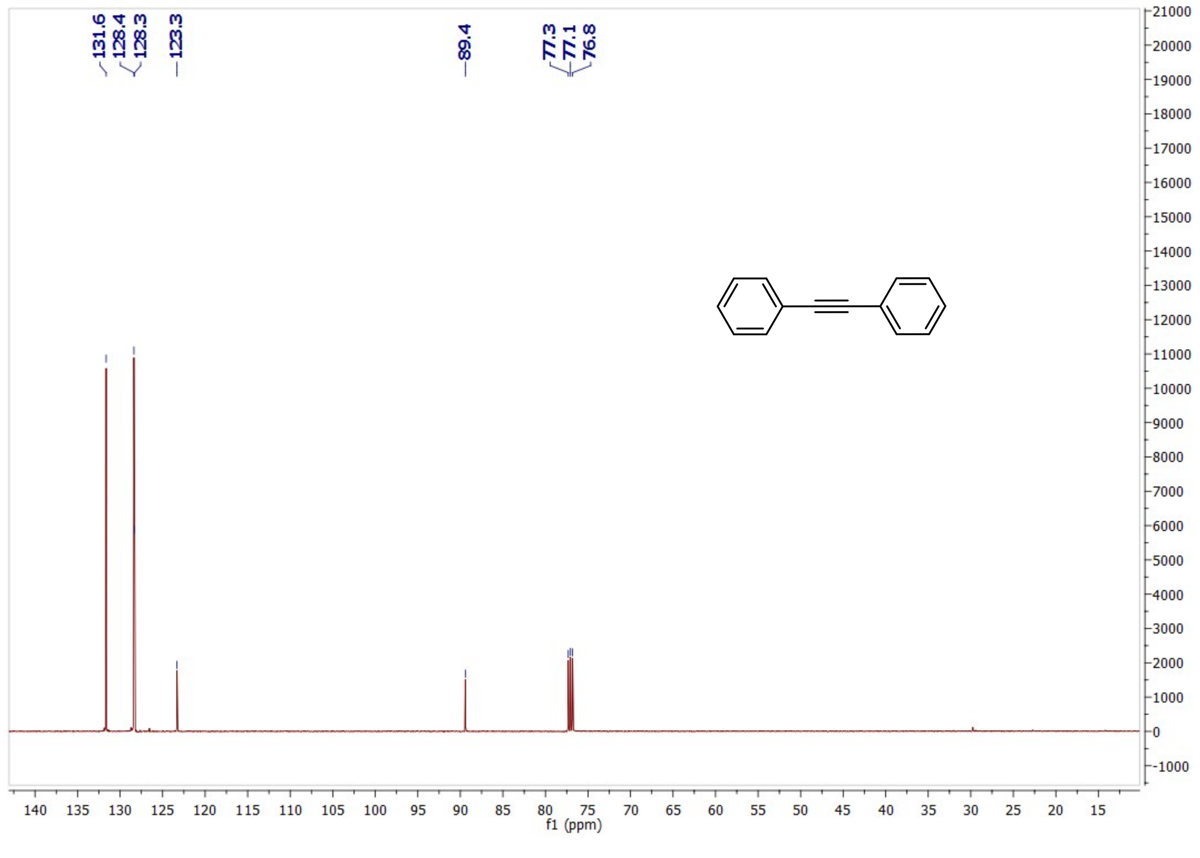

Fig. S29A: ^{1}H NMR Spectra ($CDCl_3$, 500 MHz, ppm) of compound 4d:

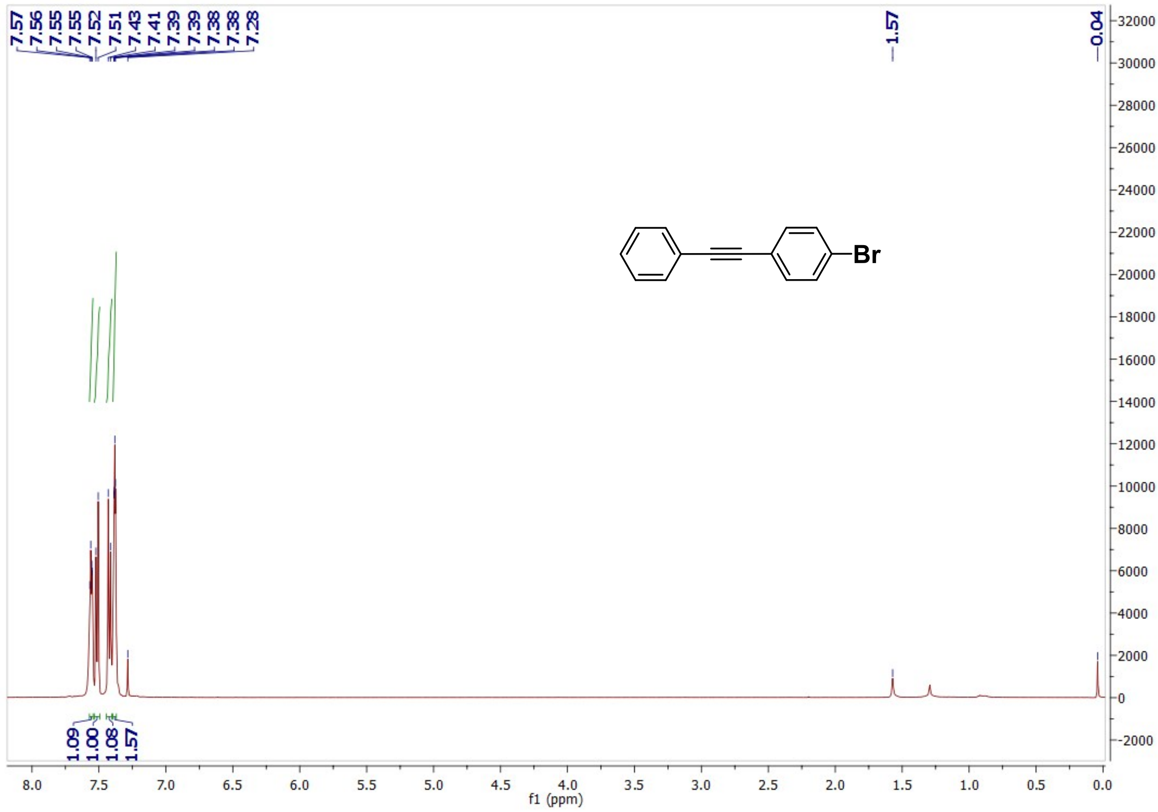

Fig. S29B: ^{13}C NMR Spectra ($CDCl_3$, 125 MHz, ppm) of compound 4d:

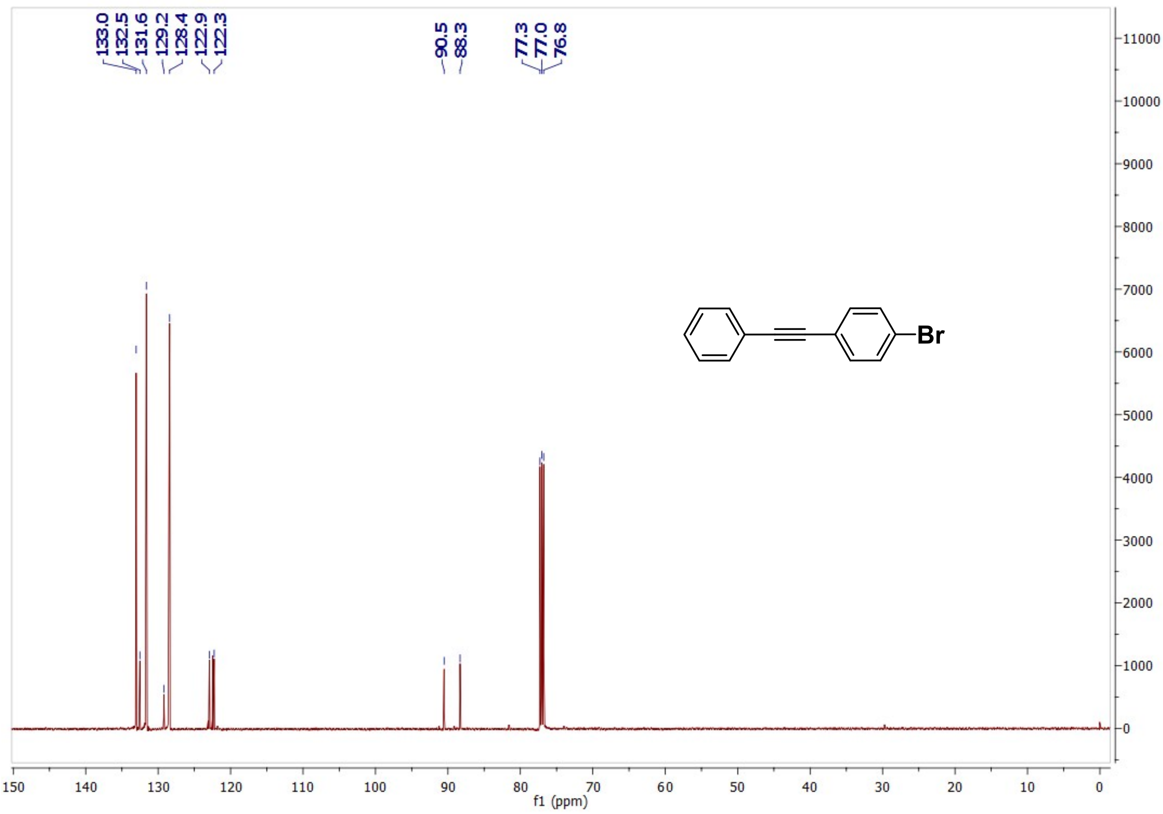

Fig. S30A: ^{1}H NMR Spectra ($CDCl_3$, 300 MHz, ppm) of compound 4e:

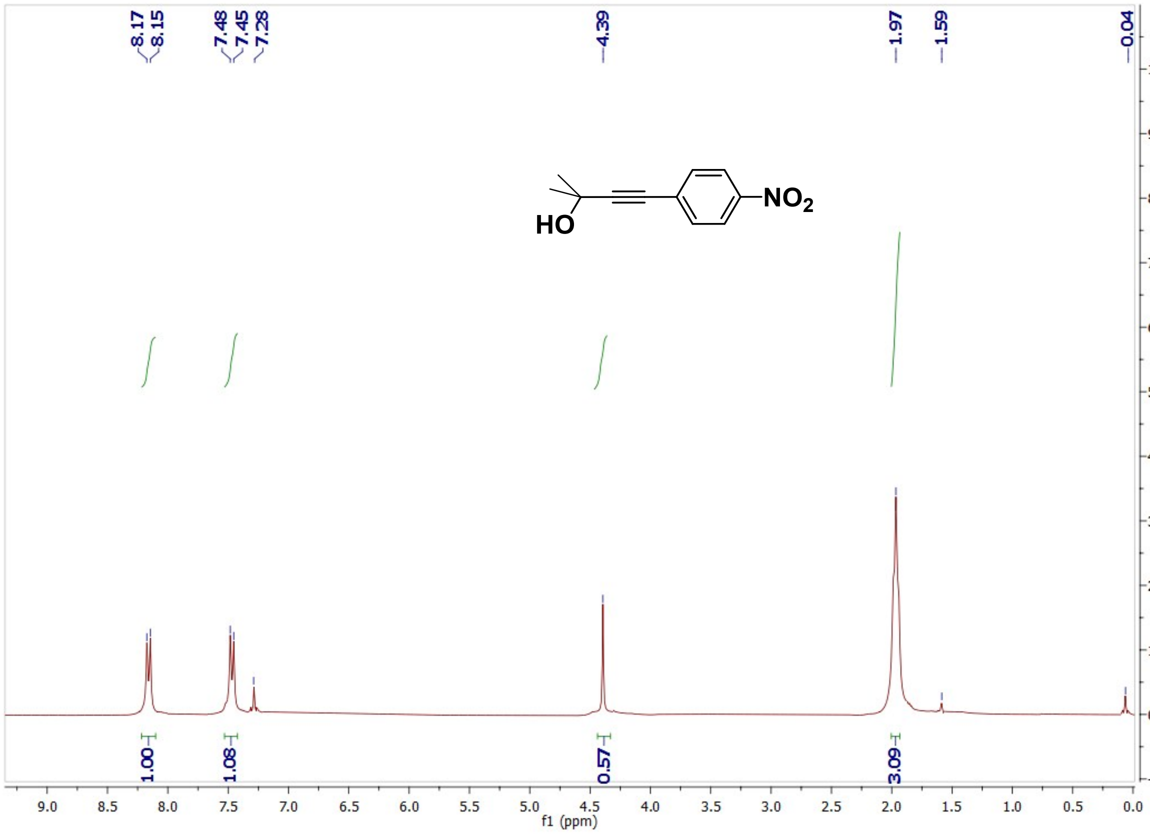

Fig. S30B: ^{13}C NMR Spectra ($CDCl_3$, 75 MHz, ppm) of compound 4e:

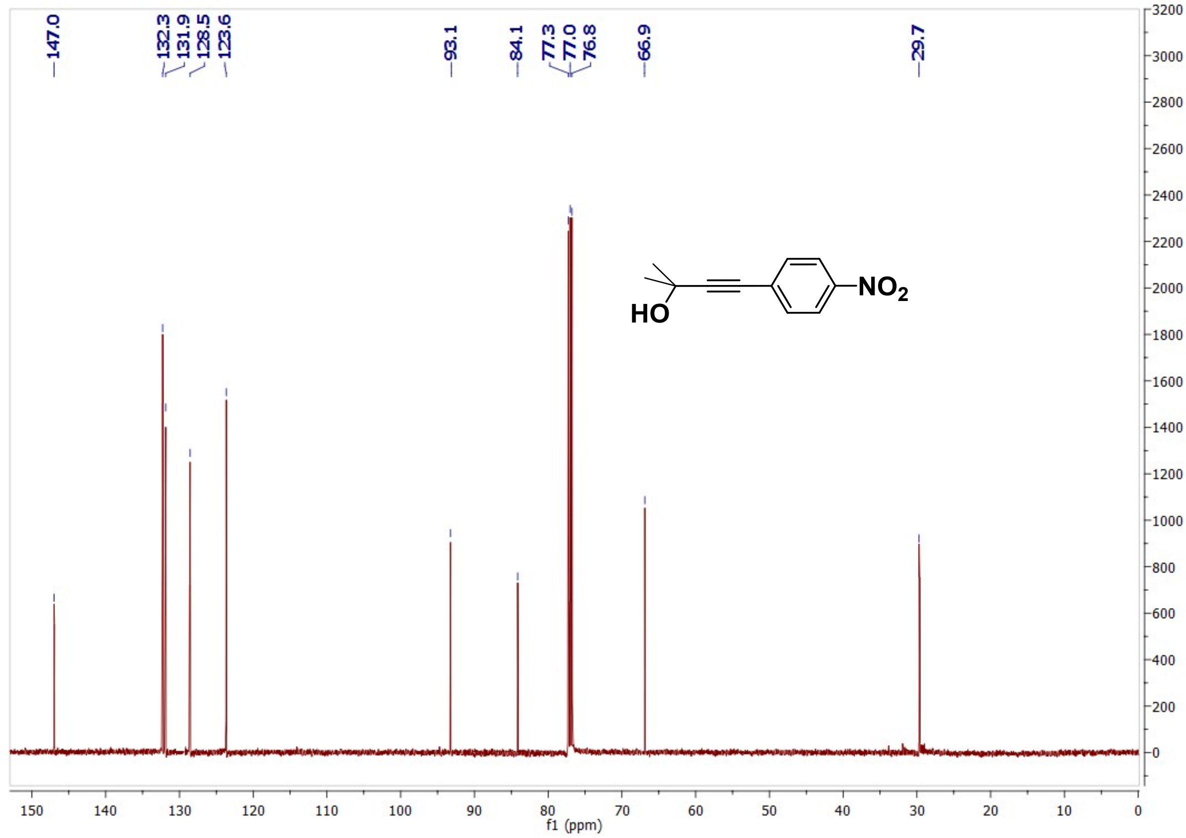

Fig. S31A: ^{1}H NMR Spectra ($CDCl_3$, 300 MHz, ppm) of compound 4f:

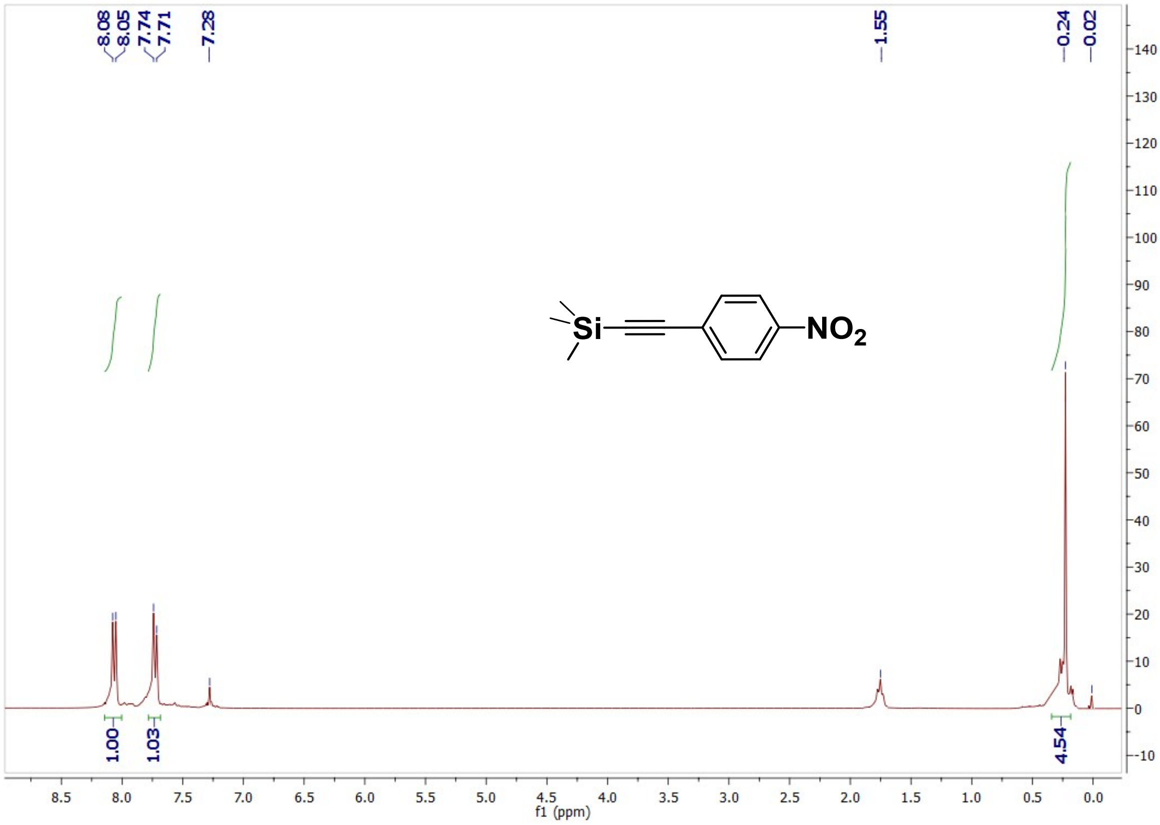

Fig. S31B: ^{13}C NMR Spectra ($CDCl_3$, 75 MHz, ppm) of compound 4f:

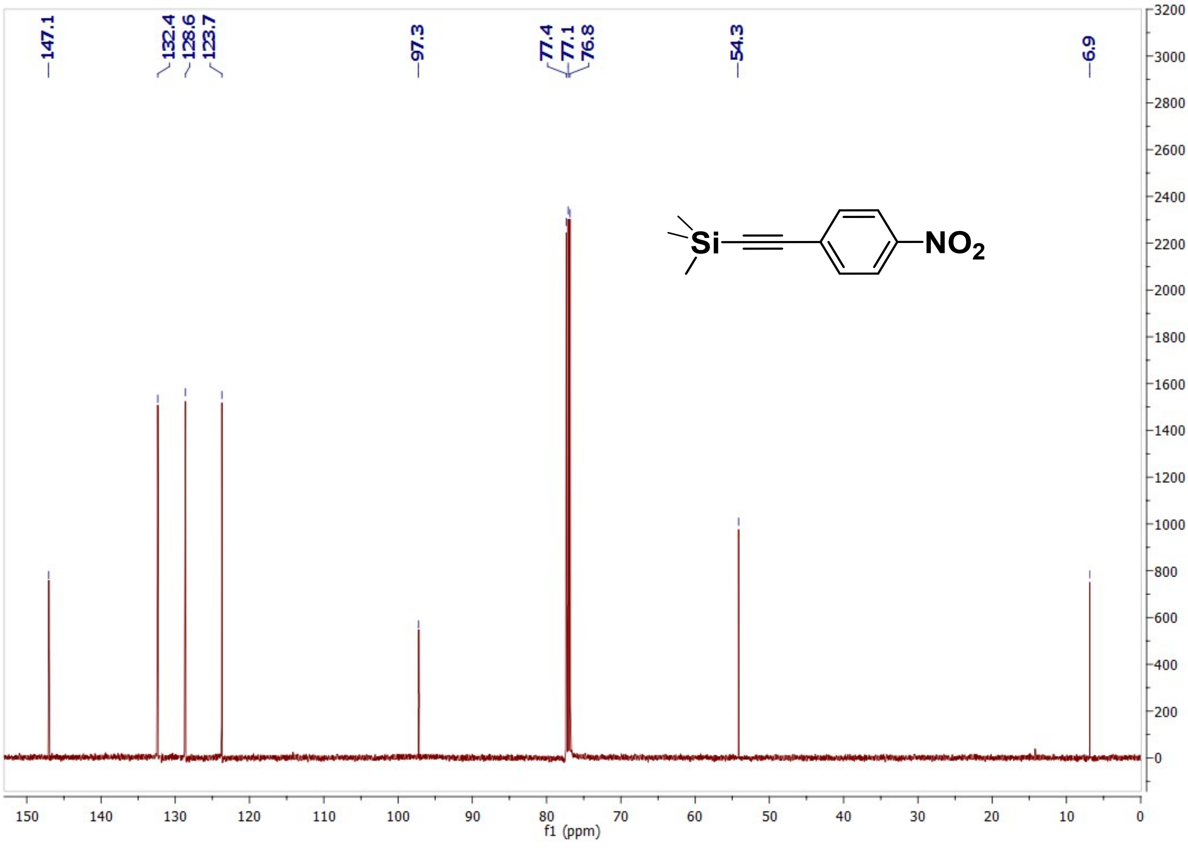

Fig. S32A: ^{1}H NMR Spectra ($CDCl_3$, 500 MHz, ppm) of compound 4g:

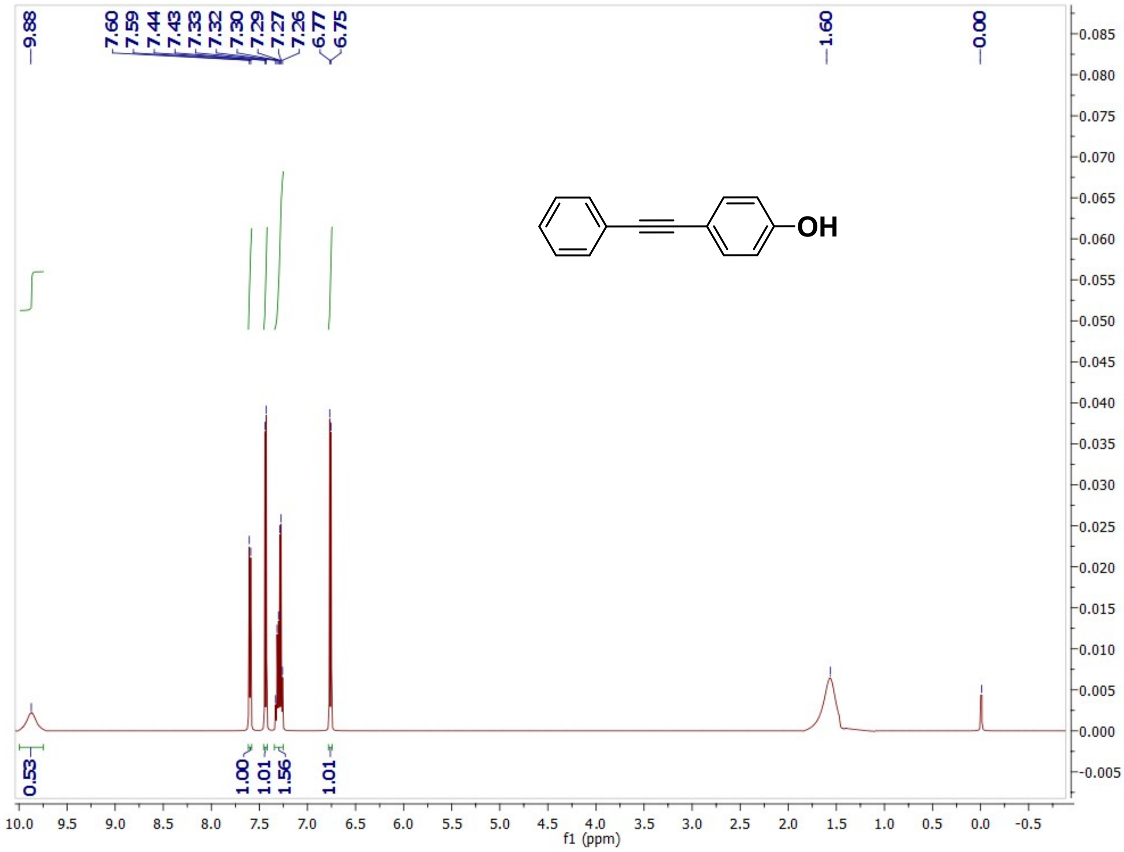

Fig. S32B: ^{13}C NMR Spectra ($CDCl_3$, 125 MHz, ppm) of compound 4g:

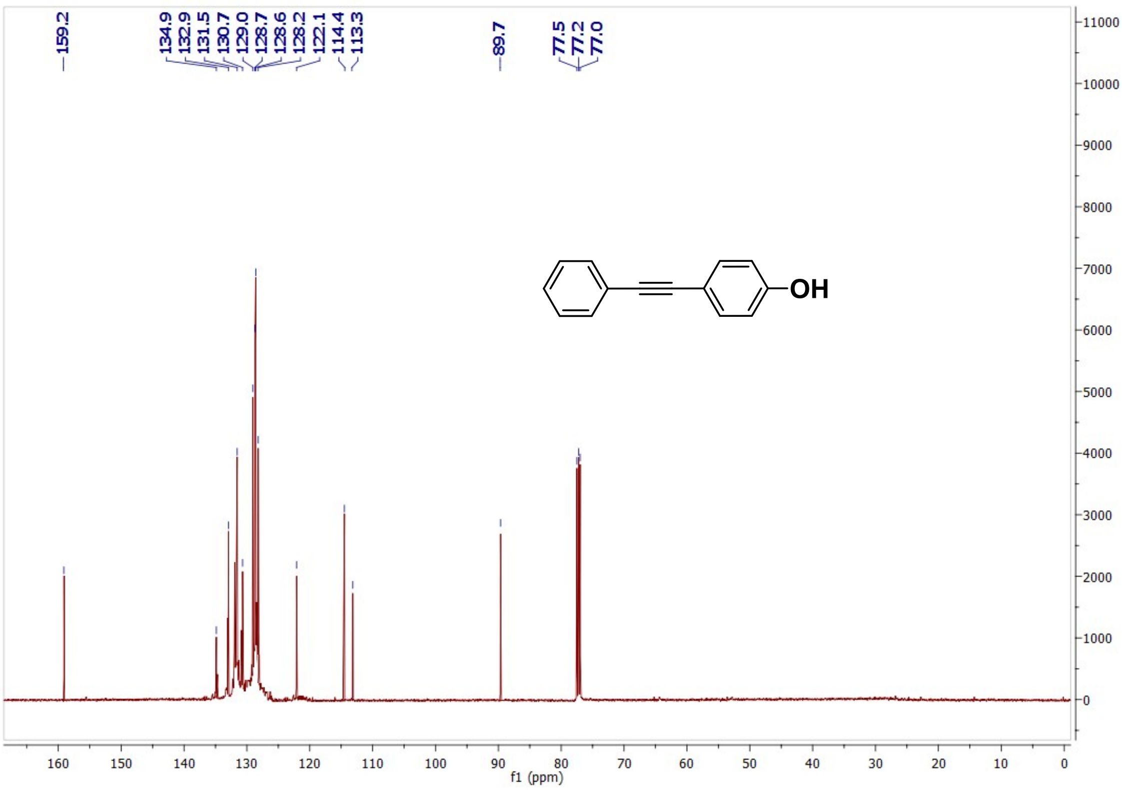

Fig. S33A: ^{1}H NMR Spectra ($CDCl_3$, 500 MHz, ppm) of compound 4h:

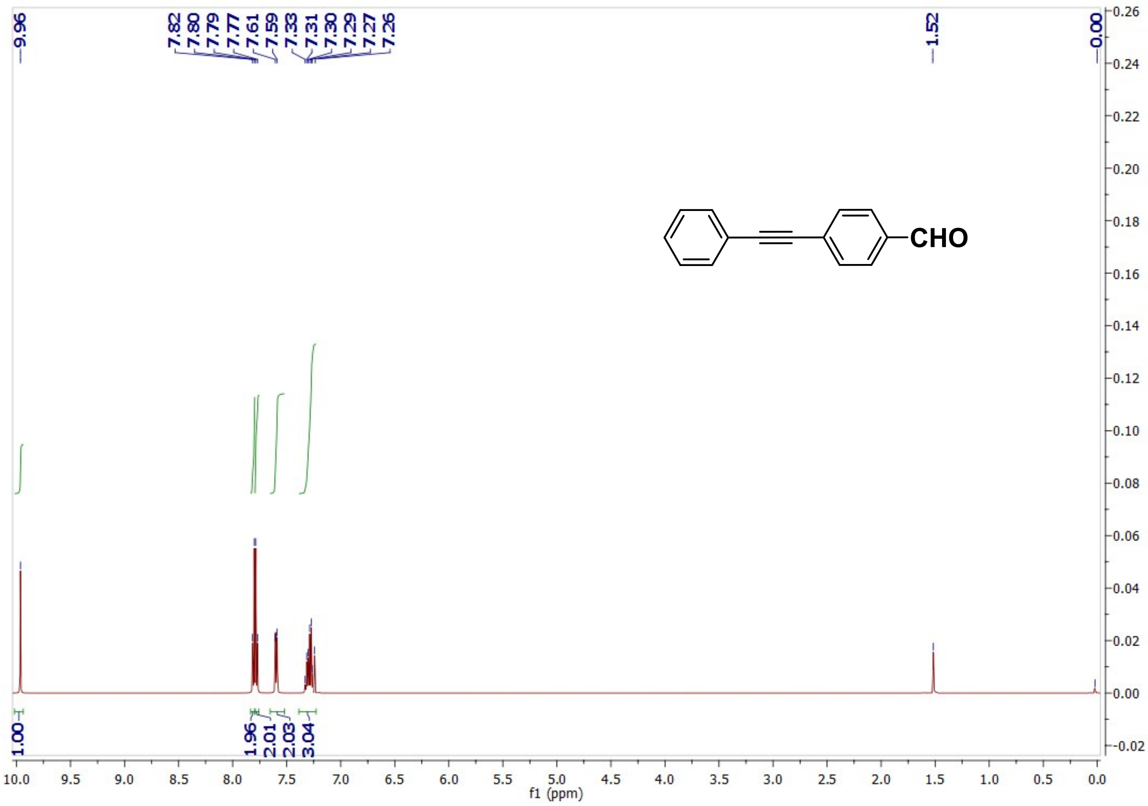

Fig. S33B: ^{13}C NMR Spectra ($CDCl_3$, 125 MHz, ppm) of compound 4h:

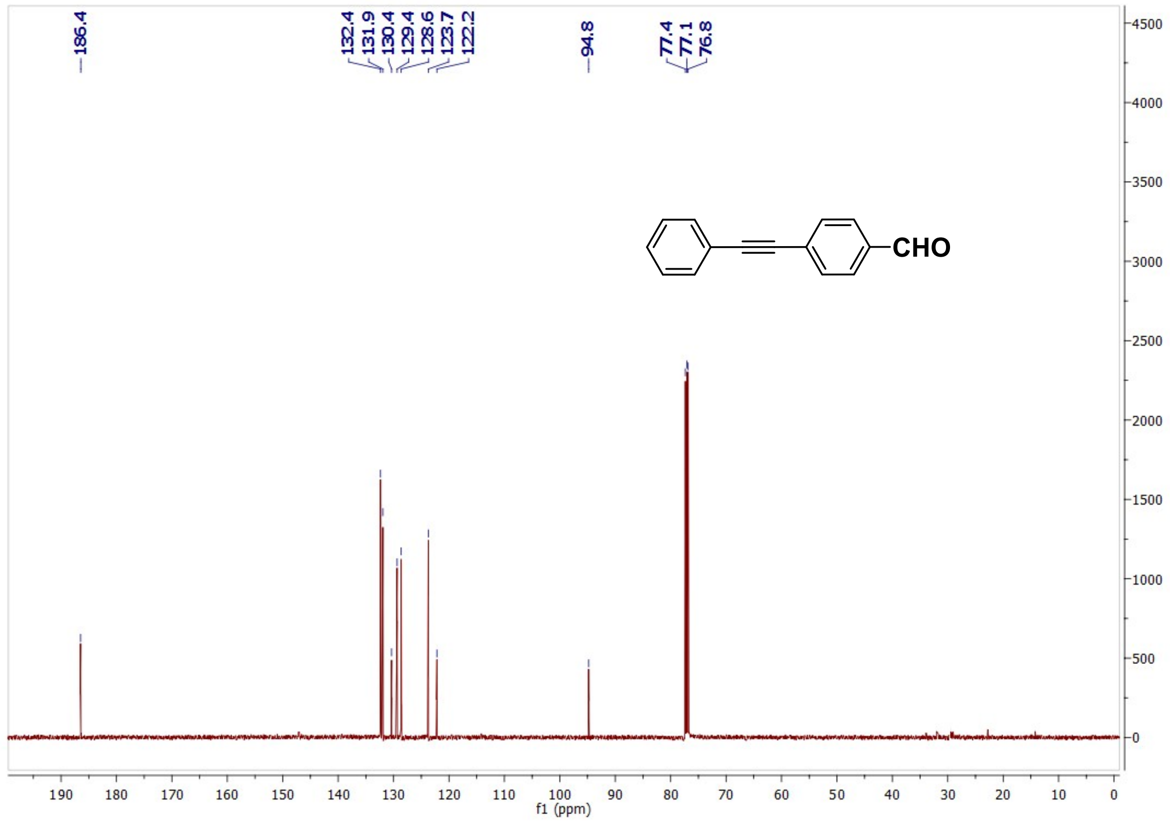

Fig. S34A: ^{1}H NMR Spectra (CDCl$_3$, 300 MHz, ppm) of compound 4i:

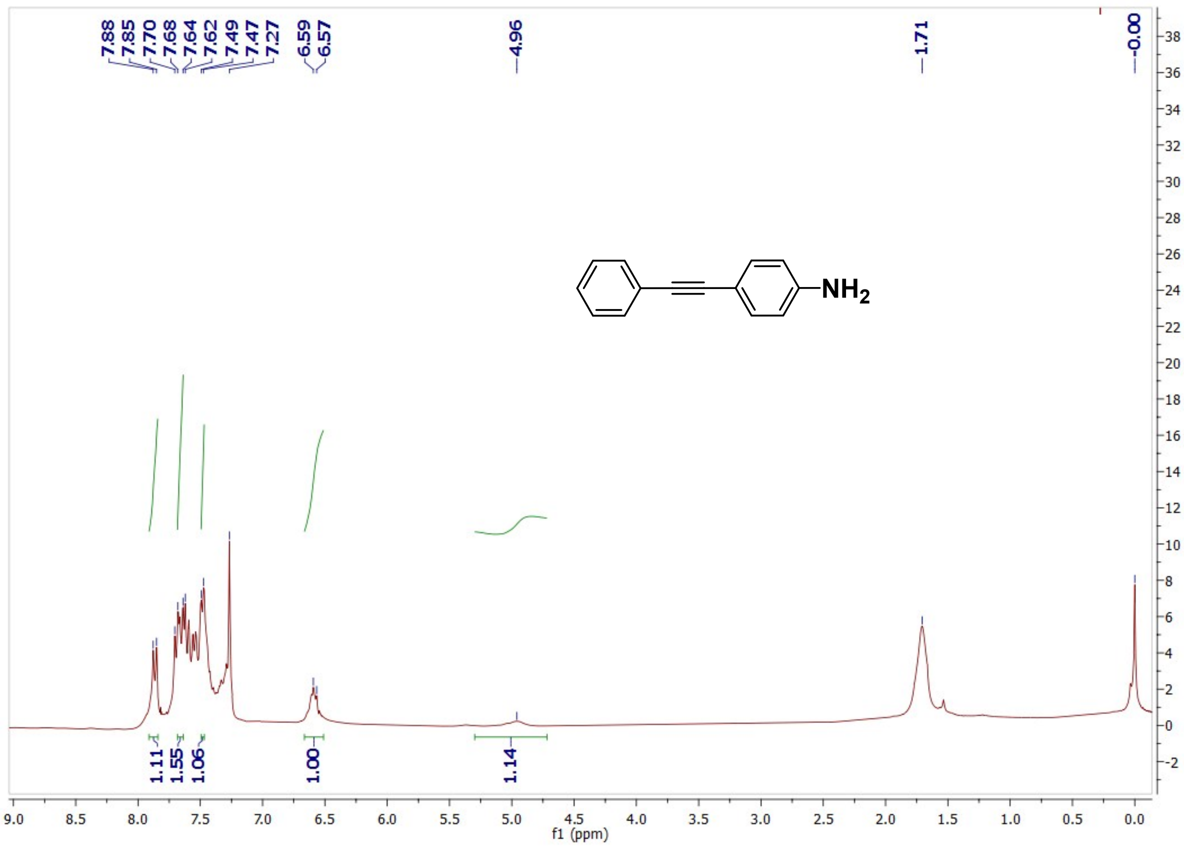

Fig. S34B: ^{13}C NMR Spectra (CDCl$_3$, 75 MHz, ppm) of compound 4i:

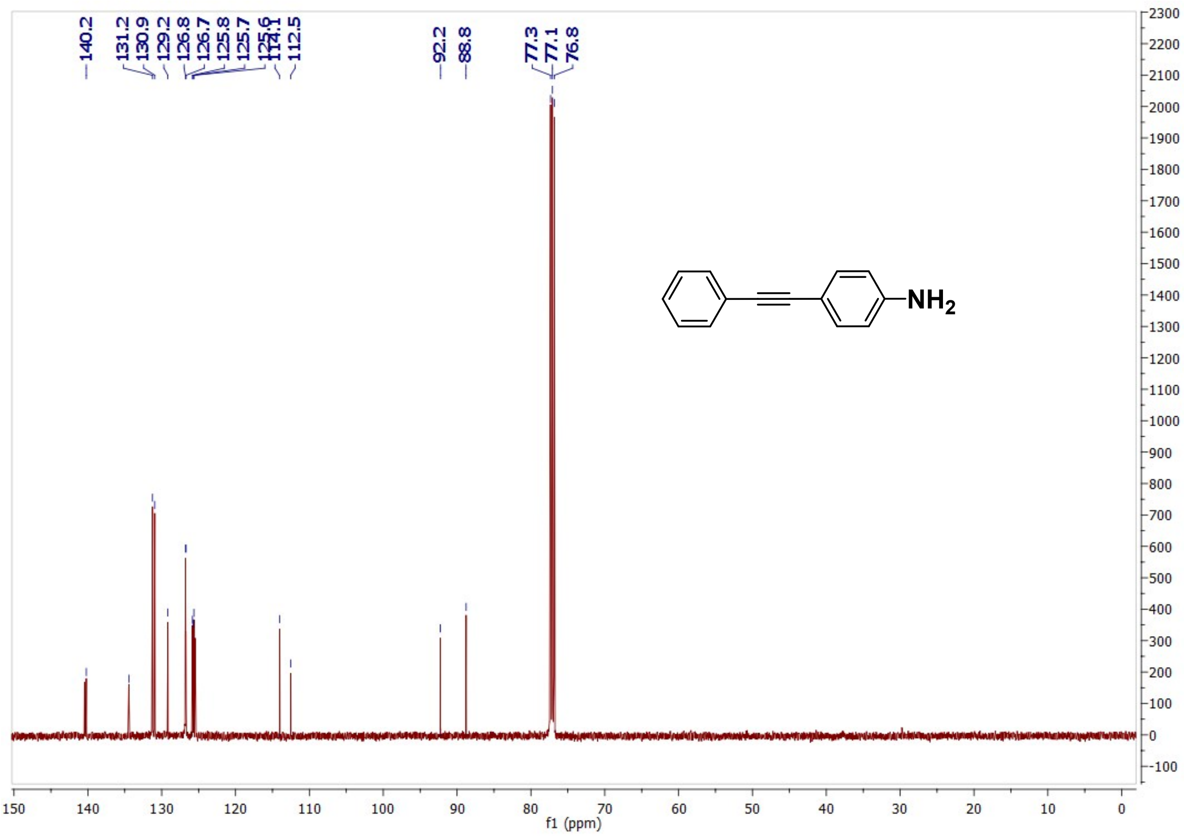

Fig. S35A: ^{1}H NMR Spectra ($CDCl_3$, 300 MHz, ppm) of compound 4j:

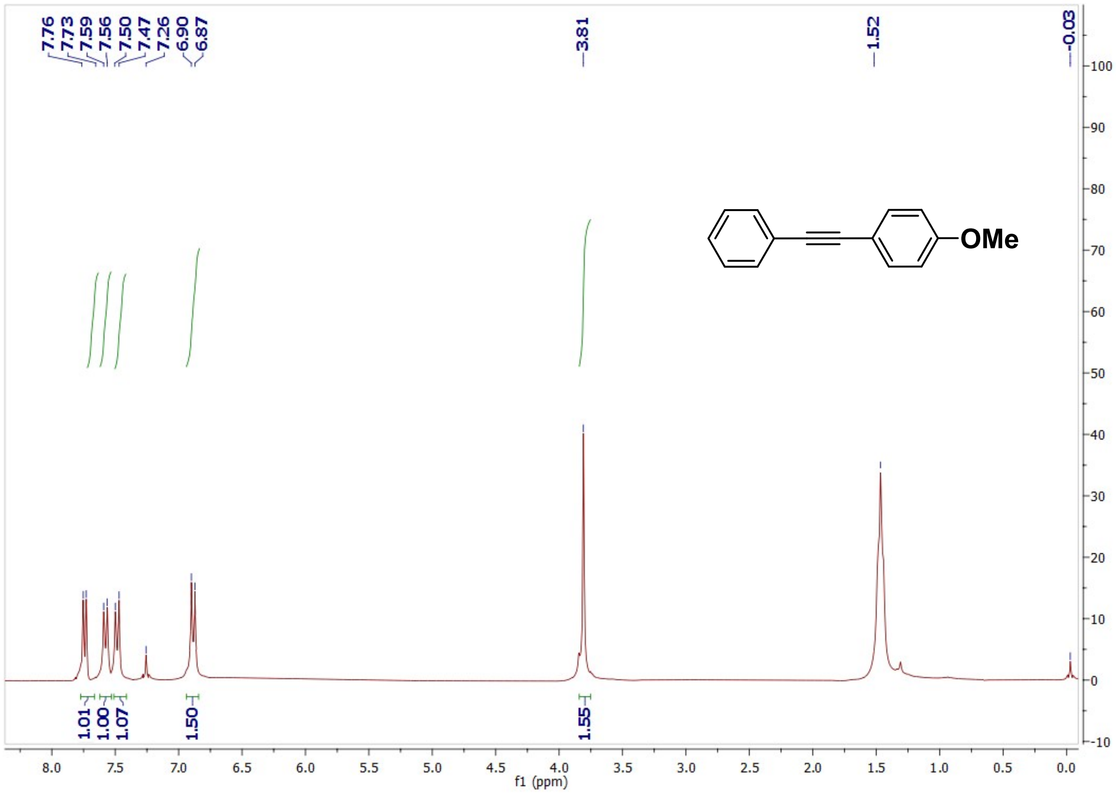

Fig. S35B: ^{13}C NMR Spectra ($CDCl_3$, 75 MHz, ppm) of compound 4j:

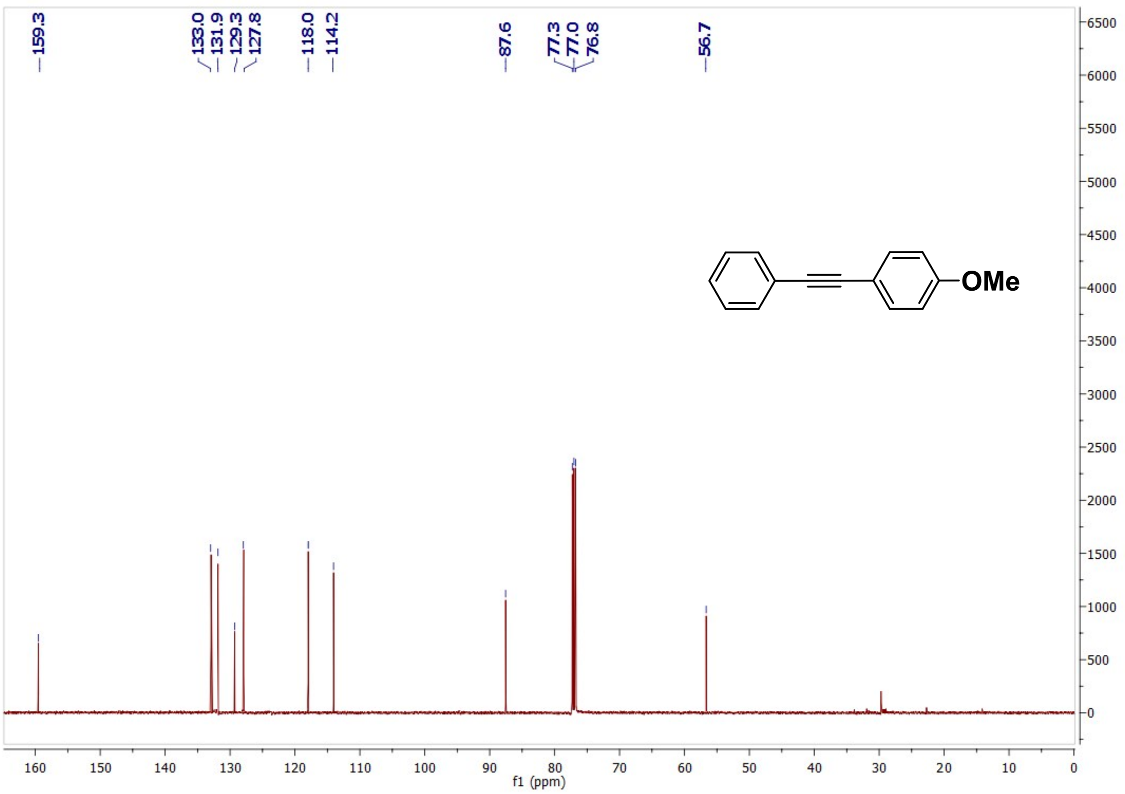

Fig. S36A: ^{1}H NMR Spectra ($CDCl_3$, 300 MHz, ppm) of compound 4k:

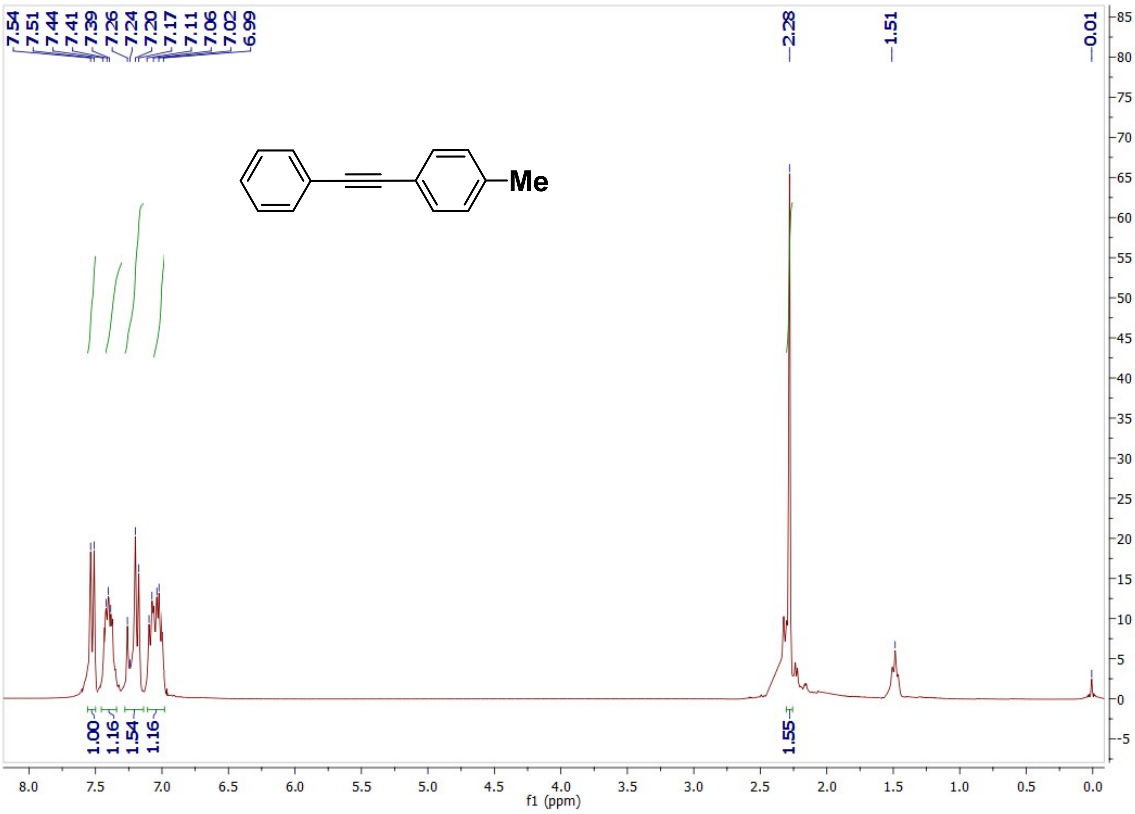

Fig. S36B: ^{13}C NMR Spectra ($CDCl_3$, 75 MHz, ppm) of compound 4k:

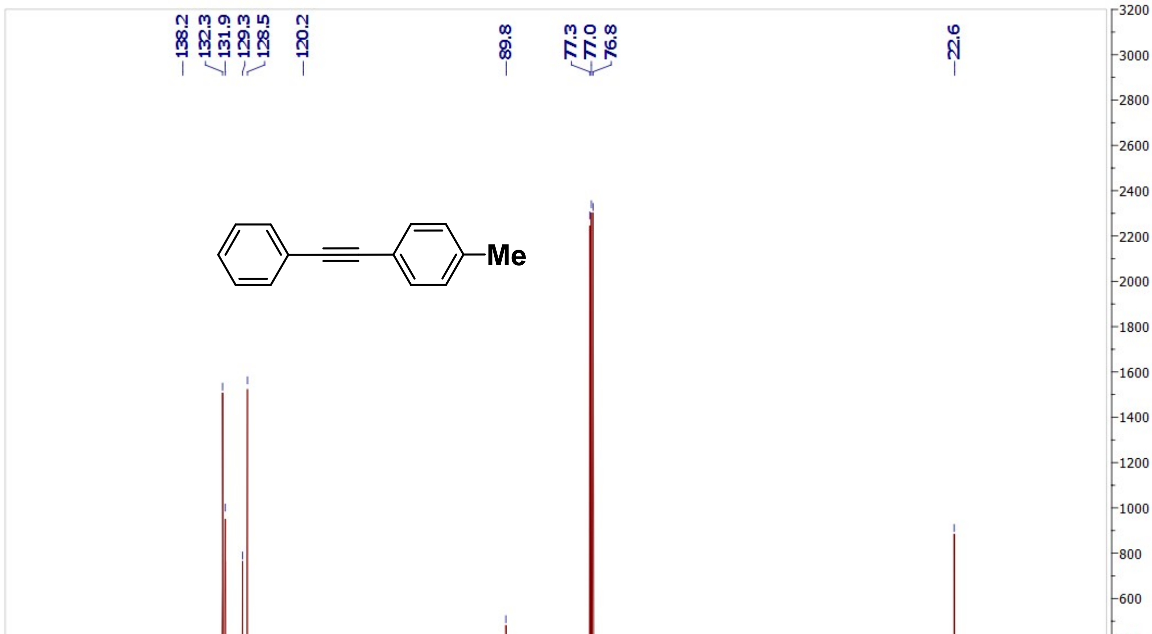

Fig. S37A: ^{1}H NMR Spectra ($CDCl_3$, 500 MHz, ppm) of compound 4l:

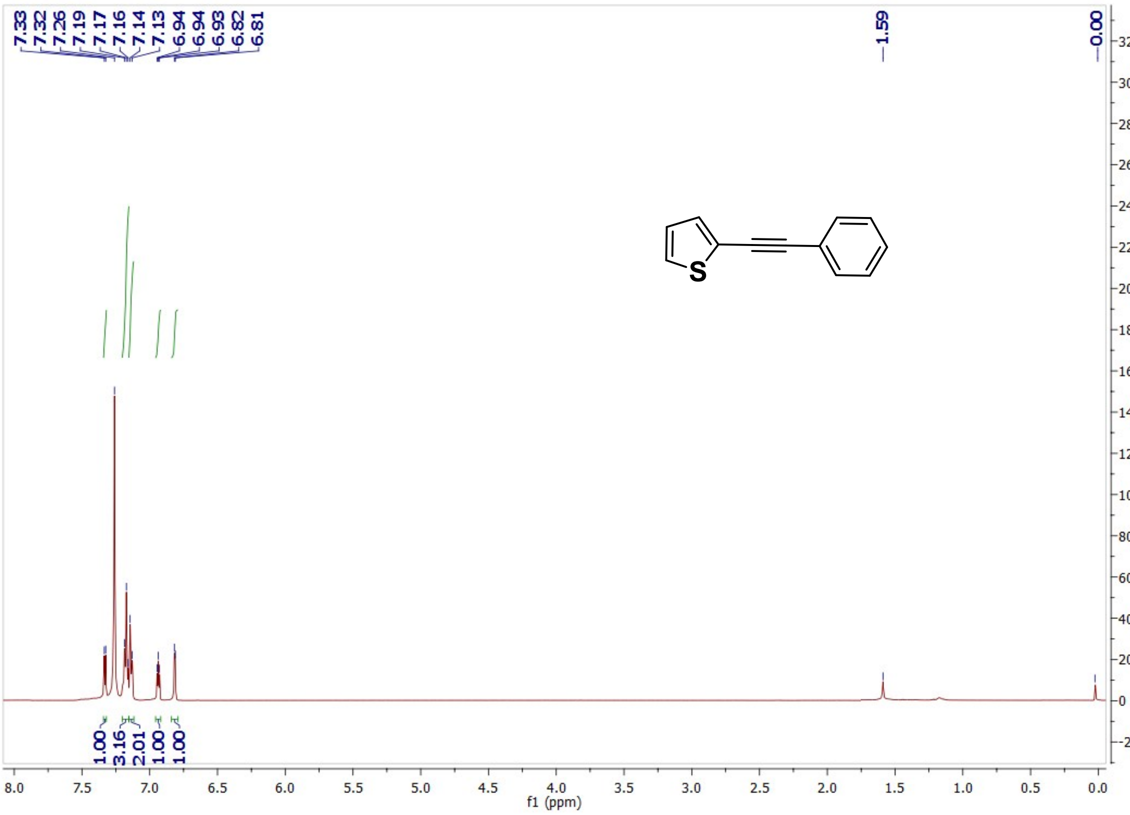

Fig. S37B: ^{13}C NMR Spectra ($CDCl_3$, 125 MHz, ppm) of compound 4l:

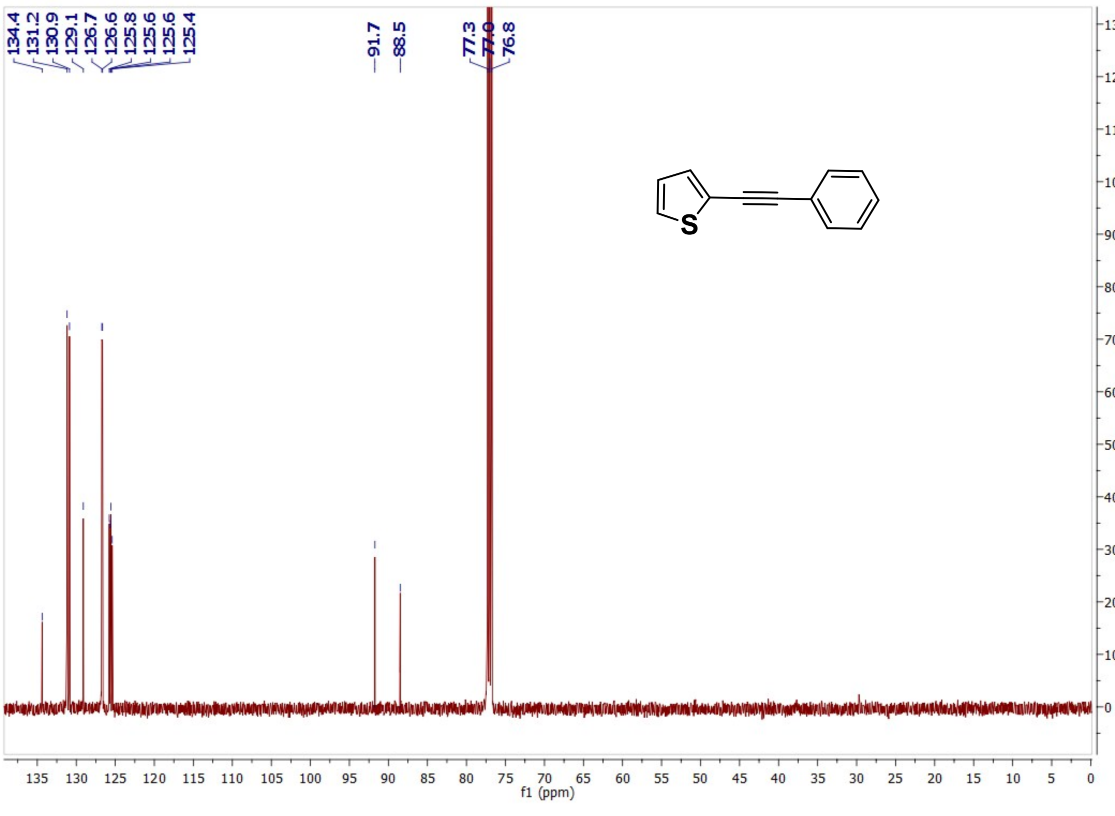

Fig. S38A: ^{1}H NMR Spectra ($CDCl_3$, 500 MHz, ppm) of compound 4m:

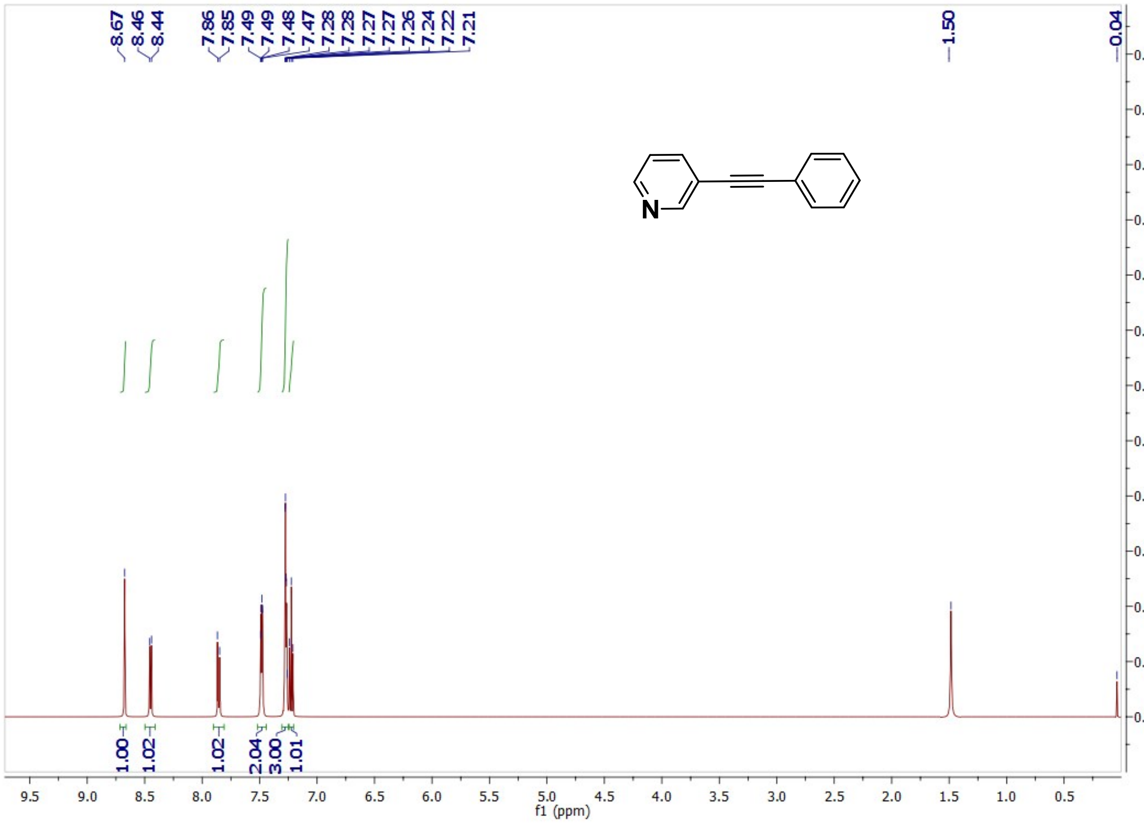

Fig. S38B: ^{13}C NMR Spectra ($CDCl_3$, 125 MHz, ppm) of compound 4m:

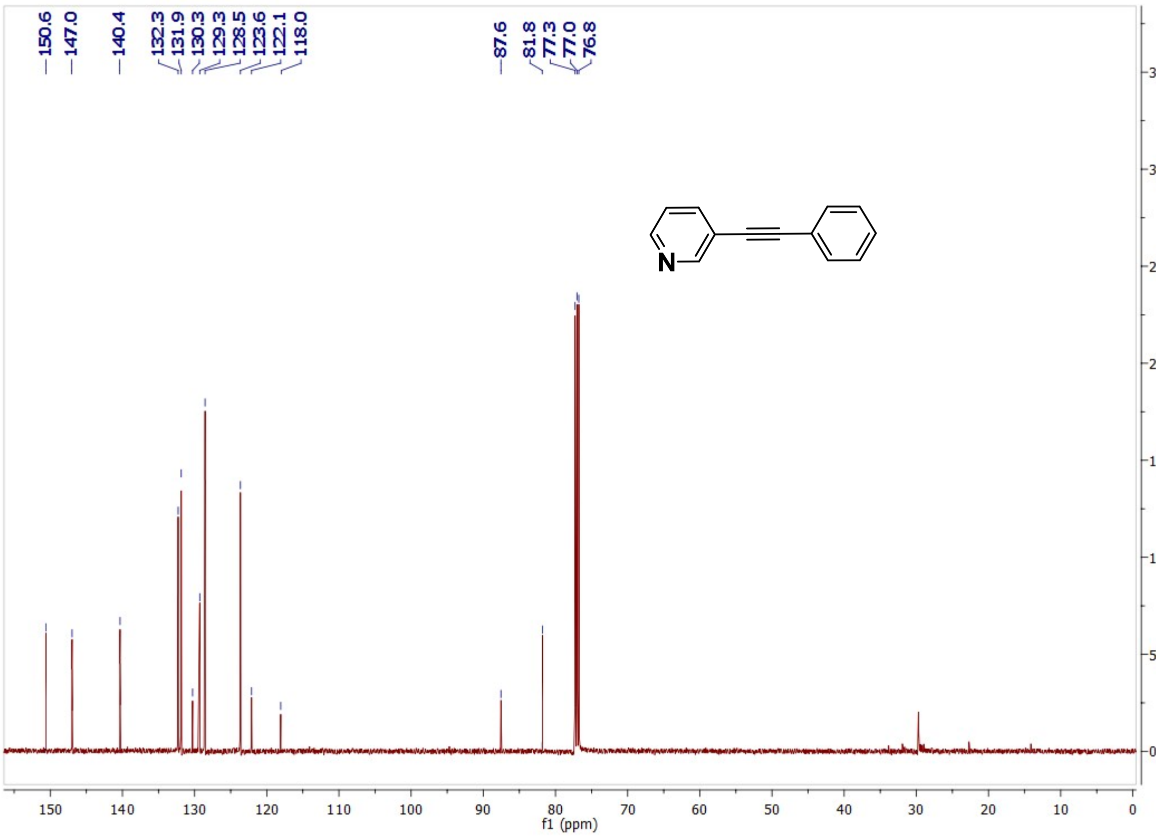

Fig. S39A: ^{1}H NMR Spectra (CDCl$_3$, 500 MHz, ppm) of compound 6:

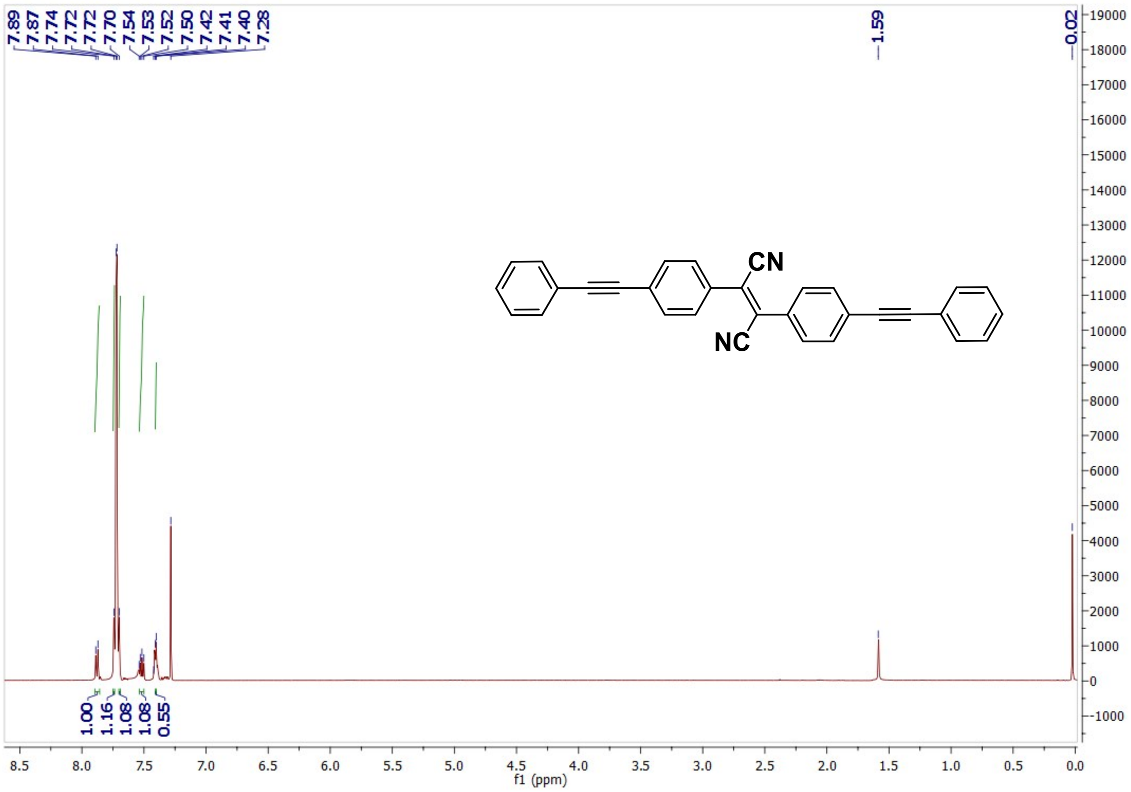

Fig. S39B: ^{13}C NMR Spectra (CDCl$_3$, 125 MHz, ppm) of compound 6:

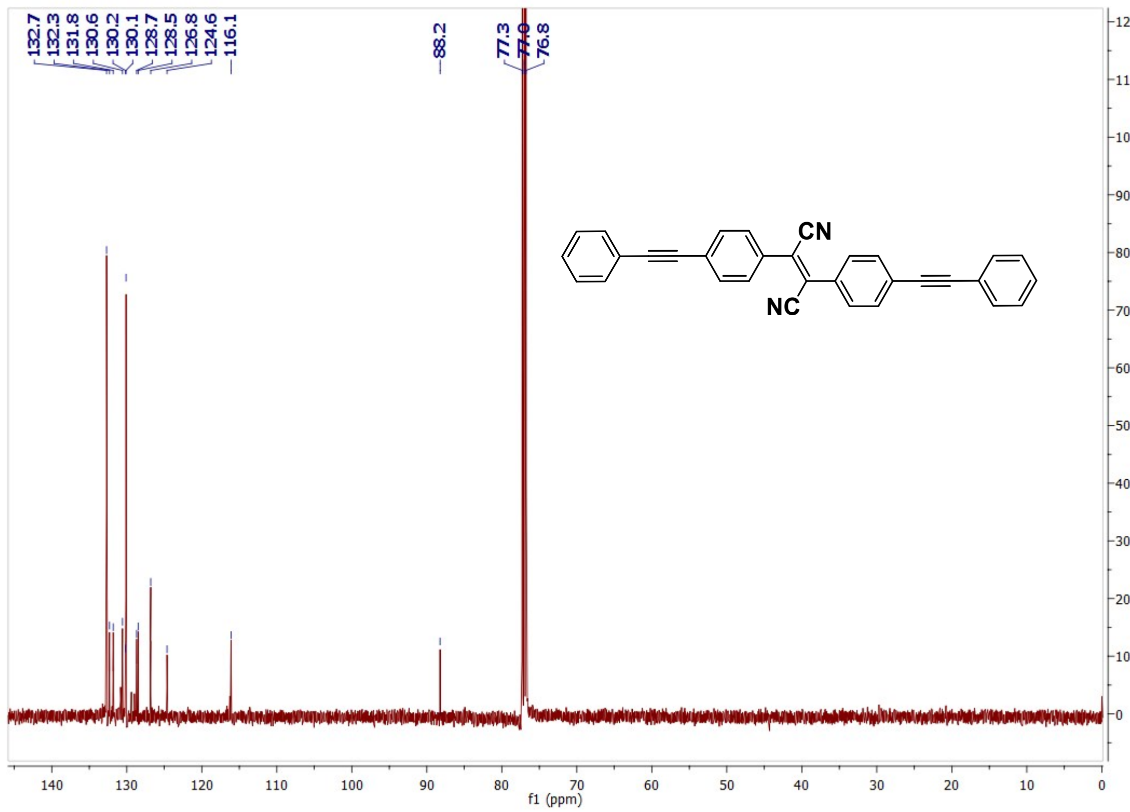

Fig. S40A: ^{1}H NMR Spectra ($CDCl_3$, 500 MHz, ppm) of compound 8:

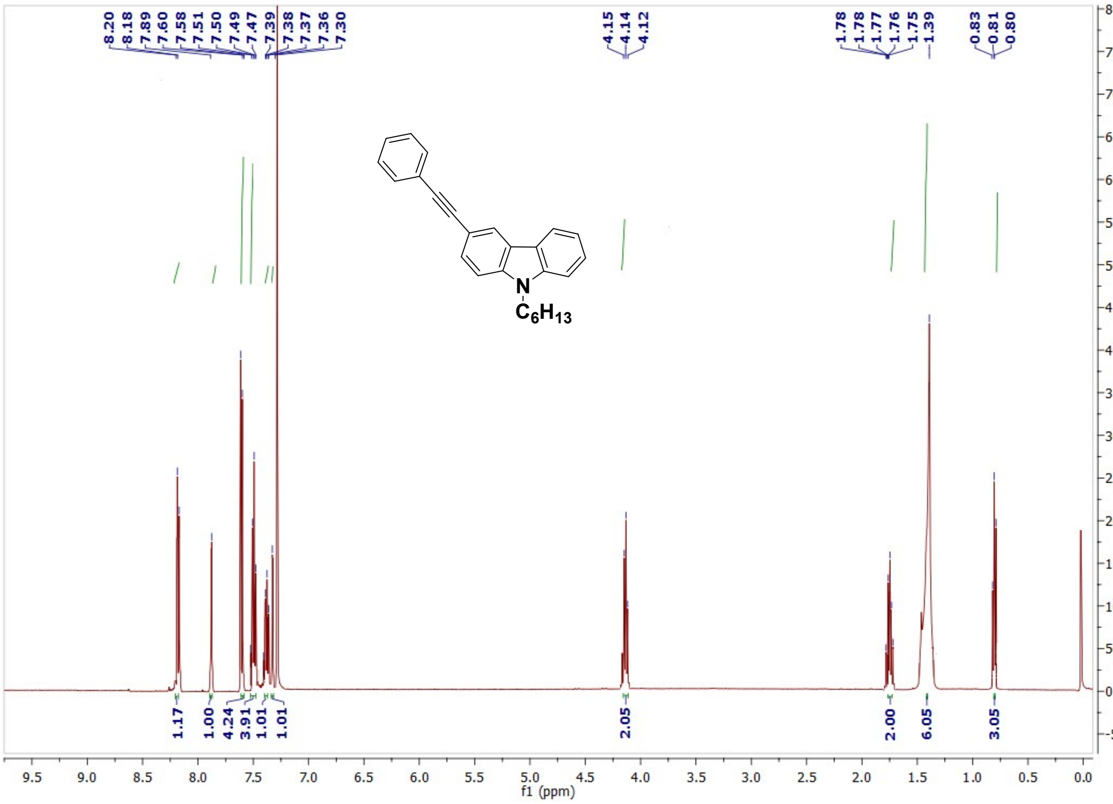

Fig. S40B: ^{13}C NMR Spectra ($CDCl_3$, 125 MHz, ppm) of compound 8:

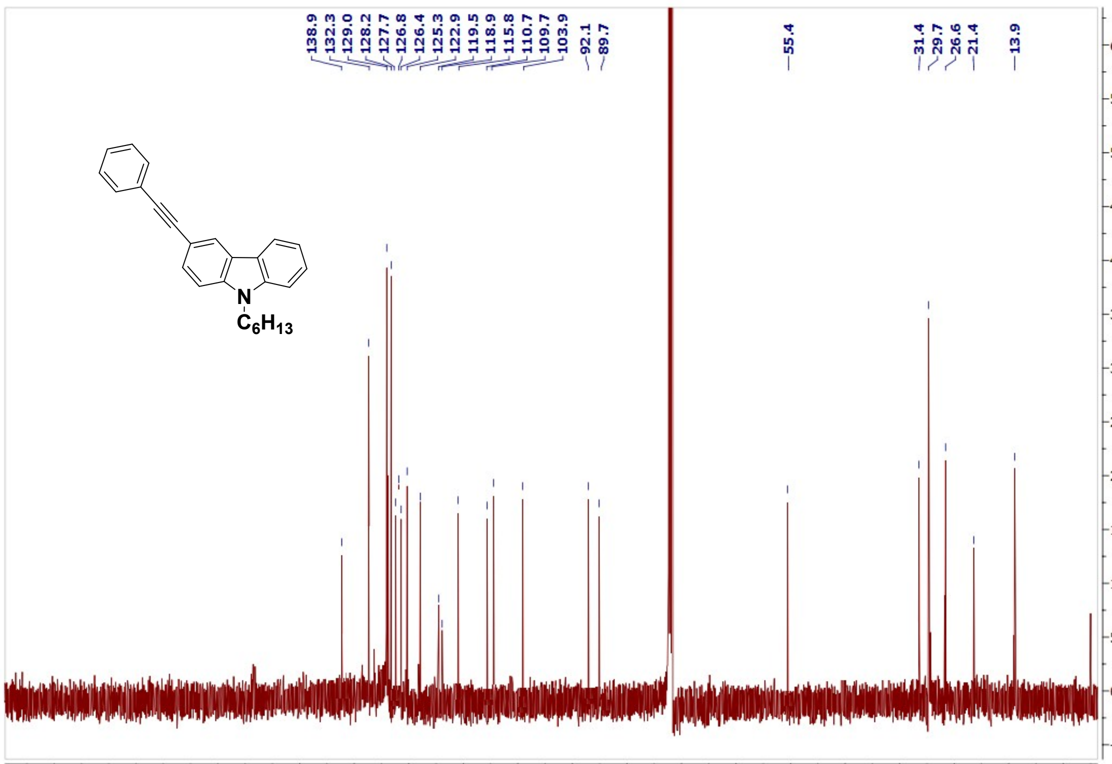

Fig. S41A: ^{1}H NMR Spectra ($CDCl_3$, 500 MHz, ppm) of compound 14a:

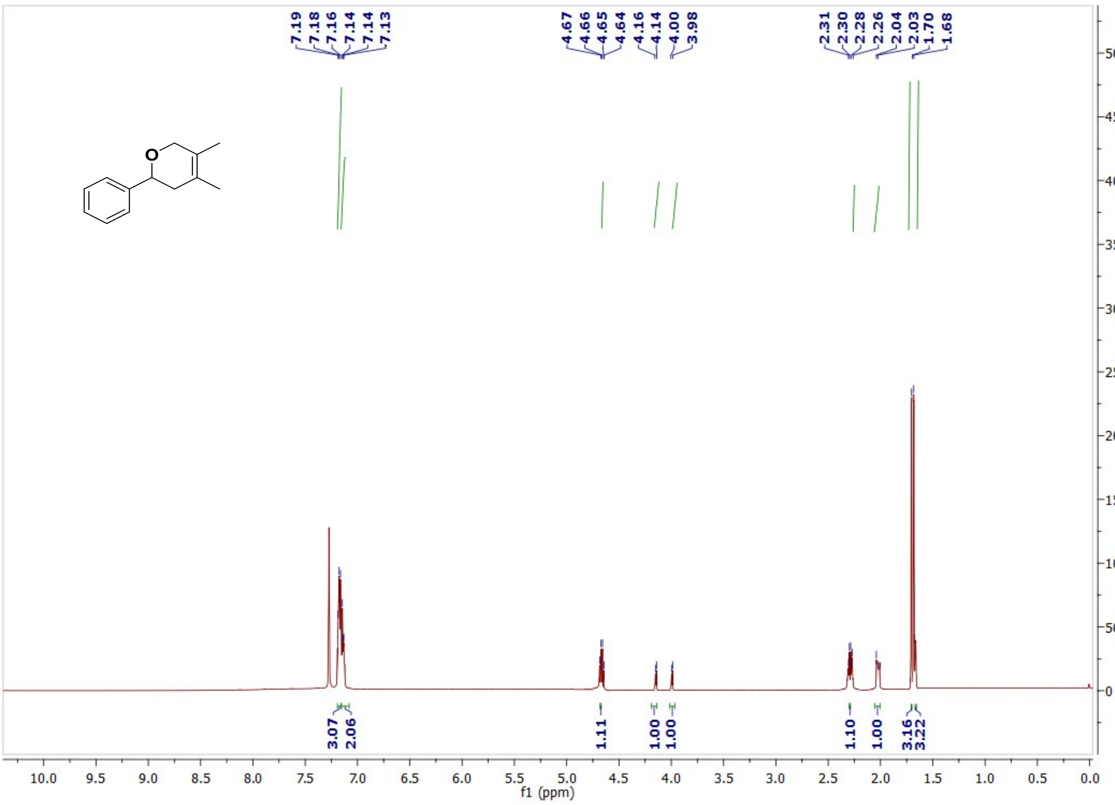

Fig. S41B: ^{13}C NMR Spectra ($CDCl_3$, 125 MHz, ppm) of compound 14a:

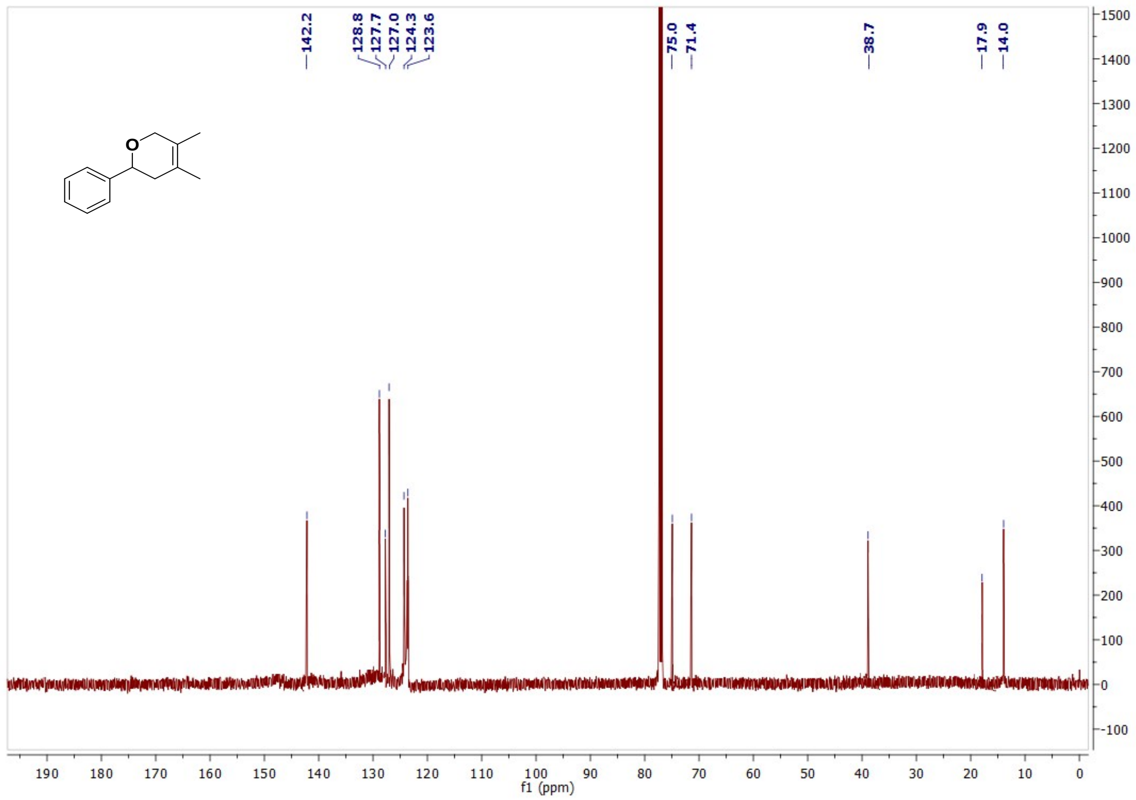

Fig. S42A: [1]H NMR Spectra ($CDCl_3$, 500 MHz, ppm) of compound 14b:

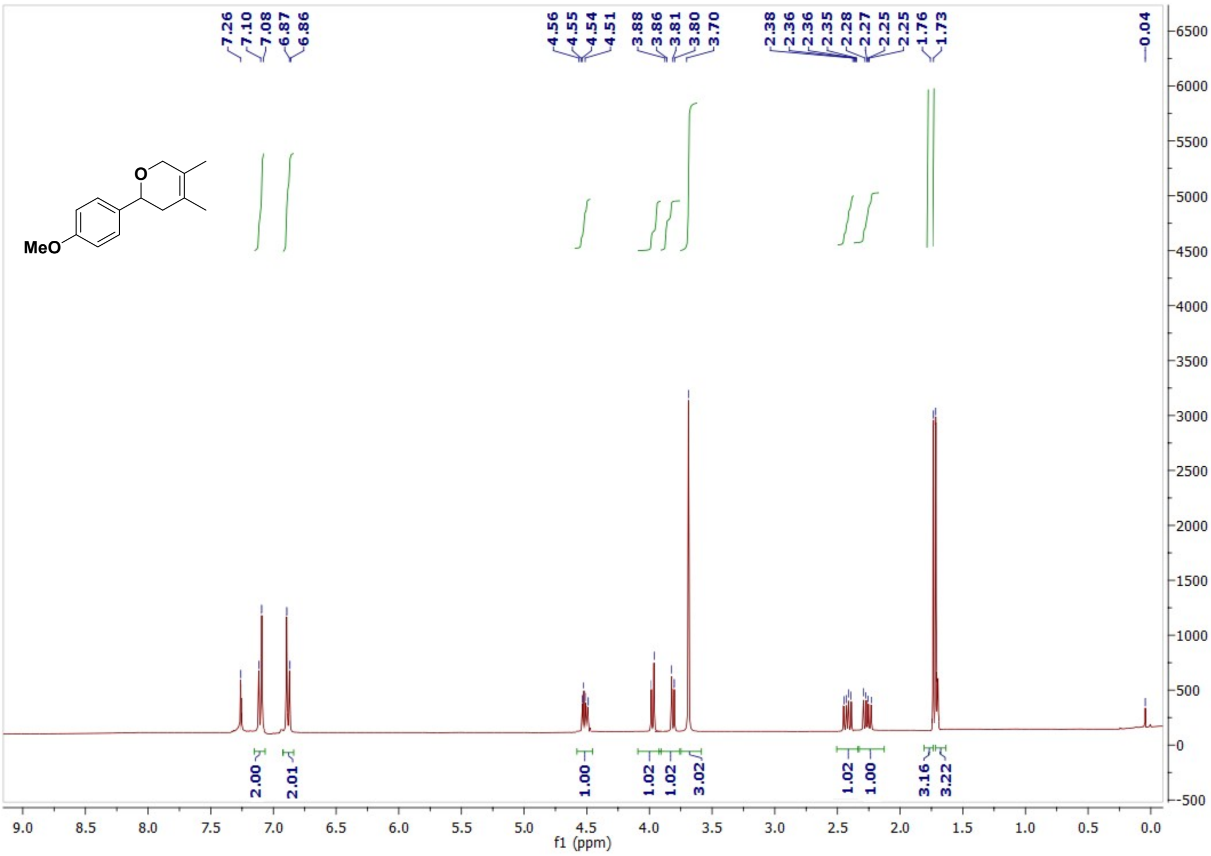

Fig. S42B: [13]C NMR Spectra ($CDCl_3$, 125 MHz, ppm) of compound 14b:

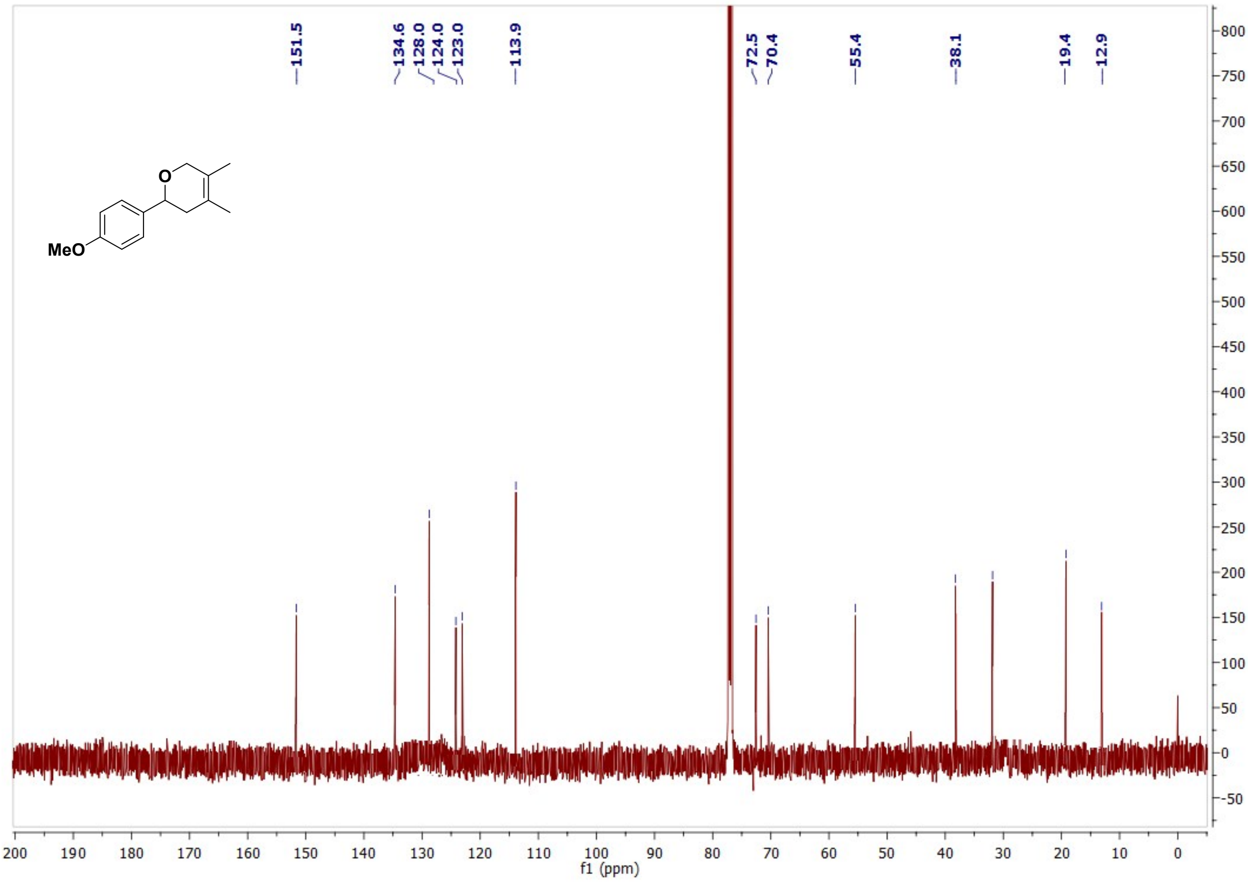

Fig. S43A: [1]H NMR Spectra (CDCl$_3$, 500 MHz, ppm) of compound 14c:

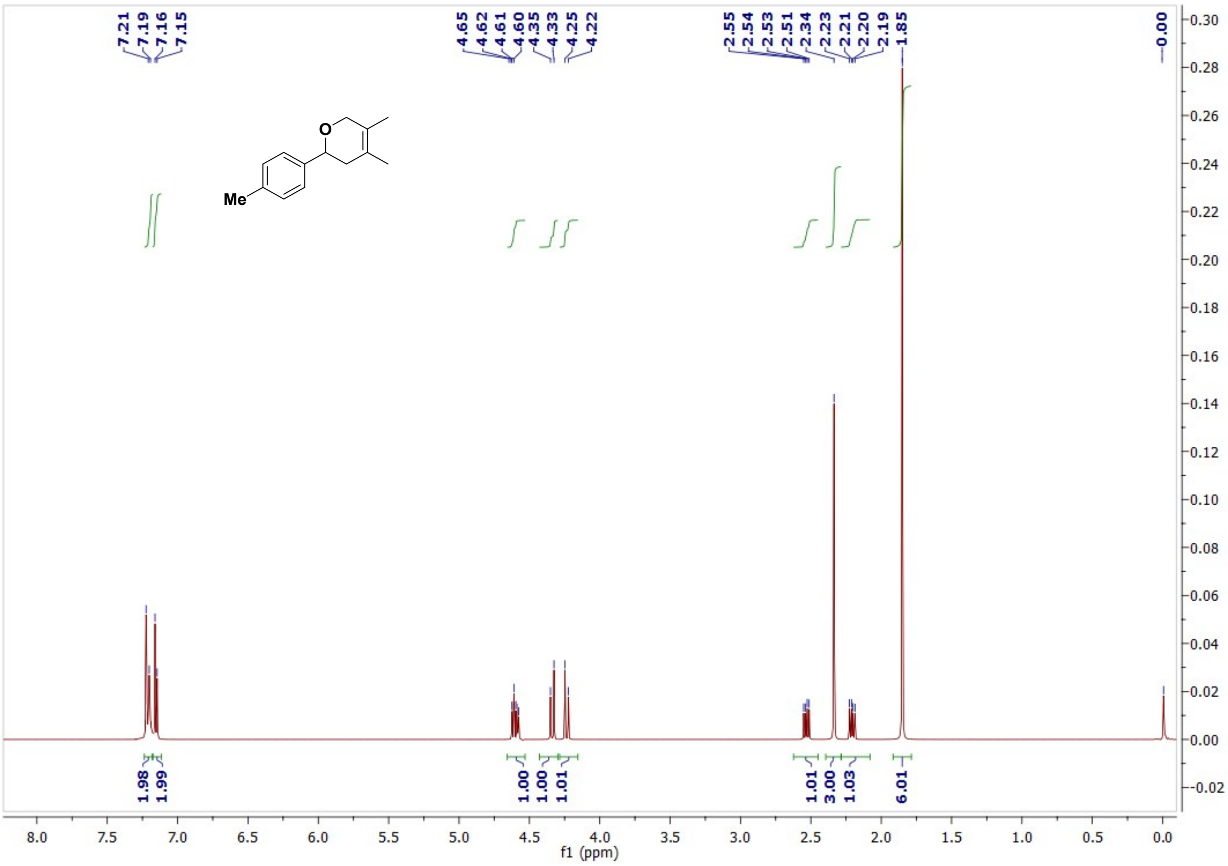

Fig. S43B: [13]C NMR Spectra (CDCl$_3$, 125 MHz, ppm) of compound 14c:

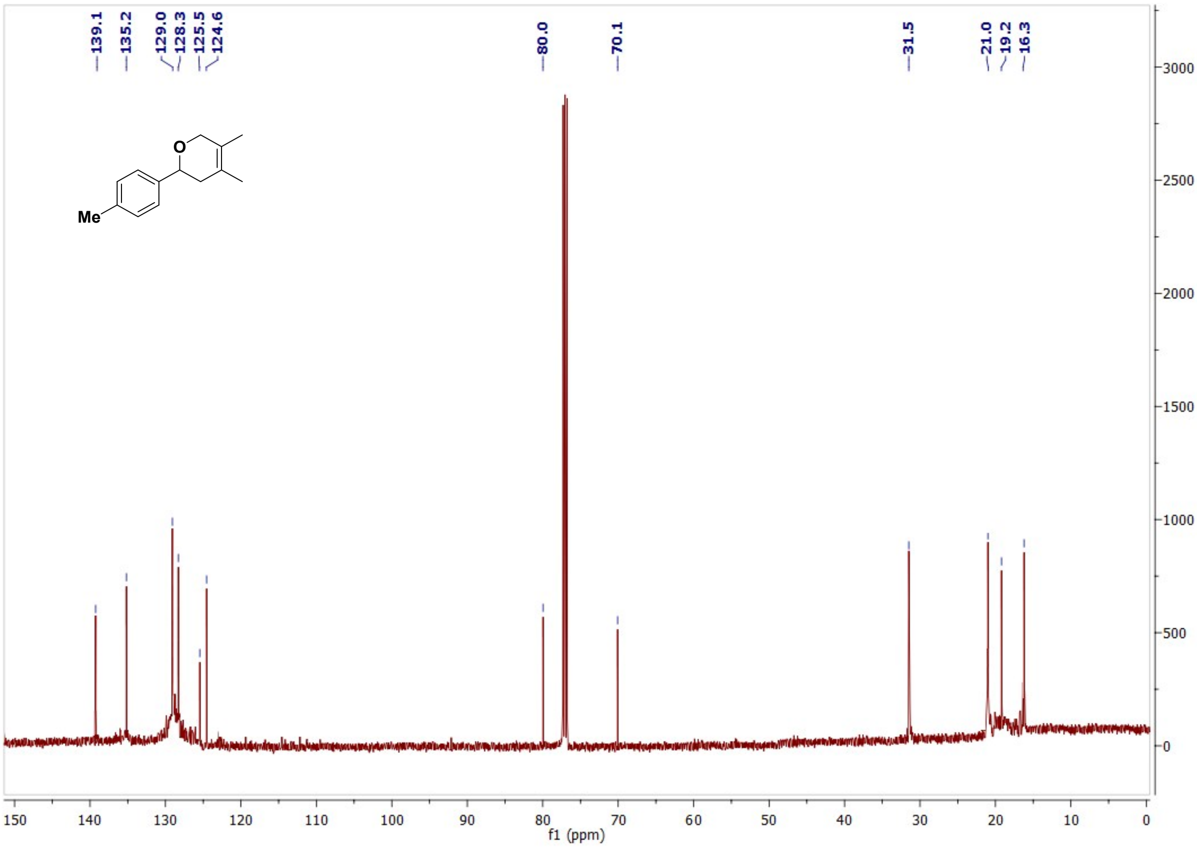

Fig. S44 A: ^{1}H NMR Spectra ($CDCl_3$, 300 MHz, ppm) of compound 14d:

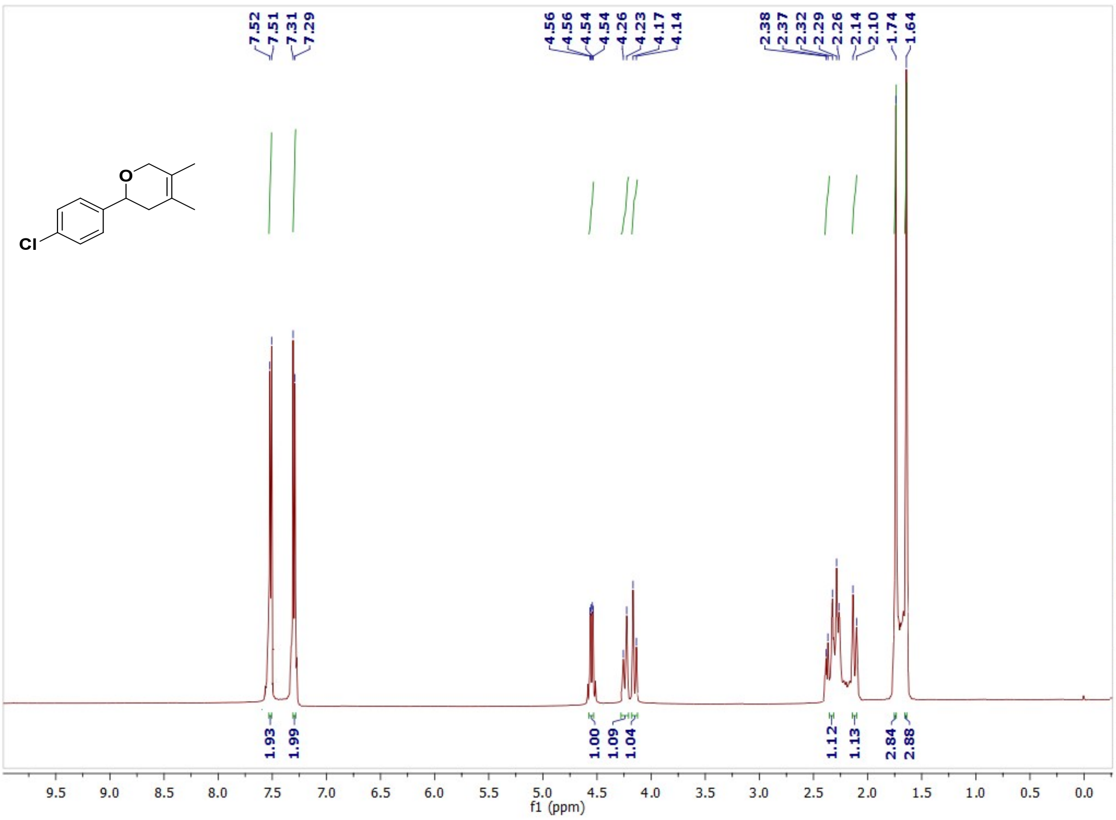

Fig. S44B: ^{13}C NMR Spectra ($CDCl_3$, 125 MHz, ppm) of compound 14d:

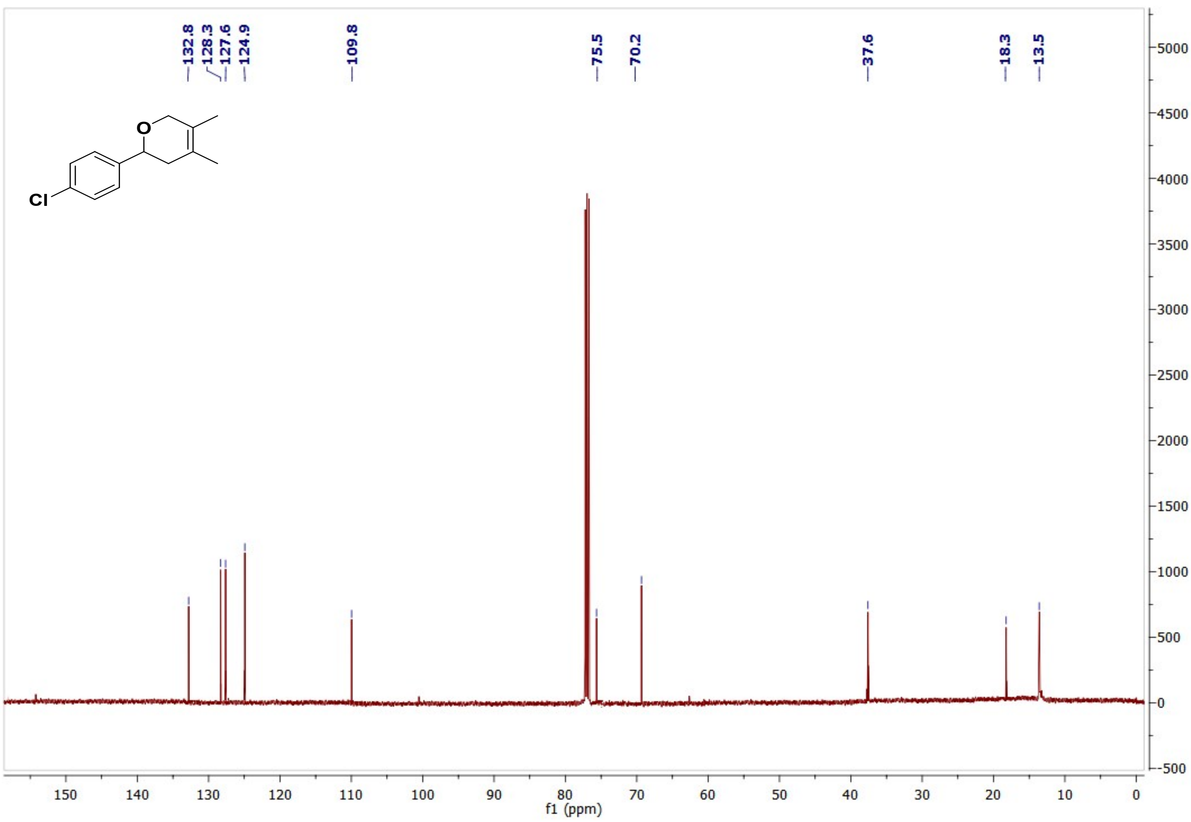

Fig. S45A: ^{1}H NMR Spectra ($CDCl_3$, 500 MHz, ppm) of compound 14e:

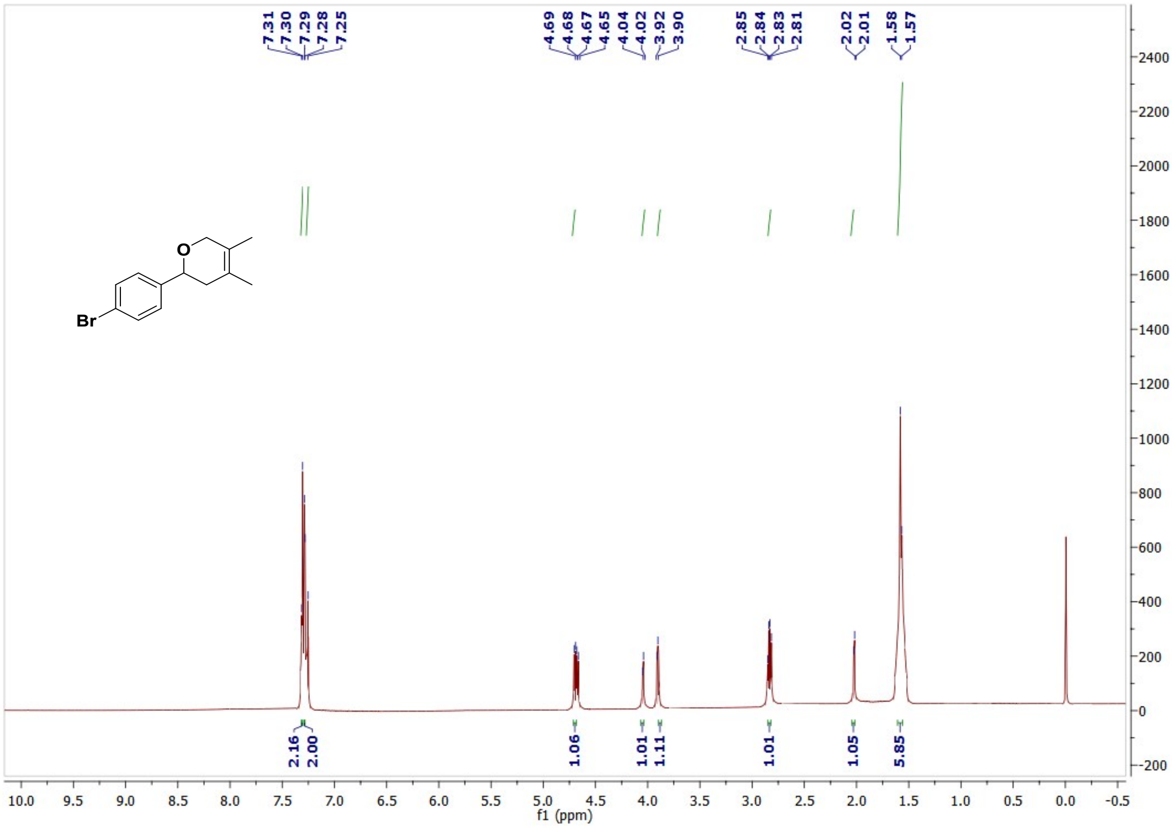

Fig. S45B: ^{13}C NMR Spectra ($CDCl_3$, 125 MHz, ppm) of compound 14e:

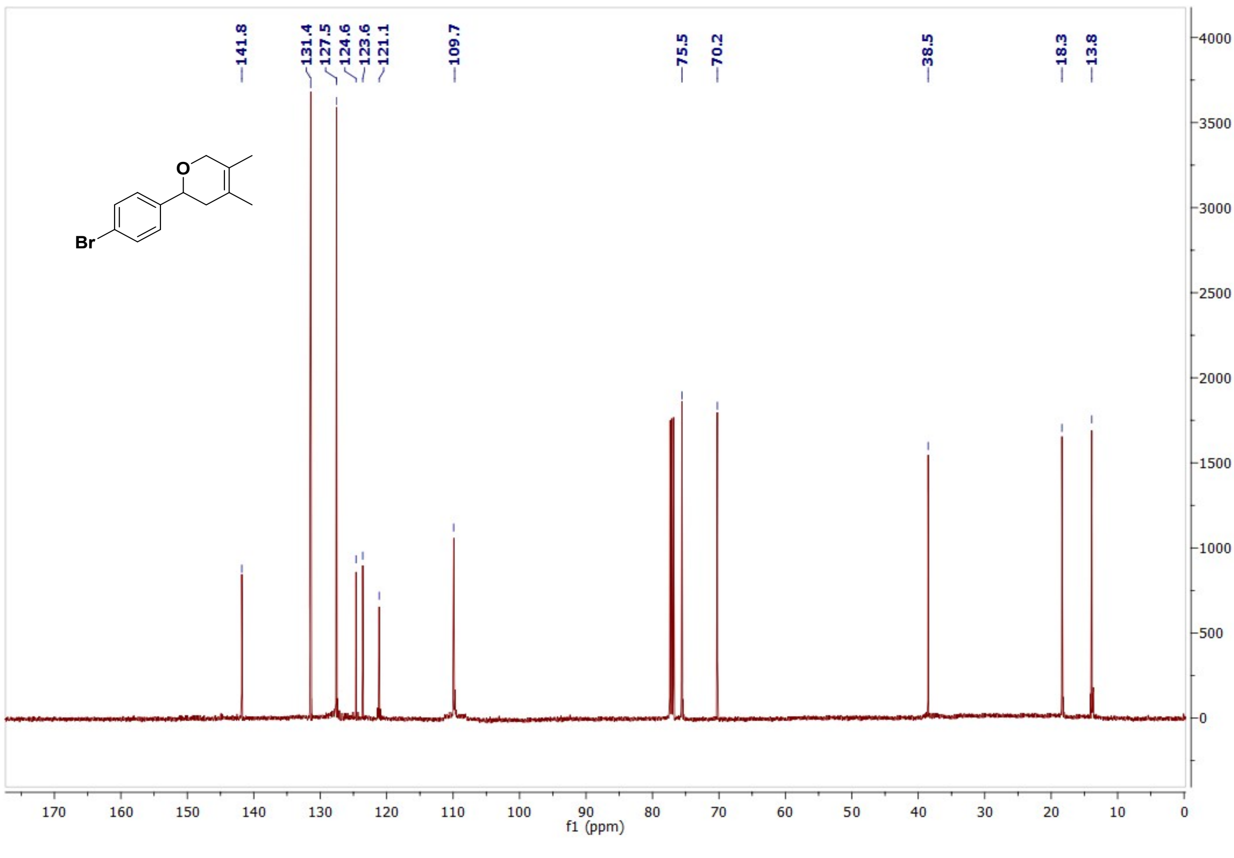

Fig. S46A: [1]H NMR Spectra ($CDCl_3$, 500 MHz, ppm) of compound 14f:

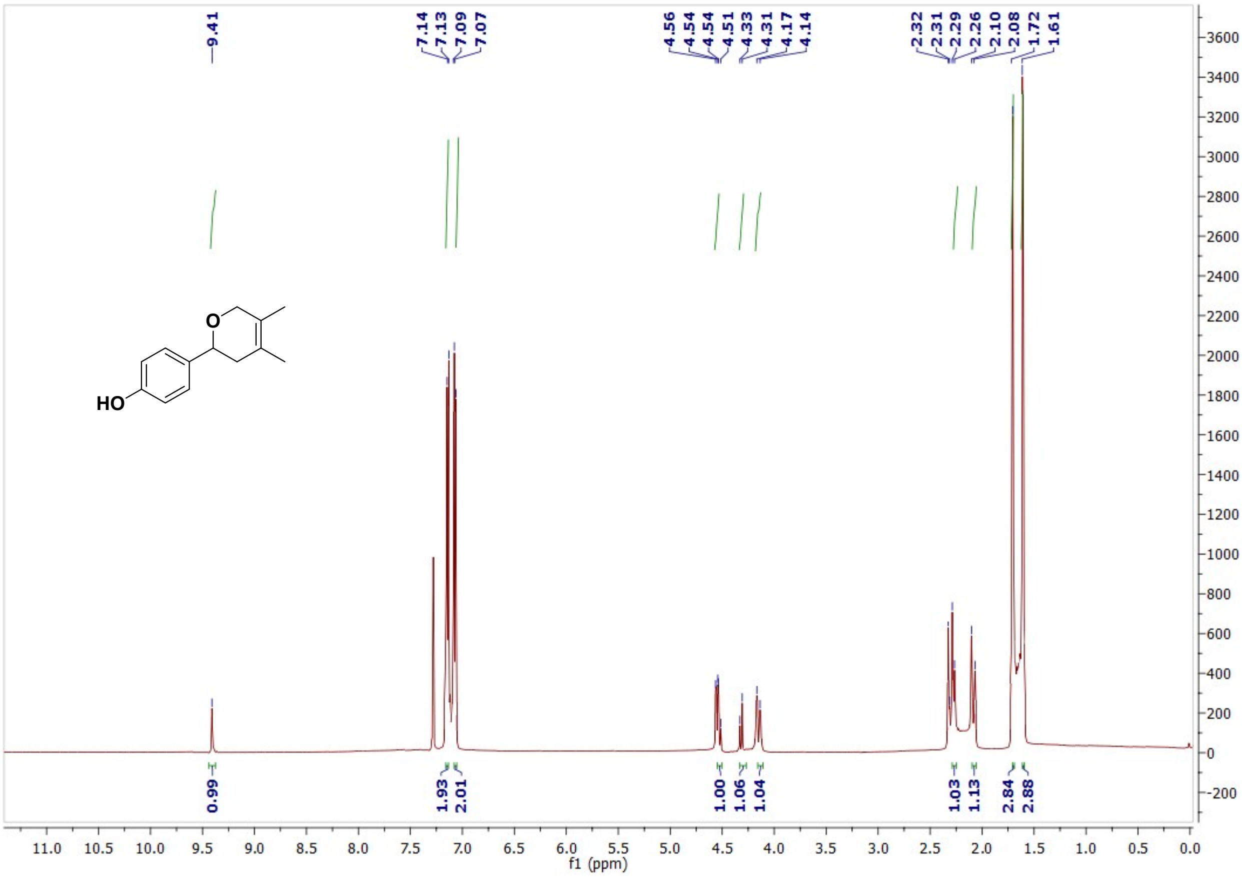

Fig. S46B: [13]C NMR Spectra ($CDCl_3$, 125 MHz, ppm) of compound 14f:

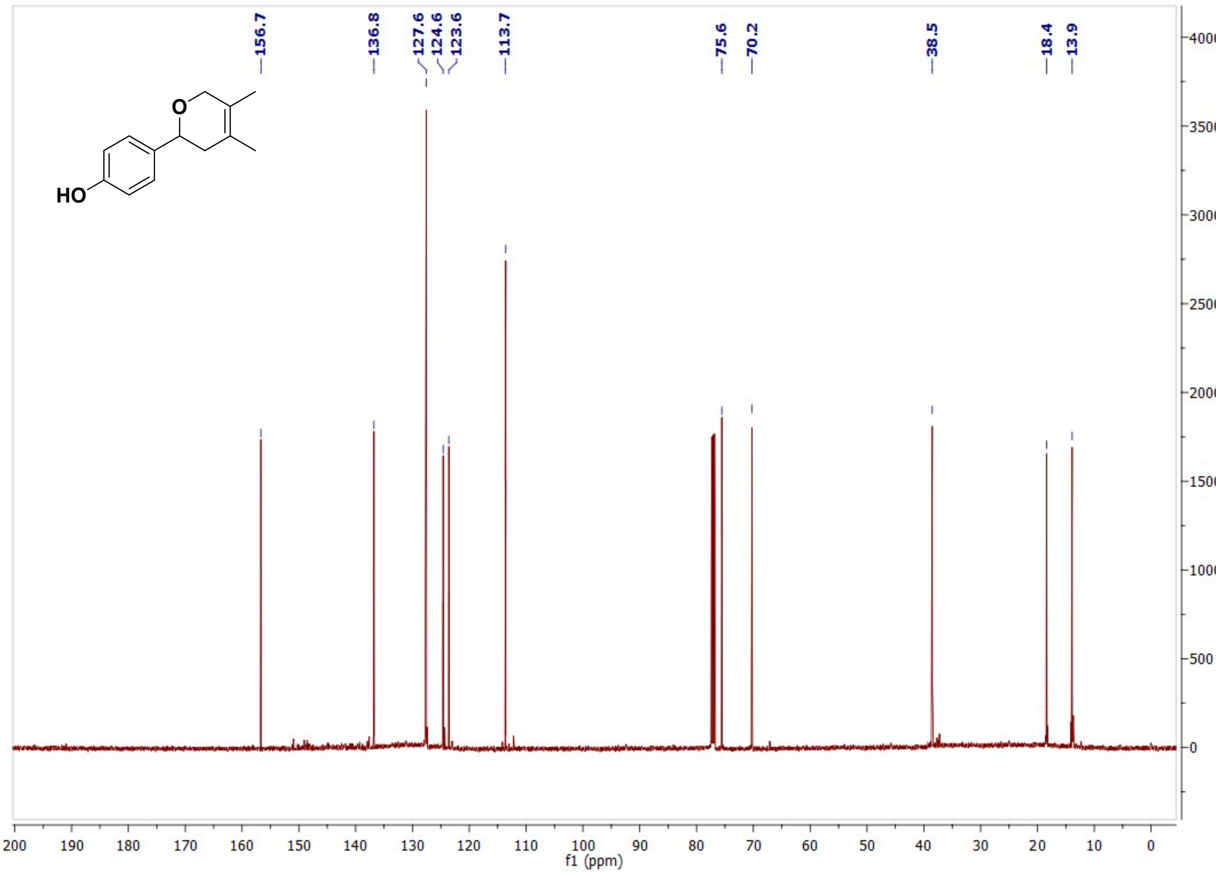

Fig. S47A: ^{1}H NMR Spectra ($CDCl_3$, 500 MHz, ppm) of compound 14g:

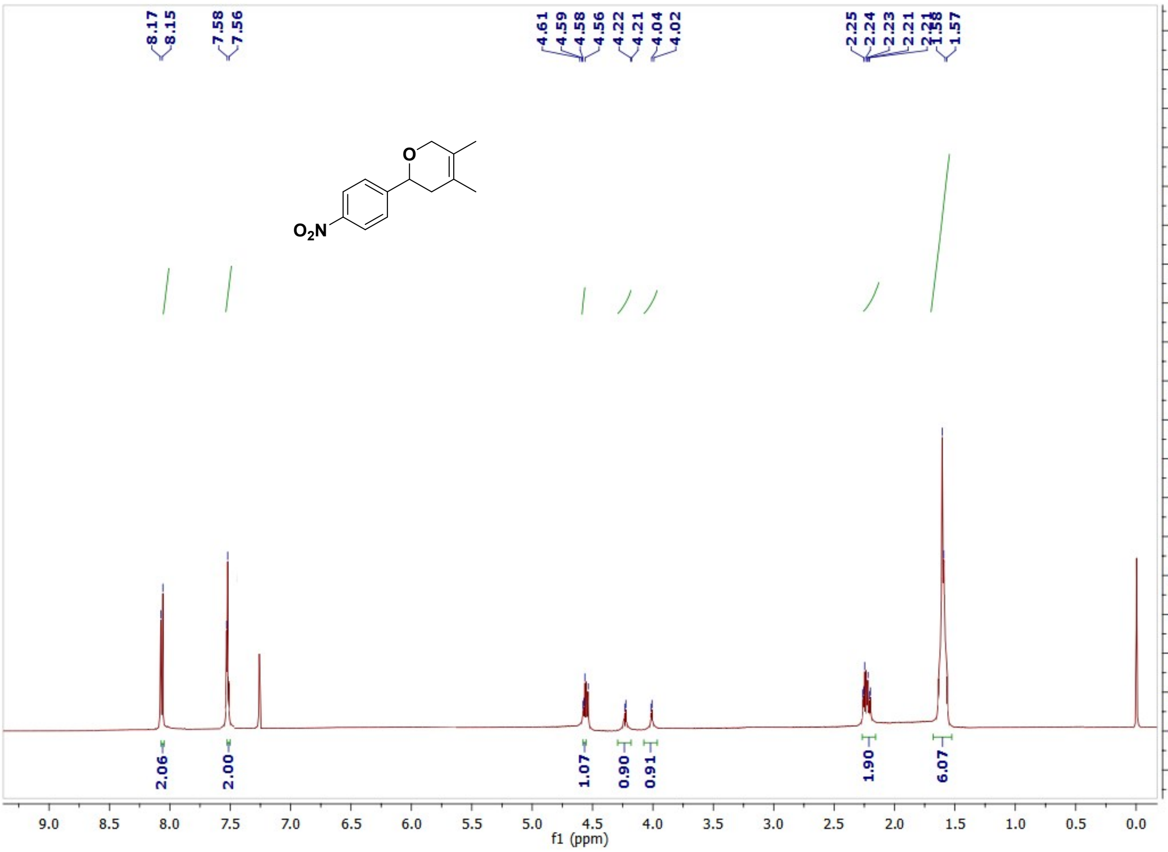

Fig. S47B: ^{13}C NMR Spectra ($CDCl_3$, 125 MHz, ppm) of compound 14g:

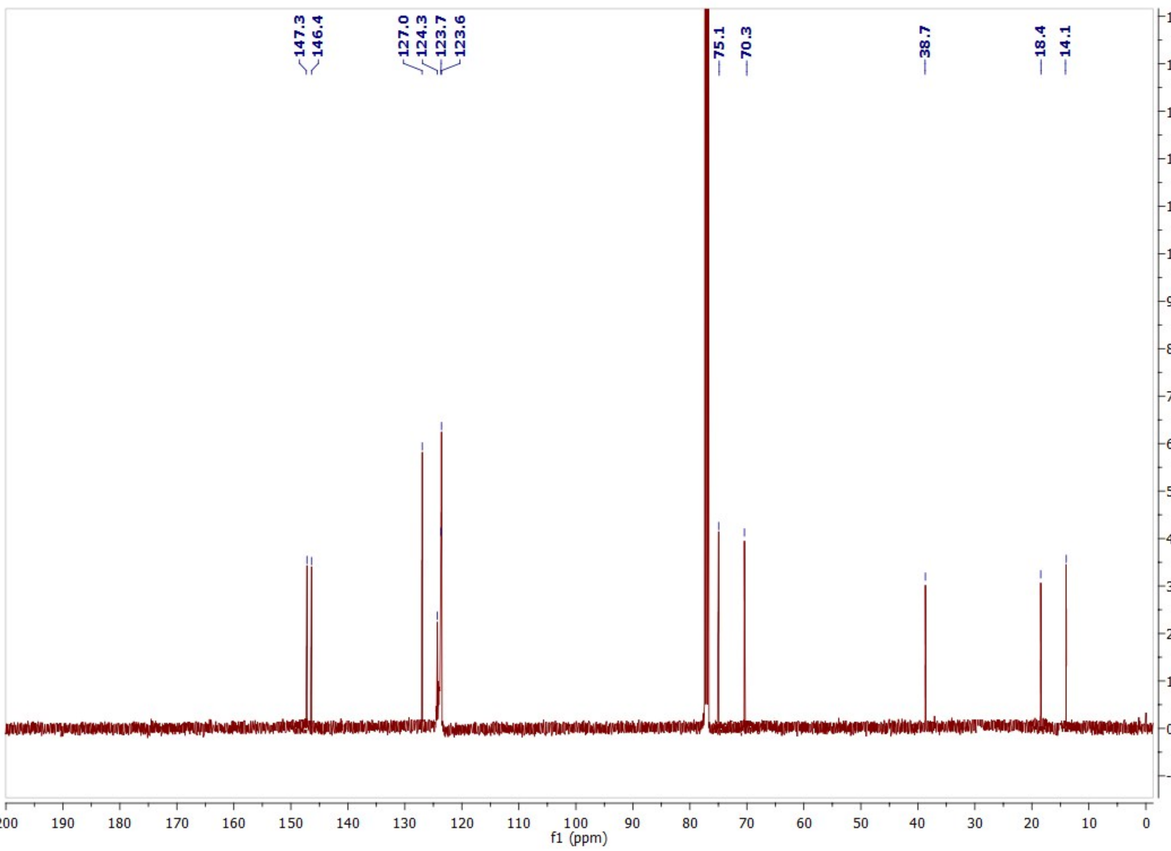

Fig. S48A: ^{1}H NMR Spectra ($CDCl_3$, 500 MHz, ppm) of compound 14h:

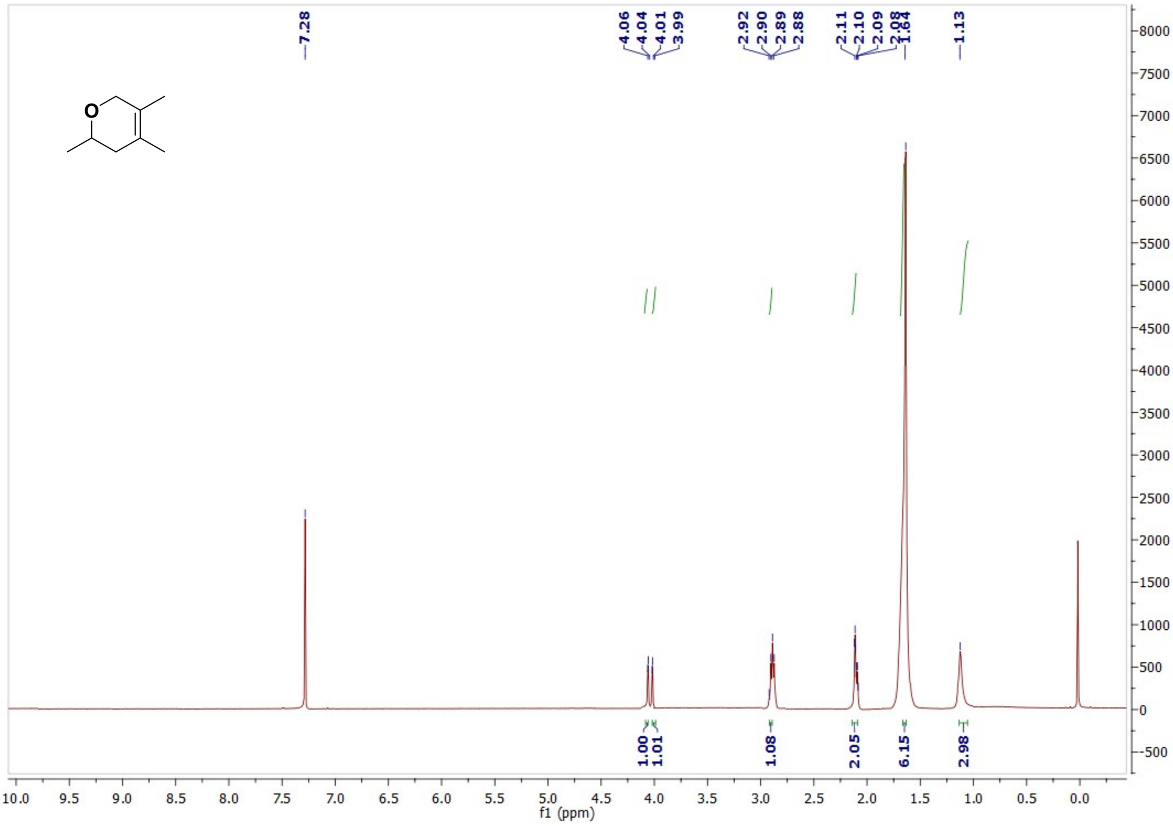

Fig. S48B: ^{13}C NMR Spectra ($CDCl_3$, 125 MHz, ppm) of compound 14h:

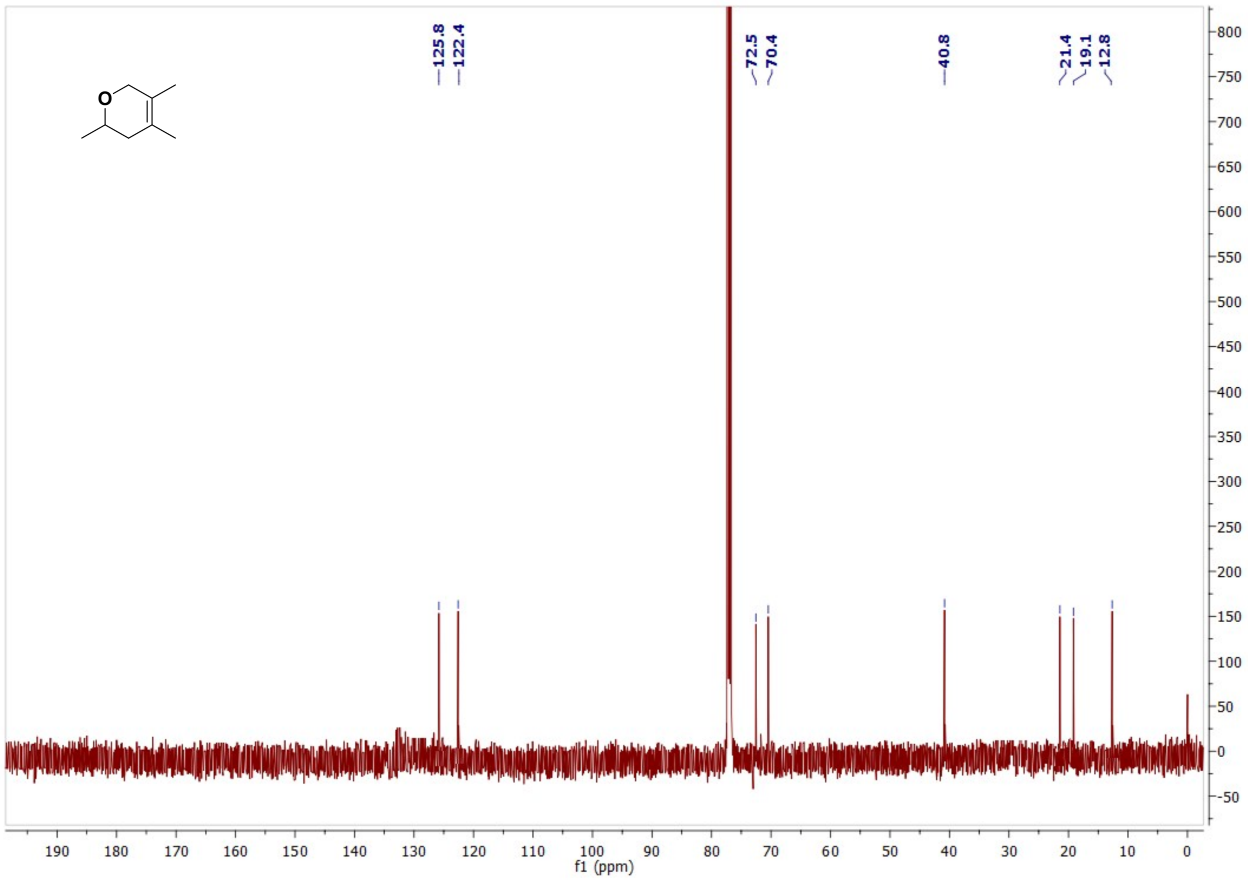

Fig. S49A: ^{1}H NMR Spectra ($CDCl_3$, 300 MHz, ppm) of compound 14i:

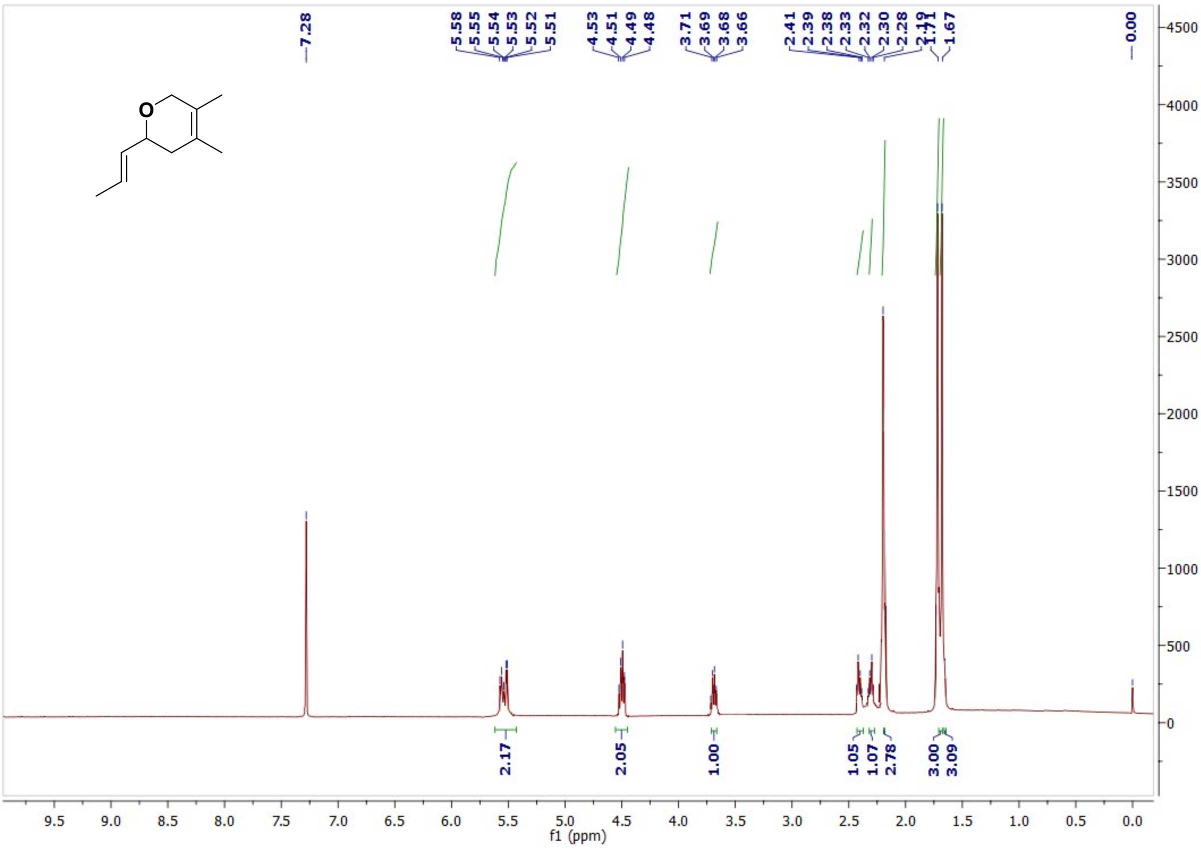

Fig. S49B: ^{13}C NMR Spectra ($CDCl_3$, 125 MHz, ppm) of compound 14i:

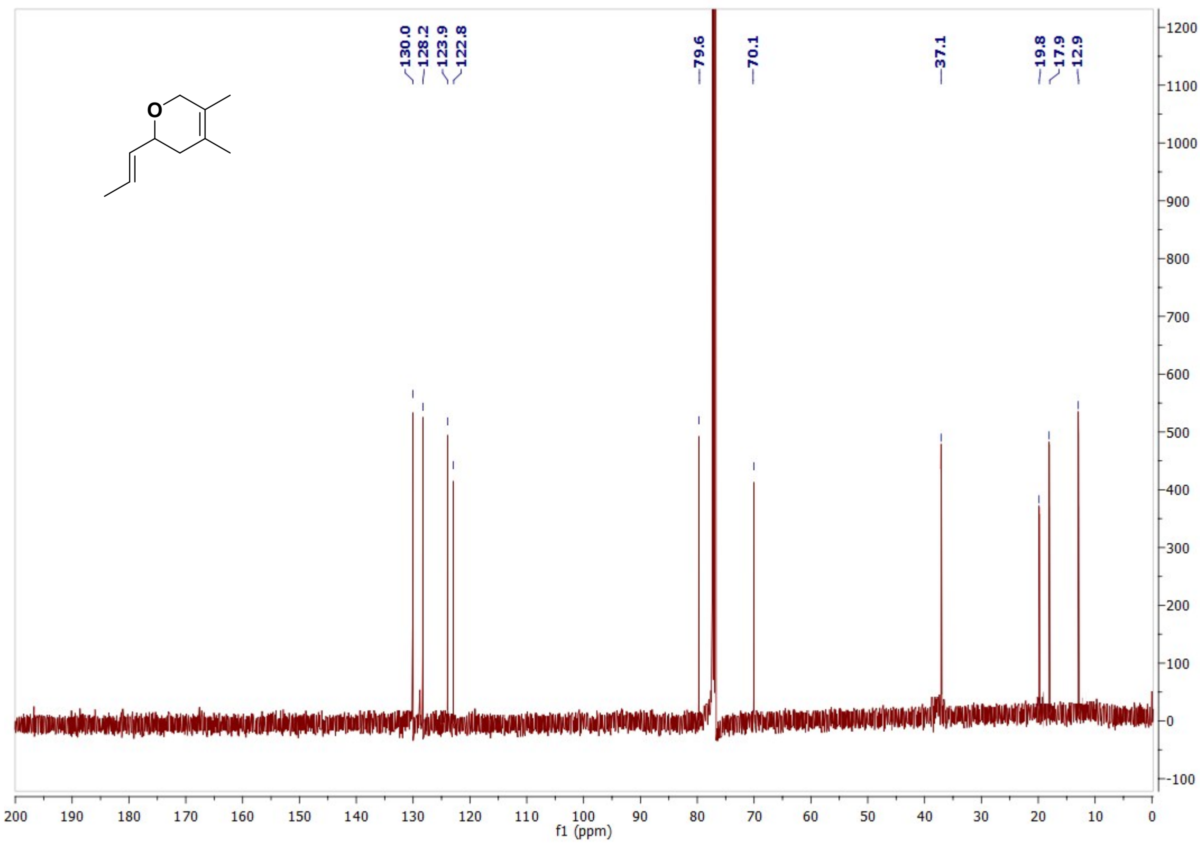

Fig. S50A: ^{1}H NMR Spectra ($CDCl_3$, 300 MHz, ppm) of compound 14j:

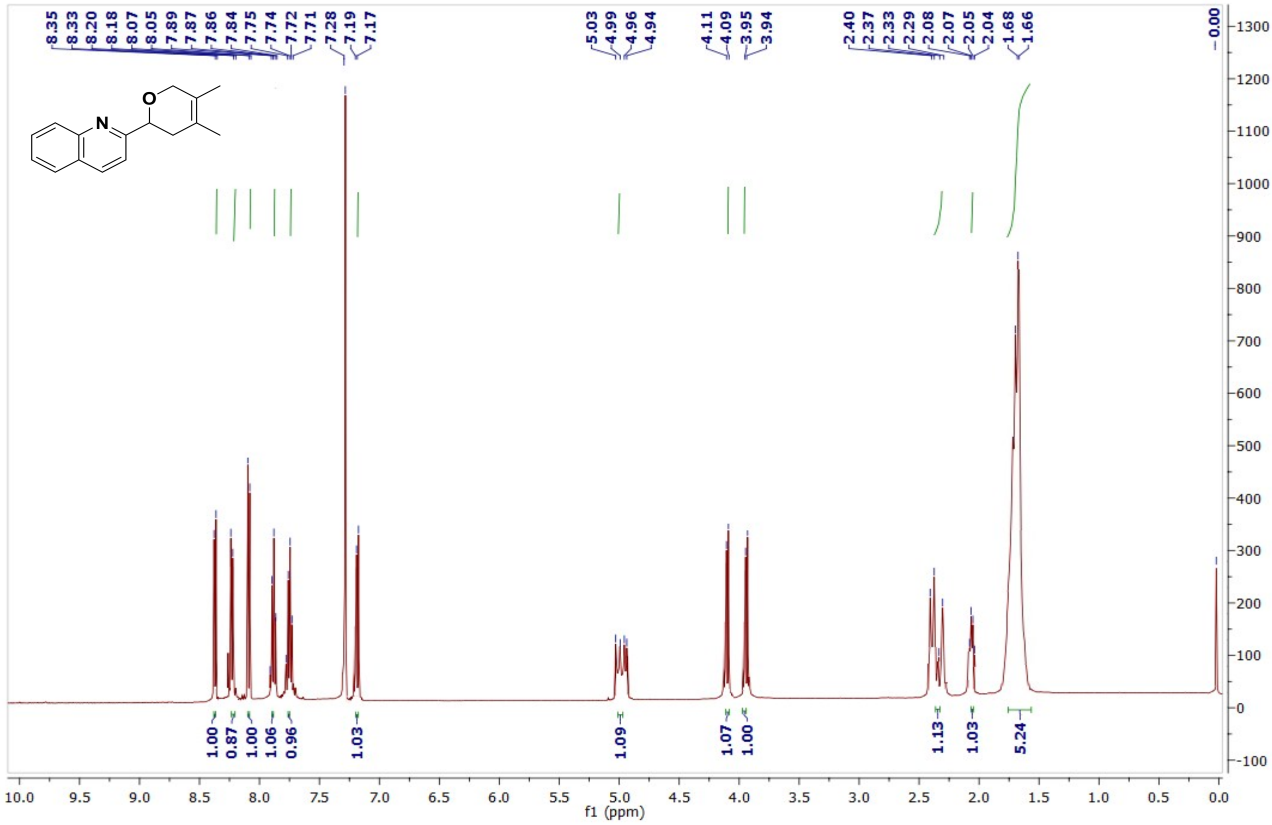

Fig. S50B: ^{13}C NMR Spectra ($CDCl_3$, 125 MHz, ppm) of compound 14j:

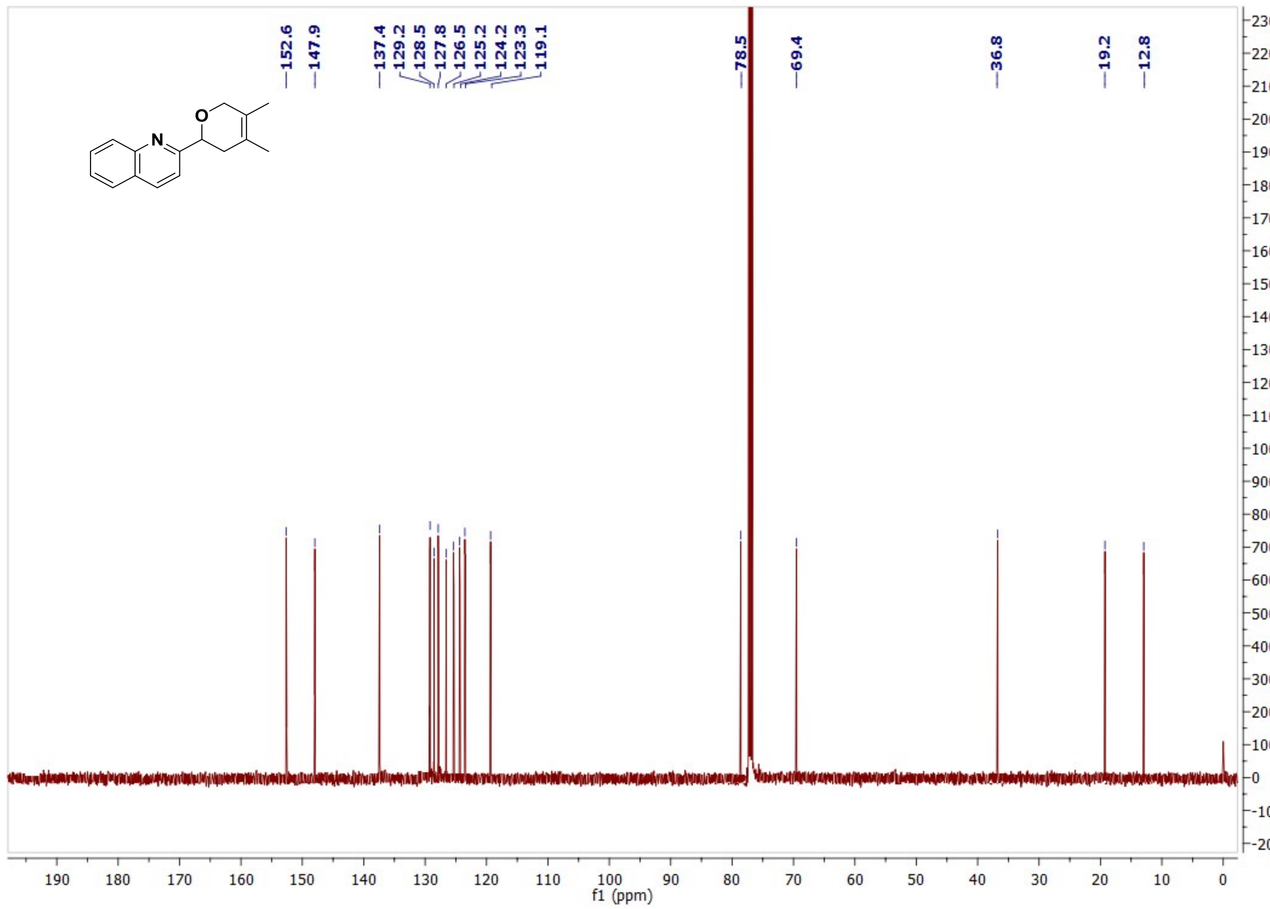

Fig. S51: ^{1}H NMR Spectra ($CDCl_3$, 300 MHz, ppm) of compound 15:

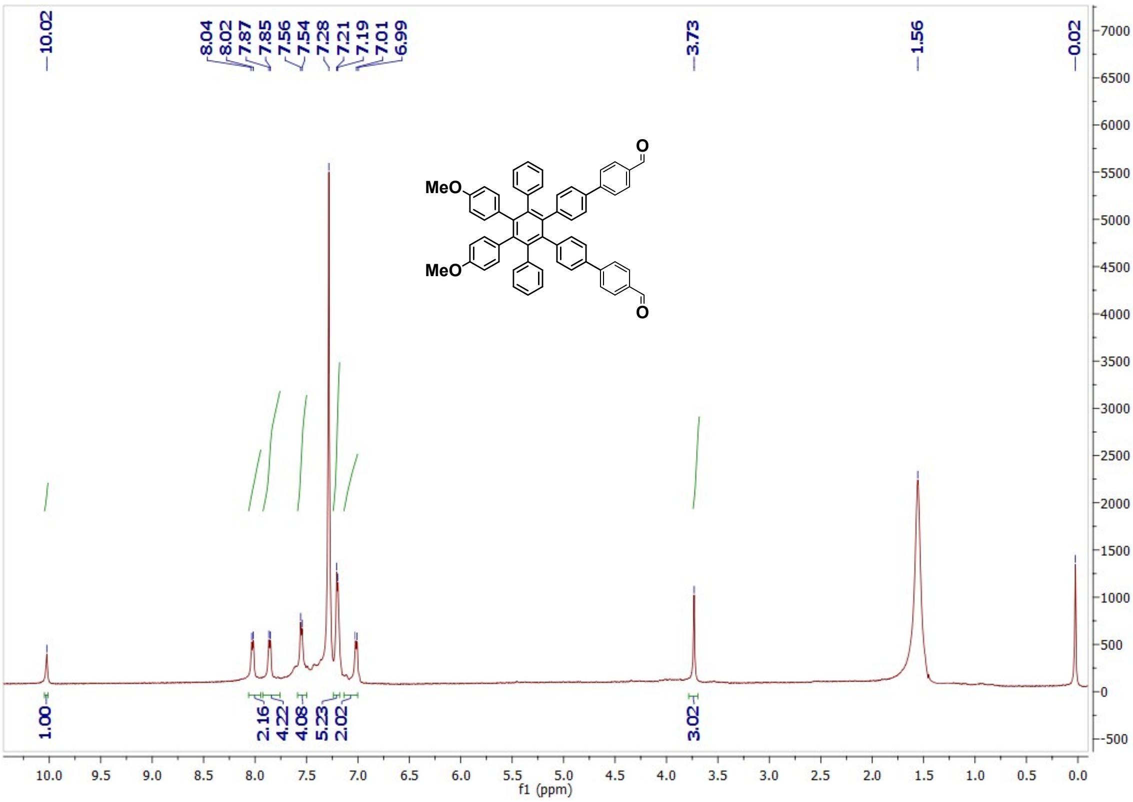

Fig. S52A: ^{1}H NMR Spectra ($CDCl_3$, 300 MHz, ppm) of compound 16:

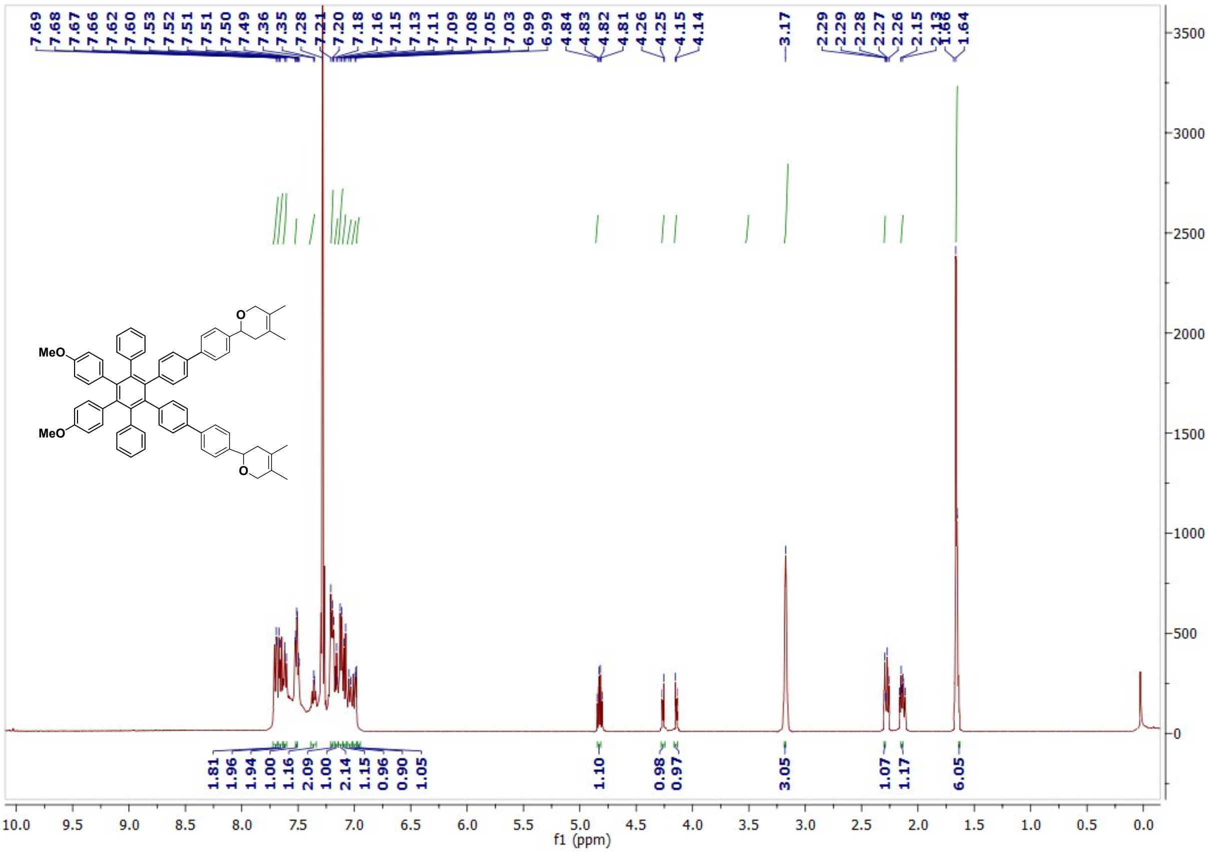

Fig. S52B: ^{13}C NMR Spectra ($CDCl_3$, 125 MHz, ppm) of compound 16: